Design of a Mobile Field Station for LEO Satellite communications

J.M. Erasmus

Thesis project presented in partial fulfilment of the requirements for the degree of Master of Science (Electronic Engineering) at the University of Stellenbosch.

Supervisor: Prof G.W. Milne

March 2000

Declaration

I, the undersigned, hereby declare that the work contained in this thesis is my own original work and I have not previously in its entirety or in part submitted it at any university for a degree.

J.M. Erasmus

Abstract

This document describes the breadboard design and practical evaluation of a mobile field station, capable of communicating with the ***SUNSAT*** microsatellite. A study of existing satellite communication systems employing LEO satellites, as well as the physical phenomena, influencing the VHF communication link between earth and such satellites was done and used to determine the specifications needed for a functional field station.

The design entailed work on different building blocks like a receiver, transmitter and modem unit as well as the writing and testing of the necessary software on a controlling personal computer. The measurements done showed that the field station satisfies most of the specifications, and that it is capable of communicating with a satellite. The document is concluded by suggesting improvements and possible further work before a commercial version of the field station may be build.

Opsomming

In hierdie dokument word die ontwerp en praktiese evaluasie van 'n mobiele veldstasie beskryf wat met die ***SUNSAT*** mikrosatelliet kan kommunikeer. 'n Ondersoek na bestaande satellietstelsels in lae-aard wentelbane en die fisiese faktore wat die radioskakel tussen die grond en sulke satelliete beïnvloed is gebruik om spesifikasies vir 'n werkende veldstasie daar te stel.

Die ontwerpstaak het werk aan 'n ontvanger, sender, modem en beheerproggramatuur ingesluit. Die voltooide veldstasie is gekarakteriseer deur 'n meetproses wat aangetoon het dat dit met 'n satelliet kan kommunikeer. Die dokument word afgesluit met voorgestelde verbeterings en verdere werk aan die veldstasie voordat 'n kommersiële weergawe daarvan voltooi kan word.

Acknowledgements

I would like to sincerely thank:

- Professor Garth Milne for his guidance.
- Everybody involved with the ***SUNSAT*** project for creating a challenging and stimulating work environment.
- Members of the Amateur Radio community for the example of their innovative and experimenting spirit.
- TELKOM SA Ltd for funding.
- My Parents.
- My wife Karina for her love and understanding.
- My Heavenly Father for the opportunity to explore and study his creation.

Contents

List of figures

List of Tables

Abbreviations

ACS	- Altitude control system
A_{Earth}	- Earth angle
A_{El}	- Elevation angle
AF	- Audio frequency
AFC	- Automatic frequency control
AFSK	- Audio frequency shift keying
A_{Sat}	- Satellite angle
BUAD	- Characters per second
CDMA	- Code division multiple access
F	- Noise Figure
FCS	- Frame check sequence
FDMA	- Frequency Division Multiple Access
FET	- Field effect transistor
FIFO	- First-in-first-out
FSK	- Frequency-shift-keying
GCC	- Gateway control centre
GEO	- Geostationary orbit satellite
GES	- Gateway earth station
GMPCS	- Global mobile personal communication systems
GNCC	- Global network control centre
GPS	- Global-positioning system
HDLC	- High level data link control
H_{Sat}	- Satellite altitude
IC	- Integrated circuit
I_D	- Drain current
IF	- Intermediate frequency
ISO	- International standards organisation
LCD	- Liquid crystal display
LEO	- Low earth orbiting
LNA	- Low noise amplifier
LO	- Local oscillator
MOSFET	- Metal oxide field effect transistor
NBFM	- Narrowband frequency modulation
NR	- Noise Ratio
NR'	- Actual noise ratio
OBC	- On Board Computer
OQPSK	- Offset quadrature phase shift keying
PCB	- Printed Circuit Board
PAM	- Pulse amplitude modulation
PID	- Protocol identifier
PLL	- Phase locked loop
PSK	- Phase shift keying
PSTN	- The public switched telephone network
PTT	- Push to talk
R_{earth}	- Earth Radius = 6378.4km
RF	- Radio frequency
RSSI	- Received signal strength indicator

SATRA	- South African Telecommunications Regulatory Authority
SINAD	- Signal plus Noise and Distortion
SRMA	- Split channel reservation multiple access
SSID	- Secondary station identifiers
SUNSAT	- Stellenbosch UNiversity SATellite
TDMA	- Time Division Multiple Access
TNC	- Terminal node controller
VCO	- Voltage controlled oscillator
VCXO	- Voltage controlled crystal oscillator
V_{DS}	- Drain source voltage
VSWR	- Voltage standing wave ratio

FREQUENCY ALLOCATIONS -	VHF	30-300MHz
	UHF	300MHz-3000MHz
	L-Band	1-2GHz
	S-Band	2-3.7GHz
	C-band	3.7-6.5GHz
	Ku-Band	11-18GHz
	Ka-band	26-40GHz

1. Introduction

The world we live in truly has gone through a communication revolution since Bell invented the first telephone in 1876. The current phase of this revolution is the meteoric rise of mobile communications. Standard cellular networks depend on limited coverage on a cell to cell basis by their very nature. To deliver truly global coverage it is necessary to use satellite communications.

Companies that employ satellites to deliver mobile communication services are using Low Earth Orbiting (LEO) satellites more and more. This trend makes it possible to manufacture mobile handsets that are comparable to terrestrial cellphones in size and cost, but with the capability of working directly to a satellite in LEO orbit. Examples of commercial companies employing this kind of satellites such as ***Iridium*** and ***Globalstar*** will be discussed in *Chapter 2.*

The Stellenbosch UNiversity SATellite (***SUNSAT***) is an experimental microsatellite build at the University of Stellenbosch, and launched by ***NASA*** on the 23rd of February 1999. ***SUNSAT*** occupies an elliptical polar orbit of between 655km and 850km giving it 4 daily passes over Southern Africa with about 10 minutes of visibility each.

1.1. Task definition

The aim of this project was to design and implement a mobile field station for satellite communications with the ***SUNSAT*** microsatellite. A field station can be defined as a minimal ground station that implements all the necessary hardware and software to communicate with the satellite, while being small and robust enough to be easily moved. The field station also needs to be commercially viable.

The technical design of the field station will be influenced by the need to be compatible to existing subsystems on the ***SUNSAT*** microsatellite.

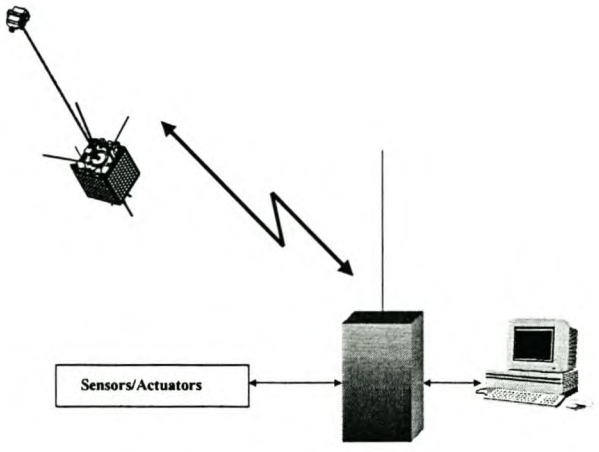

Figure 1-1 Operation of a field station

The field station must be able to communicate with a personal computer (or compatible single board computer) by using standard protocols. It should also be possible to connect the field station to sensors and/or actuators to use the field station for custom applications. To make the field station more flexible the receivers and transmitters should be designed as separate units.

1.2. Commercial applications

1.2.1. Data collection

The field station coupled to sensors can be situated in remote and difficult to reach areas and relay collected sensor information to the satellite when the user is in the satellite's footprint. This data can then be downloaded to the main groundstation where it can be relayed to the prospective users. Examples of this kind of applications include environmental monitoring such as weather stations, and also the monitoring of other assets like dams or pipelines.

With the multitude of relatively inexpensive GPS units available such a unit can also easily be connected to the field station to enable it to relay accurate information about its current position. This makes the field station useful for vehicle tracking and fleet management.

1.2.2. E-mail messaging

The field station can be connected to a personal computer or other terminal device like a palmtop computer. It will therefore be possible to exchange message files between the mobile field station and the groudstation. This service can be invaluable

in remote areas that are not covered by any other means of communication, and can be much more cost effective than voice telephony.

1.2.3. Remote asset control

The field station can be linked to simple actuators to control assets remotely. This service could make it possible to remotely open a valve, or to switch on a pump. The operation cost saved by not having to send operators to remote locations could easily cover the installation costs.

1.2.4. Technology demonstrator

The need for a technologically schooled workforce in developing countries is enormous. Unfortunately the strain on the educational system to deliver such a workforce is also mounting rapidly. One of the biggest problems is to motivate young people to follow subjects like maths and science at school that form the basis for further technological training.

The ***SUNSAT*** project has already proved that it has the potential to get pupils excited about technology. The mobile field station makes it possible to bring the interesting world of satellites and communications to the classroom. By deploying such field station at a school, pupils will be able to send and receive messages, to listen to general broadcasts and to experiment with possible new applications, all at a very competitive cost to prospective sponsors of the project.

1.3. Document overview

This document comprises the following chapters:

1.3.1. Chapter 2 - Overview of existing satellite communication systems

In this chapter the difference between GEO and LEO satellites is explained. Four commercial companies that offer LEO satellite services are discussed and the reader is introduced to the ***SUNSAT*** microsatellite.

1.3.2. Chapter 3 - The LEO Satellite communication environment

This chapter examines the physical link environment between a terrestrial field station and a LEO satellite. The combined effect of various losses are computed to specify

the required transmitter power and receiver sensitivity of the field station. The effects of Doppler frequency shift and noise are also discussed.

1.3.3. Chapter 4 - Conceptual design and specifications

In this chapter the specifications for the field station are discussed. Various possible antenna configurations are also presented.

1.3.4. Chapter 5 - Receiver design

The design of the field station receiver is discussed in this chapter. Elements of the receiver that are covered are the low noise amplifier, the input filter, the receiver module, the audio system, and a synthesised local oscillator.

1.3.5. Chapter 6 - Transmitter design

In this chapter the design of a frequency synthesised transmitter is discussed. The design is similar to the receiver synthesiser, except that it is modulated by an audio frequency source. The output of the synthesiser is coupled to a power amplifier module, which supply the required RF power output.

1.3.6. Chapter 7 - Data Communications

Besides discussing the AFSK modem used in the field station, this chapter also introduces the reader to the AX.25 data link layer protocol, and discusses the software used in the field station prototype.

1.3.7. Chapter 8 - Measurements and results

This chapter presents the measured performance of the field station.

1.3.8. Chapter 9 - Conclusions and recommendations

The thesis is concluded with an evaluation of the components of the field station. Replacements for obsolete components are presented, and possible further development is discussed.

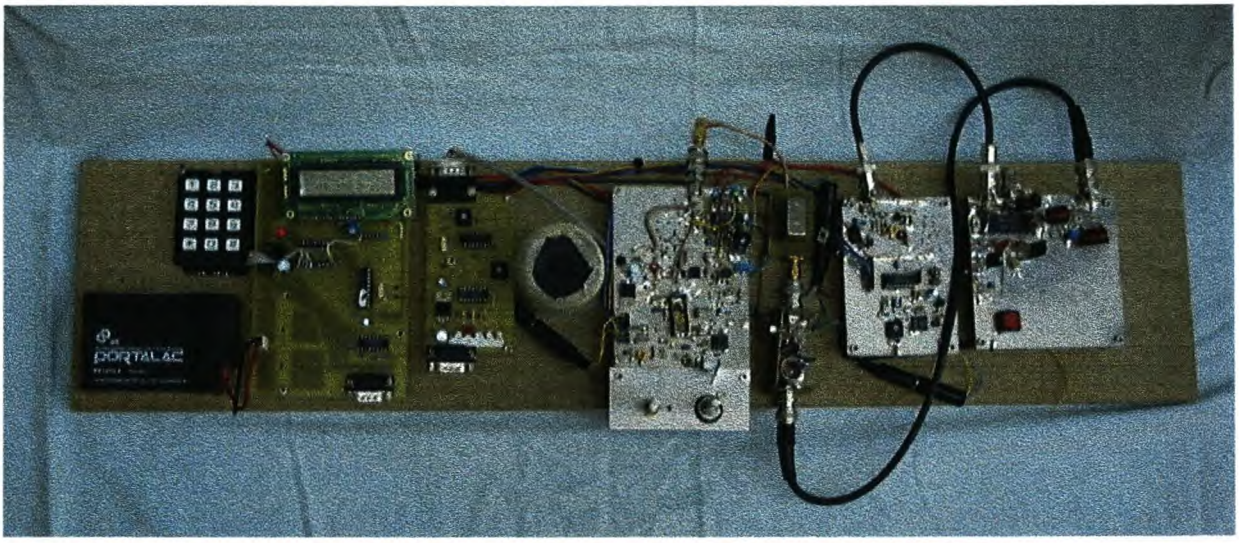

Figure 1-2 Complete Breadbord Field Station

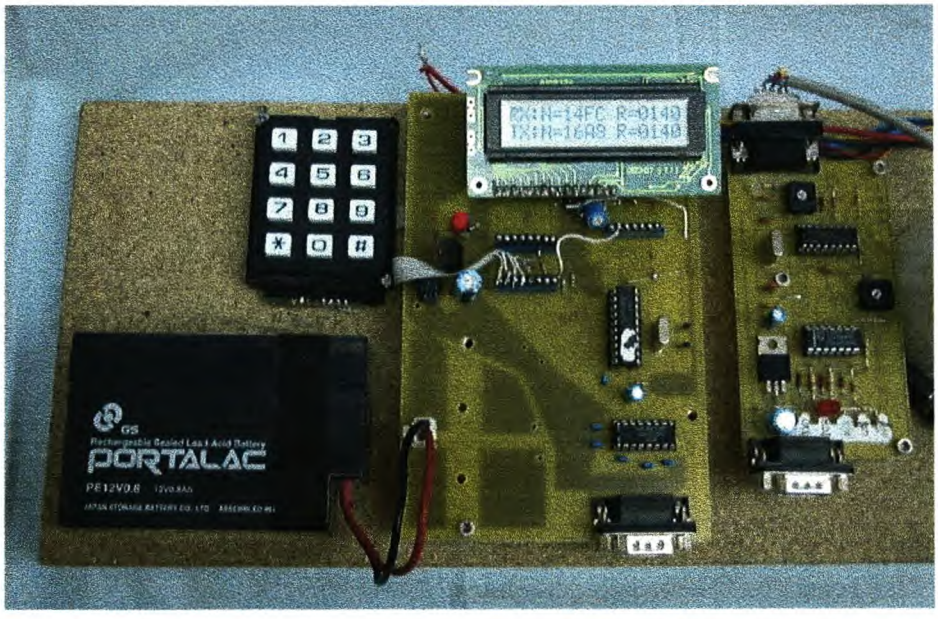

Figure 1-3 Control and modem circuits

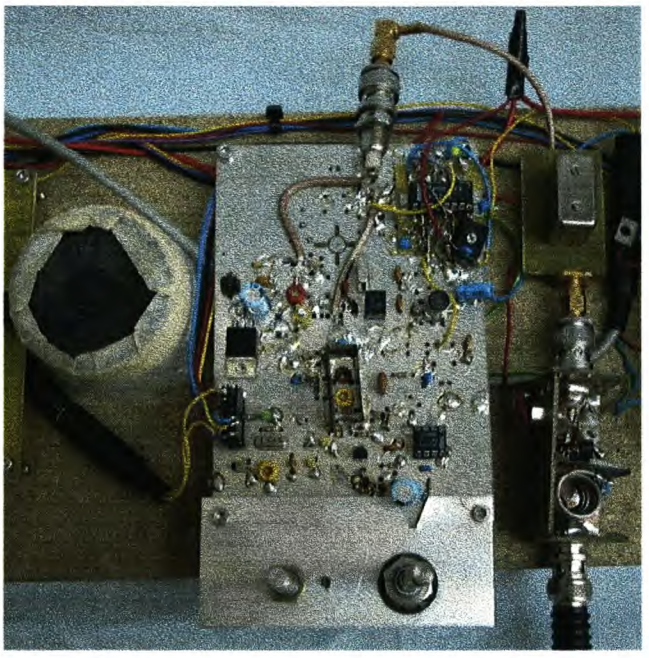

Figure 1-4 Field Station Receiver

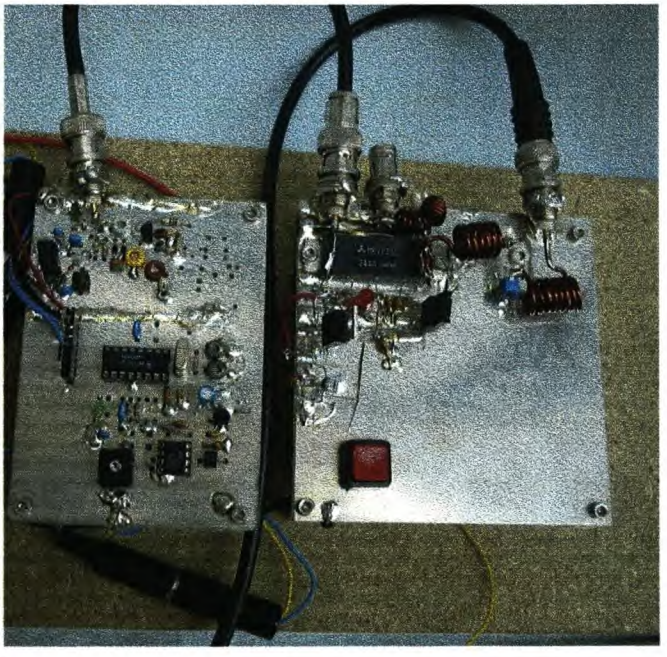

Figure 1-5 Field Station Transmitter

2. Overview of existing satellite communication systems

Mobile satellite communication has become an important concept in the communications industry. Traditionally satellite communication made use of geostationary (GEO) satellites at an altitude of 35800km[1] and with a 0° inclination. The advantages of such systems are that the satellite orbits the earth once every 24h. This means that a specific part of the earth will receive constant coverage by a single satellite. The enormous distances to the geostationary belt of satellites means that complex, high gain antennas are necessary to receive their weak signals (typically at –190dBm). The satellites themselves need to be very complicated and expensive, and it is very expensive to put a satellite in a geostationary orbit. Another problem with this kind of satellite system is that the distances the signal has to travel cause a perceivable delay of about 240ms which is especially annoying for voice communication.

With the advent of newer technologies, it became possible to make use of low earth orbiting (LEO) satellites for communication applications. The lower orbit (typically less than 2000km) means that these satellites orbit the earth in about two hours, which in turn means that a multiple satellite constellation is necessary to offer real-time coverage over the whole surface of the earth as each satellite only covers a footprint with a 3000-4000km radius. This added constellation cost can be cancelled by the fact that these satellites offer global services while generally being less expensive due to economics of scale. In cases where a constellation is not available, the satellite needs to operate in a store and forward mode.

A further advantage of a LEO system is that it makes the competitively priced production of small and easily portable receiving stations possible. These units can be of a similar physical size as commercial cellular phones.

The operations of a few companies in the field of global mobile personal communication systems (GMPCS) will be discussed to try to better understand the systems involved. While the focus of many of the current trends in LEO satellite

systems are towards voice telephony (like those services already offered by ***Iridium*** and ***Globalstar***) the systems are also well suited for data communications. *Table 2-1* gives a brief overview of some of the systems in the LEO satellite field.

Table 2-1 Comparison of LEO communication satellites

Name	Satellites	Altitude	Frequency	Data BW	Date operational
Globalstar	48	1414	L-Band (u) S-Band (d) C-band (u/d)	9.6kbs	Oct 1999
Iridium	66	780	L-Band (u/d) Ka-Band (u/d) Ka-Band (cross)	2.4kbs (1999) 9.6kbs (2000)	Dec 1998
Teledesic	288	695-705 km	Ka (u/d)	64Mbs (d) 2Mbs (u)	2003
Orbcomm	36	825	VHF (u/d) UHF (d)	2.4kbs (u) 4.8kbs (d)	Jun 1998
SUNSAT	1	655-850 km	VHF (u/d), UHF (u/d) L-Band (u) S-Band (d)	1.2/9.6kbs 1.2/9.6kbs 2Mbs 40Mbs	Feb 1999

2.1. GLOBALSTAR[2]

Globalstar lays claim to the fact that the first telephone call by LEO satellite was made through their system. By using code division multiple access (CDMA) technology the company aims to provide a high quality voice service while making efficient use of the frequency spectrum.

The 48 satellites that form the ***Globalstar*** constellation in eight orbital planes will use the design philosophy of placing the most important system technology on the ground. The satellites will act as "bend pipe receivers" that relay a user signal to a system ground station while performing minimal processing on such a signal. This means that new technology trends can more easily be applied to the system, as upgrades need only be done on the ground segment. The mass of each satellite is 450 kg with a total transponder RF power output of 1kW. The satellites are designed for an expected lifetime of 7 years.

The ground segment of the ***Globalstar*** system is made up out of several gateway earth stations around the world. These gateways divert a received call from a satellite through the public switched telephone network (PSTN) and/or cellular network. A feature for areas that have coverage by cellular networks is that the ***Globalstar*** handset is dual mode, enabling it to operate as a normal cellular telephone in such areas. Provision is also made for fixed satellite telephone booths to bring global communications to under-serviced parts of the world.

2.2. IRIDIUM[3]

This company was named after the element with 77 protons because of the initial constellation plan of 77 satellites. When the number of satellites was reduced to 66, the name remained. The 66 satellites forming the ***Iridium*** constellation are more complicated than those of other systems due to a different design philosophy of putting the latest technology in space. The ***Iridium*** system will employ a combination of Frequency Division Multiple Access (FDMA) and Time Division Multiple Access (TDMA). The satellites will aim to deploy virtual "cellular towers" in the sky and to that extent will be cross-linked to one another.

Like ***Globalstar*** the ***Iridium*** telephones will also be dual mode, enabling the use of the satellite- or terrestrial cellular systems, but additionally alphanumeric satellite pager units will also be supported. All of the ***Iridium*** services will be available on board commercial aeroplanes.

2.3. TELEDESIC[4]

The brainchild of (amongst others) Microsoft chairman Bill Gates, will aim to be a complete "Internet in the sky" solution to the problems of parts of the earth that suffer due to lack of landline communication services. The system aims to offer bandwidths comparable to that of optical fibers over radio frequency satellite links early in the next millennium. The deployment of the ***Teledesic*** network will depend somewhat on the success of the ***Iridium*** network. ***Motorola,*** the prime satellite contractor for ***Teledesic***, plans to use the lessons learned in their voice network to launch the ***Teledesic*** constellation in less than a year.

A lot of the news regarding ***Teledesic*** has been due to the company's quest to open new parts of the frequency spectrum for use by LEO satellite systems at international

regulatory authorities. In the process the ***Teledesic*** has secured 500MHz of bandwidth in the new K frequency bands between 18 and 29GHz. At present ***Teledesic*** has formed partnerships with all its main opposition, and the company is leading the way in wideband LEO data communications.

2.4. ORBCOMM[5]

ORBCOMM focus their activities on cost effective data communications. Their pricing system is designed to make short messages of typically less than 100 bytes the most cost-effective proposition for users. The main applications for this system are therefore monitoring of assets and the sending and receiving of short e-mail messages. The operation of the complete system can be seen in *Figure 2-1.*

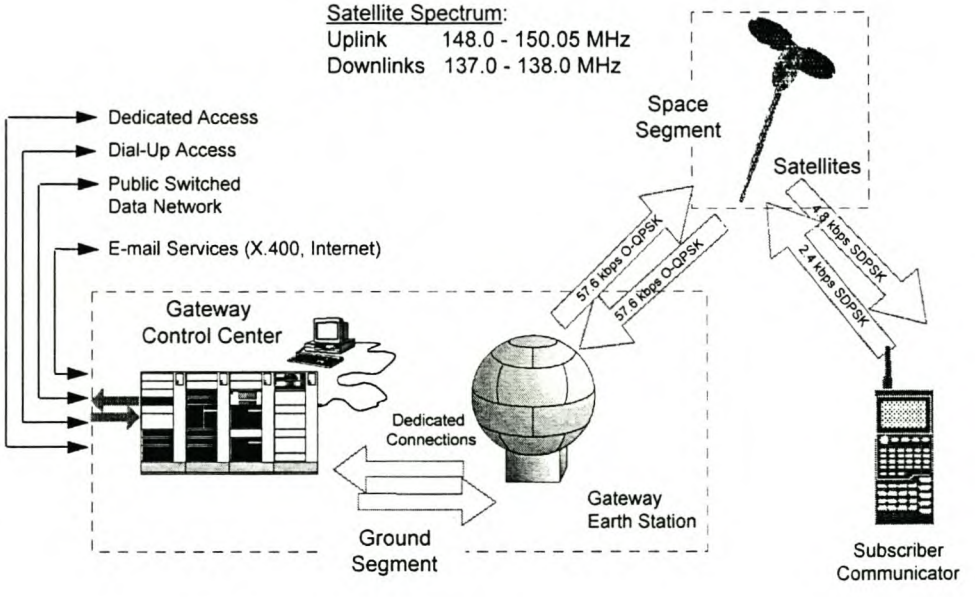

Figure 2-1 ORBCOMM System operation [5]

A unique feature of this system is its use of the frequency spectrum graphically shown in *Figure 2-1* and summarised in *Table 2-2.*

Table 2-2 Frequency use of the ORBCOMM system

Path	Frequency MHz]	Channels	Modulation	Data rate
User → Sat	148-150.5	6	SDQPSK	2.4kbs
Sat → User	137-138	12	SDQPSK	4.8kbs
Gateway → Sat	148-150.5	1	OQPSK	57.6kbs
Sat → Gateway	137-138	1	OQPSK in TDMA	57.6kbs
UHF Beacon	400.1	1		

A very important result of the use of the very high frequency (VHF) part of the spectrum is that the whole system could be designed to use relatively low cost components. For instance, low cost and simple antennas could be used, and development costs is also lower than at higher frequencies.

Special care had to be taken to be able to operate in an environment full of frequency sources generated by land mobile communication systems. To be able to do this a special protocol called the dynamic channel activity assignment system or DCAAS has been developed for the user to satellite uplink. The system makes use of a scanning receiver on board the satellite to continuously measure the interference power across the band. The satellite then assigns the users to frequency channels with the lowest amount of interference. The whole process is repeated every 5 seconds during the time of communications and gives very good results allowing the ***ORBCOMM*** system to make effective use of their allotted frequency spectrum.

The operations of the ***ORBCOMM*** company can be divided into three sections: the space segment, the ground segment, and the user segment.

2.4.1. The Space Segment

The space segment consists of 36 satellites (the company has licences for 48) positioned in such a manner that the whole earth will receive coverage on a near real-time basis, as is shown in *Figure 2-2*. Of these 26 have already been launched at the end of 1998, enabling the company to pursue viable commercial operation.

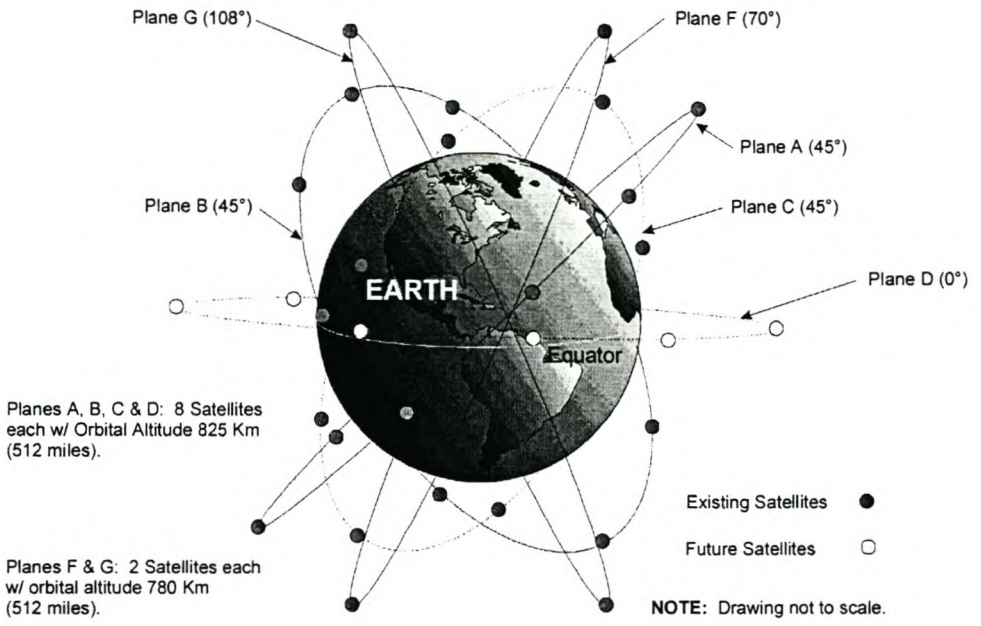

Figure 2-2 ORBCOMM constellation [5]

As can be seen, the earth will be covered by satellites in six orbital planes each designated by a letter of the alphabet. Planes A-D will orbit the earth at an altitude of 825km and the polar crossing planes F and G will have an altitude of 780km.

The satellites used are ***ORBITAL MICROSATS***^{TM} as can be seen in *Figure 2-3.*

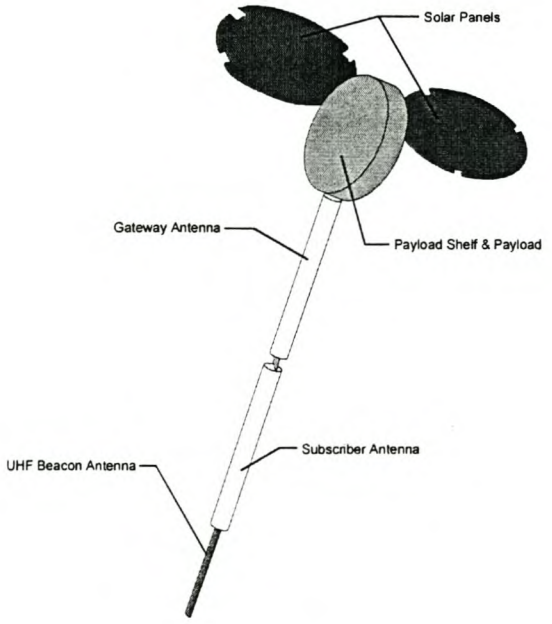

Figure 2-3 ORBITAL MICROSAT in operational mode [5]

The ***ORBCOMM*** satellites weight 43kg and in their folded state they form a disk that measures 1m in diameter and 16 cm in height. In its operational mode the solar panels unfold to give the satellite a width of 2.2m and the various communication antennas extend on a boom to a length of 4m.

A 3-axis magnetometer is also situated on the boom and this is used together with the on board Global-positioning system (GPS) receiver to calculate the position of the satellite. The on board Altitude control system (ACS) uses 3-axis magnetic control to keep the solar panels pointed to the sun and the antennas to the earth. Pressurised gas is used to perform braking when the satellites have drifted in the correct orbital position after launch.

The communication payload of the satellite includes a subscriber transmitter with a maximum capability of 40W, and 7 subscriber receivers. Of these, six are used for communicating with the subscribers and one is employed by the DCAAS. This receiver scans the uplink band with a resolution of 2.5kHz in less than 5 seconds. A 5W-gateway transmitter is used to transmit signals from the satellite to the gateway earth station. These signals transmit digital data at 57.6kbs using offset quadrature phase shift keying (OQPSK) in a TDMA format. The gateway receiver forms the reverse path.

A highly stable 1W ultra high frequency (UHF) beacon transmitter at 400.1MHz is also part of the satellite. This transmitter is included for future development of the subscriber communicators. The various actions of the satellite are controlled by a distributed network computer consisting of several microprocessors.

2.4.2. The Ground Segment

The ***ORBCOMM*** ground system is made up of satellite gateways in several countries. A gateway consists out of a gateway earth station (GES) and a gateway control centre (GCC). The GES has the necessary radio equipment to communicate with the satellites and is situated in a location favourable to space communication. The GCC controls the up- and downloading of messages from the satellites. Messages are delivered or received via the Internet to the users of the system.

The global network control centre (GNCC) of the ***ORBCOMM*** network is situated in Dulles, Virginia in North America and controls the overall flow of messages through the system.

2.4.3. The user Segment

Ground users of the ***ORBCOMM*** system are called subscribers and the units they use to communicate with the satellites are called subscriber communicators or SC's. These SC's are manufactured by various companies and the different models have different features.

A SC has the necessary radios and modems to communicate with an ***ORBCOMM*** satellite. Position reporting is also possible by receiving accurate information of the satellite's time, position and velocity (Generated by the onboard global positioning system (GPS) receiver). This data is used together with the Doppler information from the received downlink to calculate the SC position. This method gives position to an accuracy of better than $1km^2$ and it is envisioned that the UHF beacon may be used in the future to improve this accuracy.

Some SC's also have a small GPS receiver onboard that can be used to determine the position of the user more accurately. Besides this features that makes the ***ORBCOMM*** system very attractive to low cost vehicle tracking, it can also be used to remotely monitor and/or control virtually any system. To this end, a SC can be connected to either a computer or a microcontroller with sensors and/or actuators connected to it. Using a computer and the correct software it is also possible to send short e-mail messages through the system.

2.5. SUNSAT[6]

Although the Stellenbosch UNiversity SATellite (***SUNSAT***) is a single experimental satellite and seems a far cry from the commercial constellations, it serves to prove South African capabilities in the field of satellite engineering.

Work on ***SUNSAT*** started in 1992. Since then more than 70 engineering students have worked on different parts of the project. The satellite was successfully launched

in a near-sun-synchronous polar orbit (96.48° inclination) on board a ***BOEING Delta II*** rocket on February 23, 1999.

2.5.1. Overview

SUNSAT is a highly advanced microsatellite carrying various subsystems including school experiments, computer systems, a memory board, a high-resolution three band optical imager, a GPS payload for ***NASA*** and a variety of communication systems. The different subsystems of the satellite are organised in trays that are stacked on top of each other to form the square main satellite body.

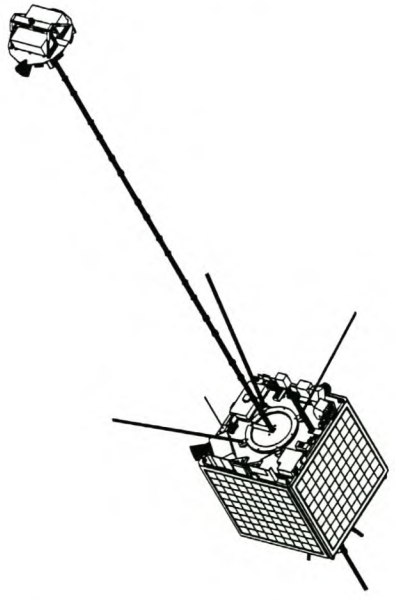

Figure 2-4 The SUNSAT microsatellite

A deployable boom separates the main satellite body and the tipmass. The tipmass houses a star camera, a magnetometer and laser reflectors, and helps to passively stabilise the satellite. Further orientation is done by means of 4 reaction wheels and 6 magnetotorquers. The satellite draws power from two battery packs that are charged by four solar panels situated on the sides of the satellite.

A telecommand system controls the configuration of the satellite while a telemetry system relays information on the state of the different subsystems on board to the groundstation.

2.5.2. The Sunsat communication system

The communication systems carried by the satellite include a VHF transceiver, UHF transceiver, L-Band receiver and S-Band transmitter. All of these different systems have been designed to operate independently to make the satellite more reliable. The VHF and UHF transceivers form the main communication path between the satellite and the earth and operate in the Amateur Radio frequency bands. This means that only an Amateur Radio licence is required to experiment with ***SUNSAT***. The microwave frequency bands are intended for wideband data communications, mainly to service the main imager. In the operation of the mobile field station the VHF transceivers on the satellite will be utilised.

2.5.3. The SUNSAT VHF communication system

A block diagram of the VHF communication system[6,7,8] is shown in *Figure 2-5*.

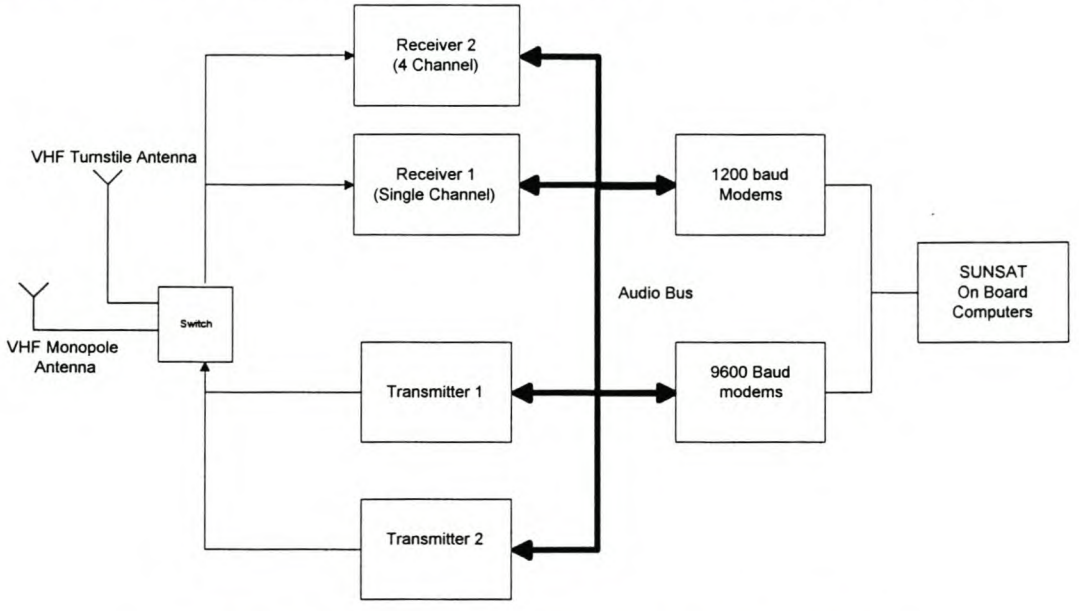

Figure 2-5 Sunsat VHF receiver block diagram

2.5.3.1. Antennas[9]

The system is fed from two external antennas made from thin beryllium copper tape. The VHF monopole antenna is situated on the bottom while the four elements of the VHF turnstile antennas are located on the top of the satellite. The two antennas are both largely omnidirectional, and therefore have little or no gain. The turnstile antennas are right-hand circularly polarised.

2.5.3.2. Receivers[6,7,8]

Two independent receivers form part of the system. The receivers are both double-conversion superheterodyne receivers that can be switched to use either crystal controlled oscillators or a frequency synthesiser as their first local oscillator (LO). In each case the two crystal controlled oscillators have been included in the design to enable ***SUNSAT*** to receive signals both in the amateur frequency band (144 to 146MHz) and the commercial mobile satellite frequency band (148 to 150.05MHz). The first receiver is a single channel receiver, which acts as the default for receiving telecommands to the satellite. The receiver also has automatic frequency control (AFC) added to compensate for up to 3.5kHz of Doppler frequency shift in the received signals.

The second receiver has four second conversion IF stages, and can simultaneously receive four adjacent channels for demodulation. Three of the four second stages have automatic frequency control added to compensate for the Doppler frequency shift in the received signals. The fourth channel has no AFC to permit more accurate Doppler frequency measurements.

2.5.3.3. Transmitters

The two identical narrowband VHF FM transmitters on the satellite are fed from the audio bus or a variety of modems. These audio-band signals are used to modulate a 20MHz oscillator, which is mixed either with crystal based oscillators or a frequency synthesiser. The output signal is connected to two power amplifier modules. The output power of these modules can be switched between one and five watts.

2.5.3.4. Modems

Two types of data modems can be interconnected to send data to and from the satellite. The most basic type uses audio frequency shift keying (AFSK) to send and receive digital data up to a rate of 1200baud. The second is G3RUH compatible modem developed by James Miller to send and receive data at a data rate of 9600baud. Only the 1200baud AFSK modem will be utilised for the field station.

2.5.3.5. On Board Computers (OBC's)

SUNSAT has two OBC's. The main computer has an 80188 processor and is responsible for the control of most of the main functions of the satellite. The

secondary computer has an 80386 processor and supplies the backup for the first computer. It will also be used for the processing of computationally intensive algorithms. Both computers are connected to a Ram tray, which has 64Mb of storage space and can be completely reprogrammed from the ground.

2.6. References

1. Barry Millar, *Satellites free the mobile phone*, IEEE Spectrum, March 1998-09-28
2. Globalstar Web Site, http://www.globalstar.com
3. Iridium Web Site, http://www.iridium.com
4. Teledesic Web Site, http://www.teledesic.com
5. ORBCOMM Global L.P., *ORBCOMM System Overview*, ORBCOMM Document A80TD0008 – Revision B
6. Mostert, Schoonwinkel & Milne, *Pre-flight performance of the communication payloads on SUNSAT, South Africa's first microsatellite*, 8th Bi-annual Conference & Exhibition on Telecommunications in Southern Africa, 1997
7. P van der Westhuizen, *A VHF and UHF receiver for the SUNSAT microsatellite* (Afrikaans), Thesis for masters in Engineering (Electronic) at University of Stellenbosch, January 1994
8. J.J Roux, *The design of a VHF and UHF Receiver Front-end for the SUNSAT micro satellite*, Thesis for masters in Engineering (Electronic) at University of Stellenbosch, January 1998
9. N.J.J Bornman, *Design of an antenna system for the VHF communication link of the SUNSAT micro satellite*, Thesis for masters in Engineering (Electronic) at University of Stellenbosch, November 1993

3. The LEO Satellite communication Environment

Electromagnetic waves that travel through any medium are influenced by such a medium. This is also true for radio waves travelling between a LEO satellite and the earth and it is therefore essential to understand the influence of all the relevant atmospheric phenomena on a radio link to be able to design a functional field station.

3.1. Satellite Orbit

Satellite orbits are described by means of the Keplerian elements. These elements describe the shape, size and orientation of the orbit at a specific time. Various software packages exist that use these elements to do orbit predictions and they can be very useful to determine when the satellite is above the viewer's horizon.

For a satellite in an elliptical orbit, the distance closest to earth is known as the perigee, and the distance farthest from earth is known as the apogee.

3.1.1. Slant Range

The distance between the satellite and the field station on the surface of the earth is known as the slant range of the satellite. The trigonometric relation between the earth, satellite altitude and the position of the ground station is shown in *Figure 3-1*.

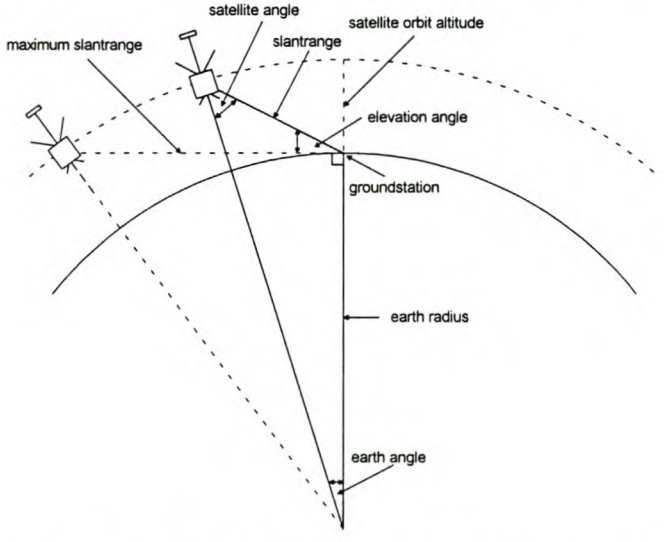

Figure 3-1 Determining the Satellite Slant range[4]

Electromagnetic waves of VHF and higher frequencies travel more or less in a straight path. The angle between the earth's horizon (below which the satellite cannot be seen) and the satellite is known as the elevation angle (A_{El}). The two other important angles of the triangle are known as the satellite angle (A_{Sat}) and the earth angle (A_{Earth}). The relation between these angles and the distances involved can be found from the sine law as follows:

$$\frac{\sin(A_{El}+90°)}{R_{earth}+H_{Sat}} = \frac{\sin(A_{Sat})}{R_{Earth}} = \frac{\sin(A_{Earth})}{Slant\_Range}$$

In this equation, the earth's radius (R_{earth}) is taken as 6378.4km[6]. The satellite altitude (H_{Sat}) at perigee and apogee will be used to calculate the minimum and maximum slant range. The values of 650 and 850km will be used respectively representing the orbit of the ***SUNSAT*** microsatellite. By assuming an elevation angle between 0° and 180°, equating the angles of the triangle to 180° and using the above equation, the slant range can be determined for different elevation angles. This is done in a ***MATLAB*** routine given in *Appendix A* and the results plotted in *Figure 3-2*. The solid line represents the slant range with the satellite at apogee and the dotted line the case with the satellite at perigee.

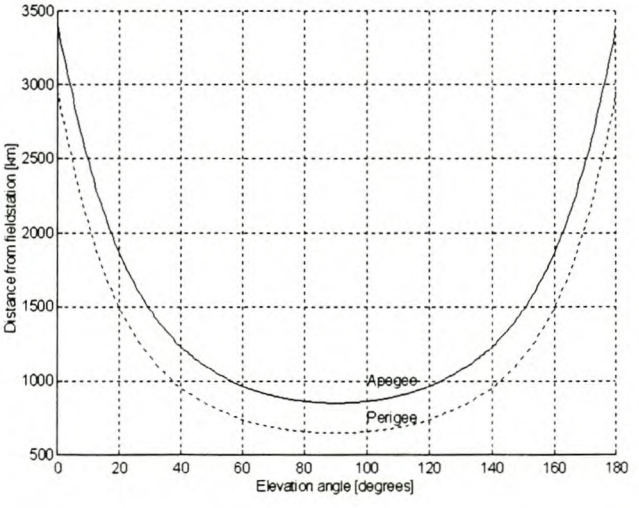

Figure 3-2 Slant range of satellite

The distance covered by the electromagnetic waves through the bottom 100km of the atmosphere is important in calculating the losses that such waves will undergo as will be discussed in *Section 3.3.* This distance can be calculated by using the above method and assuming a satellite orbit of 100km. This has been done, and the results are plotted in Figure 3-3.

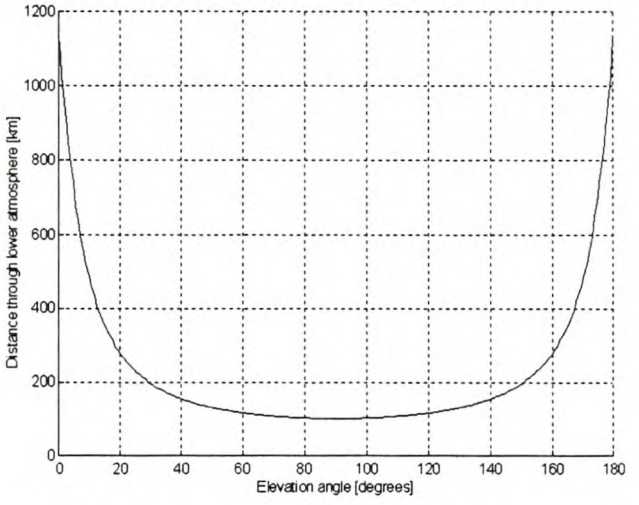

Figure 3-3 Slant range through lower Atmosphere

The satellite angle determines which part of the gain pattern of the transmitting antenna of the satellite to use for calculations. This angle is plotted for a direct overhead pass of the satellite at perigee in Figure 3-4.

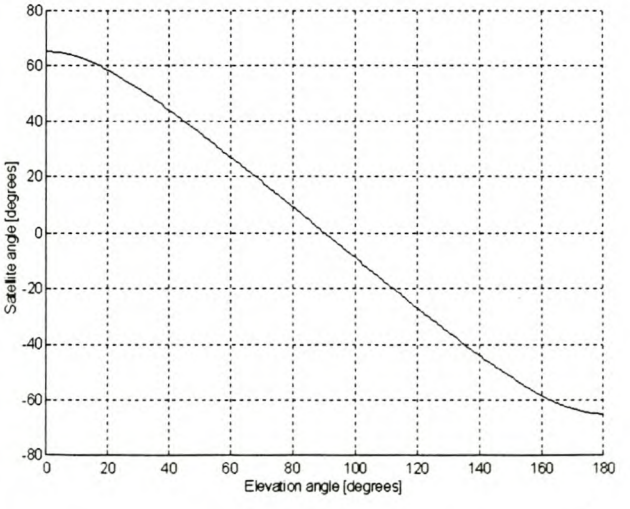

Figure 3-4 Satellite angle at perigee

As can be seen with the satellite at perigee the part of the radiation pattern between -69° and 69° will be used. When the satellite is at apogee only the part of the pattern between -61° and 61° will be used.

3.1.2. Satellite speed and pass Time

The time it takes for the satellite to travel from one horizon to the other is determined by the speed at which the satellite travels through space. This time can be calculated if it is remembered that a satellite will orbit the earth at a distance where the gravitational force between the satellite and the earth is in balance with the centrifugal force on the satellite caused by its motion. These restraints cause the speed of satellites in a circular orbit to be given by the following equation [2,6]:

$$v_{sat} = \sqrt{\frac{GM_{earth}}{R_{earth} + H_{sat}}}$$

In this equation, G represents the universal gravitational constant, M_{earth} the mass of the earth, R_{earth} the radius of the earth, and H_{sat} the height of the satellite above the surface of the earth. In this manner it can be calculated that the speed of a satellite (with its height varying between 650km and 850km) will vary between 7.6km/s and 7.4km/s. This in turn means that the satellite will take between 102 and 97 minutes to orbit the earth.

If *Figure 3-1* is considered again it can be seen that this is the time that it will take the earth angle to change from 0° to 360°. To calculate the time the satellite is above the horizon, the following relation can be used:

$$\frac{T_{pass}}{T_{orbit}} = \frac{2*\phi}{360°}$$

In this equation, Ø represents the earth angle when the satellite starts to rise above the horizon. This means that the total direct overhead pass time will be 15.9 minutes at apogee, and 12.8 minutes at perigee.

3.2. Path Loss (Free Space Attenuation)

The amount of attenuation an electromagnetic wave will undergo in free space can be determined by modelling the transmitting signal as a point source in the middle of a

sphere. The power density at a distance d away from a source transmitting P_t *[W]* is given by[1,2,3]:

$$\rho_r = \frac{P_t}{4\pi d^2}\left[W/m^2\right]$$

The power received by a receiving antenna is given by the product of the power density and the effective antenna area A_e. For an isotropic antenna this area is given by:

$$A_e = \frac{\lambda^2}{4\pi}\left[m^2\right]$$

Combining the above two equations lead to the following equation path loss of a signal received with an isotropic antenna:

$$L_{FS} = 10\log\left(\frac{4\pi d}{\lambda}\right)^2$$

In this equation λ represents the wavelength of the radio waves. The path loss for a VHF signal travelling through ***SUNSAT's*** slant range has been calculated with the ***MATLAB*** code given in *Appendix A* and is represented in *Figure 3-5*.

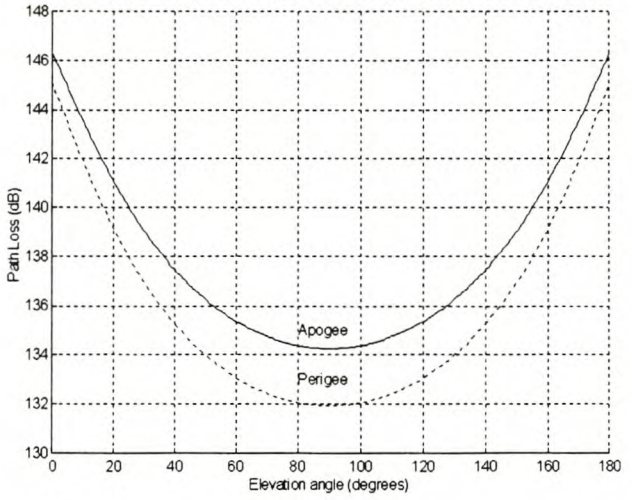

Figure 3-5 Path loss

3.3. Atmospheric absorption

Gasses like oxygen and uncondensed water vapour common to the bottom part of the atmosphere absorb a part of the energy of electromagnetic signals travelling through this layer. The amount of energy absorbed depends on the frequency used, the density of the gasses and the path length. Previous studies[1,4] used the data given in Collin[3]

which states that this absorption leads to an attenuation of about 0.005dB for every kilometre travelled. These studies then used a distance of 100km for the height of the atmosphere and assumed a uniform atmospheric density in this layer. The distance that the electromagnetic waves have to travel through this layer was calculated in *Section3.1.1*. This distance varies between 100km and 1133km, giving rise to the presumed absorption loss plotted *Figure 3-6*.

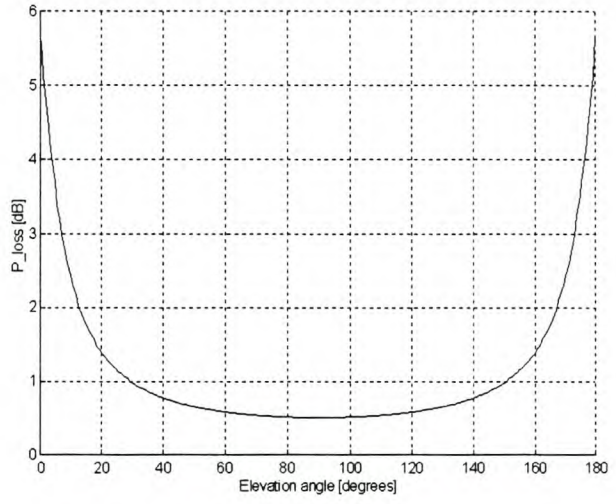

Figure 3-6 Atmospheric absorption loss

The values for absorption losses seem very high, with more than 1dB of absorption loss at elevation angles lower than 30°. This can be explained if it is remembered that the data used were intended for point to point links on the surface of the earth, and therefore does not take the lower air pressure at higher altitudes into account. The method is therefore overestimating the absorption loss and will only be used as a worst case approximation.

3.4. Ground reflection

When the satellite is on the horizon (low elevation angle) a situation may arise where ground reflection of the signal causes multipath effects. In this case the transmitted signal reaches the receiver via the direct line-of-sight path, as well as a path reflected from the surface of the earth. These multiple signals interfere with each other and can momentarily attenuate or amplify the received signal.

According to Collin[3] an appropriate gain factor for the signal can be found for the lowest 5 degrees of elevation. This equation (which assumes a flat earth) is given below:

$$F_{dB} = 10\log_{10}\left(2*\left|\sin\left(\frac{2\Pi h}{\lambda}*\tan(elevation)\right)\right|\right)$$

In this equation h represents the height of the antenna above the ground, and λ refers to the wavelength of the signal. The gain factor was computed for antenna heights of 1,2 and 5 metres and the result is given in *Figure 3-7.*

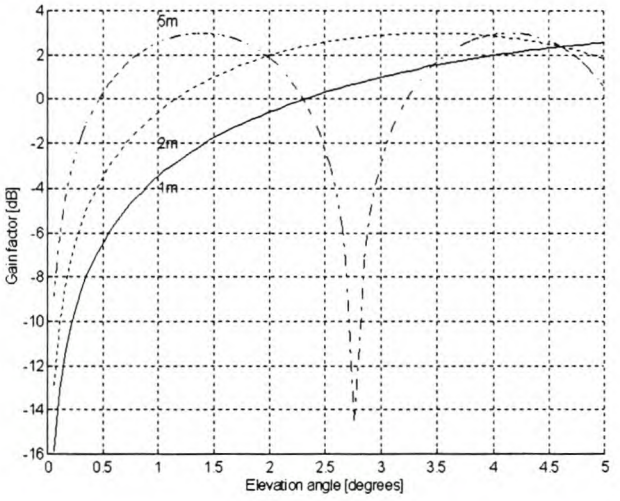

Figure 3-7 Ground reflection loss

As can be seen from the graph there are some special circumstances where the result of ground reflection can be a net gain. This is the case when positive interference takes place between the main signal and its reflected counterpart accounting for the maximum of 2dB gain visible on the plot.

It should be stated that the above calculation only serves to give an indication of the effect of ground reflection. The true signal strength is also polarisation dependent and vary significantly with the movements of a mobile field station.

3.5. Antenna gain patterns

To complete the link budget between the satellite and the earth it is necessary to include the gain patterns of both the transmitting and the receiving antennas.

The effect of the transmitting turnstile satellite antennas for different elevation angles of a direct overhead pass of a stabilised ***SUNSAT*** has been computed and is

represented in *Figure 3-8.* This gain pattern is computed for a satellite angle varying between -69° and 69° as was computed in *Section 3.1.1.*

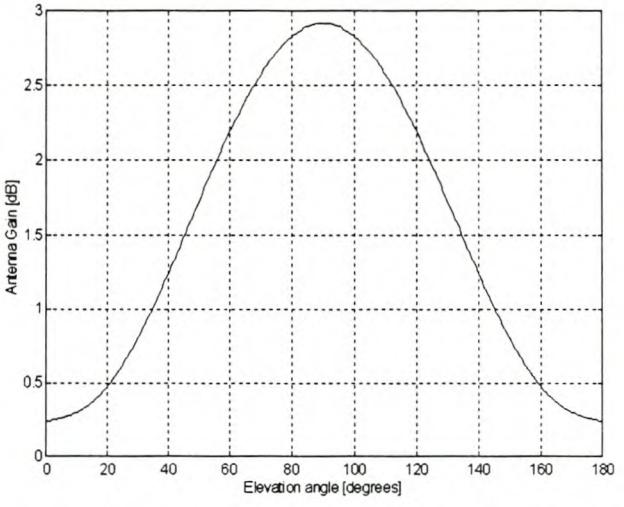

Figure 3-8 SUNSAT transmitting antenna gain patterns

If it is assumed that the receiving antenna will be a monopole, a gain pattern like the one given in *Figure 3-9* will be typical[7].

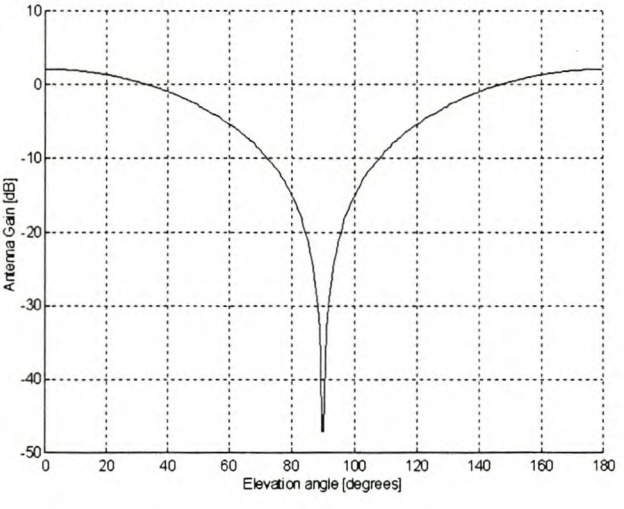

Figure 3-9 Receiving Monopole antenna gain pattern

3.6. Faraday rotation

The wavefront of a signal travelling through the ionosphere is rotated, causing changes in its polarisation. The rotation rate depends on the frequency (the rotation is reduced at higher frequencies), the strength and orientation of the earth's magnetic field at a specific point , ionic densities and the path length[2]. For a VHF signal the

plane will rotate about 4 to 5 times at low elevation signals, and about 1.4 times for an elevation angle of 90°.

When a signal with a rotating wavefront is received with a linear antenna, variable fading caused by polarisation mismatch may be experienced. To alleviate the problem, the receiving and transmitting antennas should be circularly polarised. If this is not possible and only one of the two link antennas the can be made circularly polarised, a constant 3dB reduction in signal strength will be experienced.

3.7. Doppler shift

A satellite will always be in motion relative to a fixed (or relative slowly moving) ground station. This means the relative velocity between these two points will also change bringing about a change in frequency owing to the phenomena called the Doppler effect. This change in frequency is given by[2,4]:

$$f_{Doppler} = f_{operating} \frac{v_{relative}}{c}$$

In the above equation $v_{relative}$ represents the relative velocity between the satellite and the groundstation, and c represents the speed of light in a vacuum.

As was stated in *Section 3.1.2* the speed at which the satellite will orbit the earth will vary between 7.4 and 7.6km/s. To determine the relative speed between the satellite and the stationary ground station, the trigonometric relations *Figure 3-1* is used once again. The component of the speed vector of the satellite between the satellite and the ground station is given by:

$$v_{rel} = v_{sat} \cos(90° - A_{Sat})$$

When this values is computed for the different elevation angles and substituted in the equation the results of *Figure 3-10* are obtained.

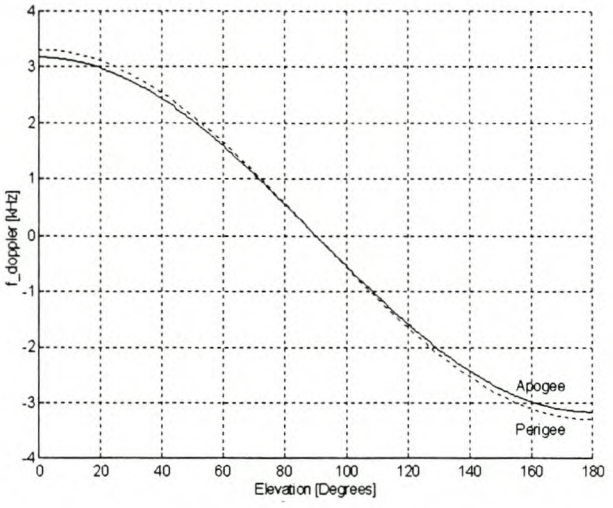

Figure 3-10 Doppler frequency shift

The result of Doppler shift is a maximum frequency shift of about 3kHz at a frequency of 145MHz. This effect is proportional to frequency, giving a maximum shift of about 10kHz at UHF.

3.8. Noise

Several sources of unwanted signals or noise exist that degrade the quality of the wanted signal. The receiver itself forms one of these sources because of the inherent noise generated in the components of the receiver. The effect of internal noise will be discussed in *Chapter 4* while this section will investigate the effect of noise external to the receiver.

Noise received by the antenna of the satellite ground station can be generated by both natural and man-made sources[8] and the amount of average noise power that can be received by such an antenna is given by:

$$N = kTB$$

In this equation N represents the average noise power in watts, T the noise temperature in Kelvin and B the bandwidth of the measurement in Hz The constant k represents Boltzman's constant with a value of $13.8*10^{-24}$ $J.K^{-1}$.

The magnitude of typical noise sources is shown in *Figure 3-11*[10] and will be discussed in the following sections.

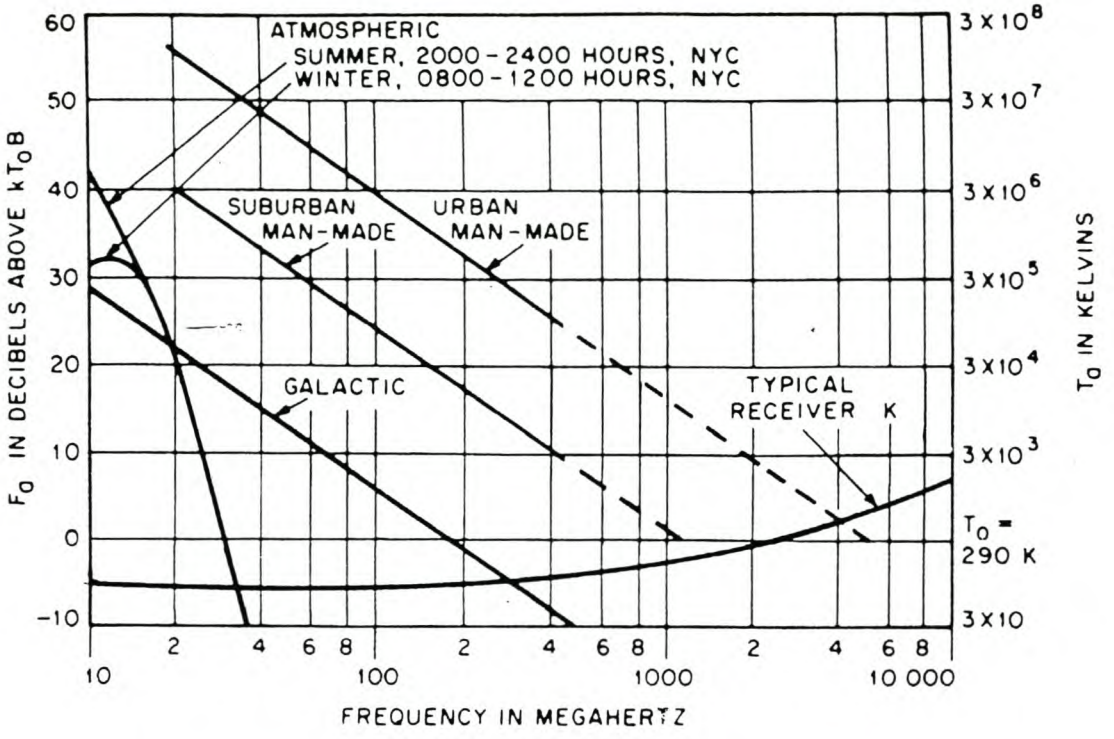

Figure 3-11 Typical Noise Sources (Received with Omnidirectional antenna)[10]

It can be observed that emissions from most noise sources decrease with an increase in frequency, or the distance from urban centres.

3.8.1. Natural noise

Atmospheric noise is mostly generated by lightning and electrical storms, and is therefore a largely localised phenomenon. Its occurrence is difficult to predict, but can generally be ignored for frequencies above 50MHz.

Galactic noise is caused by noise sources such as the sun or other stars. A receiver connected omnidirectional antenna following a satellite across the sky will experience an increase in received noise when a large group of such stars is in its main lobe. The effect of galactic noise is to raise the receiver noise floor by about 3dB at VHF frequencies as can be seen in *Figure 3-11*. This value gives rise to an ambient noise level of about 580°K.

Thermal noise generated by the components of the receiver will also degrade the received signal, but proper design of a low-noise receiver can alleviate this problem.

3.8.2. Man-made noise

In some instances it is possible to suppress man-made noise that is degrading the received signal of a satellite field station. The unwanted emissions caused by ignition systems, electric motors or computers are examples of this. Controlling such emissions can become more troublesome, and sometimes impossible for a mobile field station of which the movement cannot be determined.

Should high levels of radiation cause the field station to momentarily loose contact with the satellite, a packet type data protocol will permit effective data transfer by retransmitting only a part of the message instead of restarting the transmission.

3.9. Other lesser phenomena

The following effects of atmospheric phenomena on electromagnetic waves are included for the sake of completeness. Their influence is either so small that it can be ignored at the chosen frequency, or their occurrence is so unpredictable that it is not possible to do anything to combat their effect other than to specify a sufficient safety margin in the link budget.

3.9.1. Refraction

The path of the electromagnetic waves is bent as it passes through the ionosphere, but this is not significant at VHF. For the sake of the above calculations it is assumed that the radio waves travel in a straight path.[8]

3.9.2. Diffraction[2,8]

The effect of buildings, trees or mountains that block the path of electromagnetic waves is to attenuate the received signal strength. It is virtually impossible to predict this effect due to the random nature of the field station's movements. To ensure minimal effect there should be an unobstructed signal path to the satellite. This is also an operating factor for the mobile satellite telephone systems discussed in *Chapter 2*, and restricts coverage in some areas like city centres.

3.9.3. Spin modulation[2]

The rotating motion of a satellite as it travels through space can sometimes cause the received signal strength to vary periodically. This is especially true on satellites, which have very complex antenna systems with gain patterns that are not omnidirectional in the satellite's spinning axis. Once ***SUNSAT*** is properly stabilised,

its rotational movement should have little influence on the signal strength due to the omnidirectional VHF antennas used.

3.9.4. Sporadic E-fields[2,5,8]

The density of the E-layer of the ionosphere undergoes sporadic changes. Sometimes thin layers of enhanced ionisation can be formed that are dense enough to reflect radio waves with such a frequency that normally would have gone straight through these layers. Although this phenomenon is used to great effect by radio amateurs to "bounce" their signals and therefore communicate over further distances in exceptional circumstances, it is not desirable for satellite communications. The effect is normally more marked at frequencies below 100MHz.

3.9.5. Scintillation[5,8]

This effect describes an arbitrary and sudden change in the amplitude and phase of signals travelling through space and the ionosphere and brought about by ionised plasma. It can especially cause havoc in wideband signals that depend on phase information for modulation. It is not very common over the middle latitudes, which fortunately includes much of the area in which ***SUNSAT*** will be actively used.

3.9.6. Precipitation

Cloud cover, rain, fog and snow can alter both the magnitude and phase of electromagnetic waves, but the effect is only evident at frequencies above 500MHz.

3.10. Combined effect

The effects of the above phenomena can be combined to give the total loss between the satellite and the field station. This figure can then be used to specify the design of the field station transmitter and receiver. The total path loss is computed in *Appendix A* and plotted in *Figure 3-12*

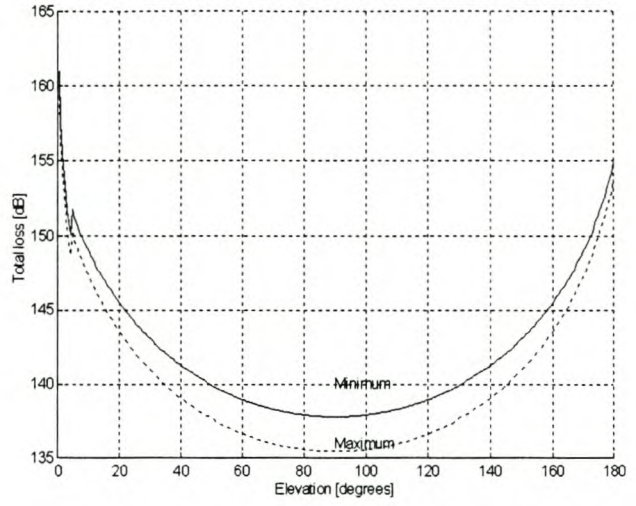

Figure 3-12 Total loss between LEO satellite and ground station

When it is considered that the power transmitted by ***SUNSAT*** can vary between 1W and 5W the received power can be computed by using the following equation:

$$P_{received} = P_{transmitted} + G_{ant\_trans} + G_{ant\_rec} - P_{loss\_tot}$$

The received power was computed for the best (maximum transmitted power and minimum losses) and the worst case (minimum transmitted power and maximum losses) respectively and is shown in *Figure 3-13.* Also included in this figure is a line representing the achieved sensitivity of the ***SUNSAT*** receivers at –120dBm.

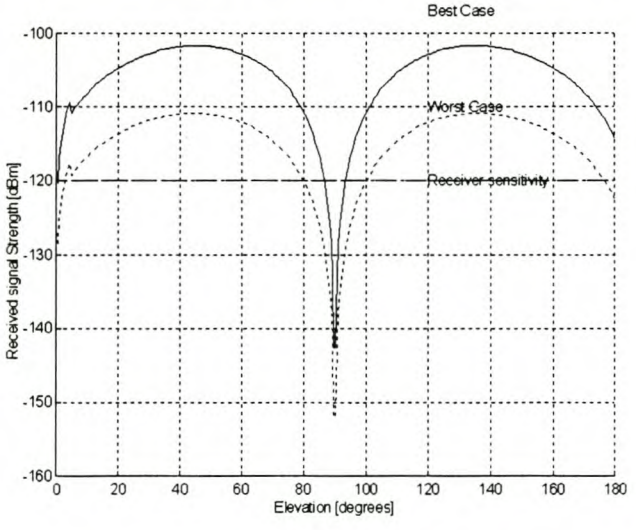

Figure 3-13 Total Received power

The difference between the sensitivity of the receiver and the received signal strength is known as the link margin. A link margin of 10dB gives rise to a link reliability of 90%[9]. A receiver with sufficient sensitivity should therefore be able to receive the high power VHF signals transmitted from ***SUNSAT*** with a 90% link reliability for

90% of the satellite pass using a monopole antenna. It should even be possible to make short contacts with the satellite while it is operating on its minimum output power level, but the percentage of a pass that will be useable for communication with a field station will be less for this scenario.

3.11. References:

1. N.J.J Bornman, *Design of an antenna system for the VHF communication link of the SUNSAT micro satellite*, Thesis for masters in Engineering (Electronic) at University of Stellenbosch, November 1993
2. Martin Davidoff, *The satellite experimenter's handbook - 2nd Edition*, ARRL, 1990
3. Robert E. Collin, *Antennas and radiowave propagation*, Mcgraw-Hill international student edition 1985
4. J.J Roux, *The design of a VHF and UHF Receiver Front-end for the SUNSAT micro satellite,* Thesis for masters in Engineering (Electronic) at University of Stellenbosch, January 1998
5. John Brannegan, *Space radio handbook*, RSGB, 1990
6. Serway, *Physics for scientists and engineers – Third edition*, Sauders College publishing, 1992
7. Ramo, Whinnery & Van Duzer, *Fields and waves in communication electronics*, Johan Wiley and Sons, Third Edition, 1994
8. Hall, Barclay & Hewitt, *Propagation of radiowaves*, The institute of Electrical Engineers, 1996
9. Stephen J. Erst, *Receiving Systems Design*, Artech House Inc, 1985
10. International Telephone and Telegraph Corporation, *Reference data for radio engineers 6th Edition*, Howard W. Sams Co., 1975

4. Conceptual design and specifications

4.1. Choice of Frequency

It was decided to use the VHF part of the spectrum for this project mainly because the VHF transceivers on ***SUNSAT*** were available for experimenting. The VHF frequency spectrum utilised by ***SUNSAT*** is shown graphically in *Figure 4-1*.

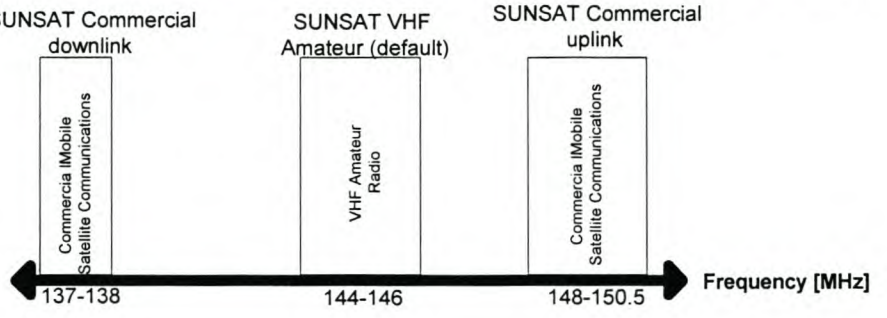

Figure 4-1 VHF Frequency allocatement

For the initial design, the frequency band that is allocated for Amateur Radio use in South Africa will be used (144-146MHz). Should the system be successful a prospective commercial user thereof can go through the process of applying for a licence to use the commercial VHF satellite bands.

Advantages of using VHF frequencies are that the design and construction of the field station are less difficult than at higher frequencies, and that the cost of a VHF field station should be less. An important requirement of a competed system would be that the rate of data throughput should be comparable to that of the commercial systems discussed in *Chapter 2*. The initial objective for the field station is for a data rate of 1200 baud.

Negative aspects of the usage of the VHF bands are that these bands are tightly populated by terrestrial commercial services like paging and mobile radio. The field station will have to be designed to withstand interference from these signal sources and the high ambient noise levels typical at VHF frequencies.

4.2. Choice of modulation scheme and communication protocol

Narrowband frequency modulation (NBFM) with a maximum deviation of 3kHz is a suitable modulation scheme for the relatively low data rate that is required. To supply

the wanted data rate of 1200 baud, audio frequency shift keying (AFSK) modems will be used. These devices send and receive bandwidth limited audio tones across the radio channel to relay digital information.

The communication protocol that is used on board ***SUNSAT*** is oriented towards the amateur radio public. The AX.25 protocol implemented in the software of the satellite is a radio amateur protocol used for packet-type radio communications. A previous study[1] showed that AX25 is not the most effective protocol to use for a store and forward satellite application where multiple groundstations try to access the satellite channel simultaneously. Split channel reservation multiple access (SRMA) is presented as a better alternative. For the initial testing of the field station, experiments will be carried out using the standard AX25 protocol.

4.3. System Block diagram and description

A block diagram of the field station is represented in *Figure 4-2*.

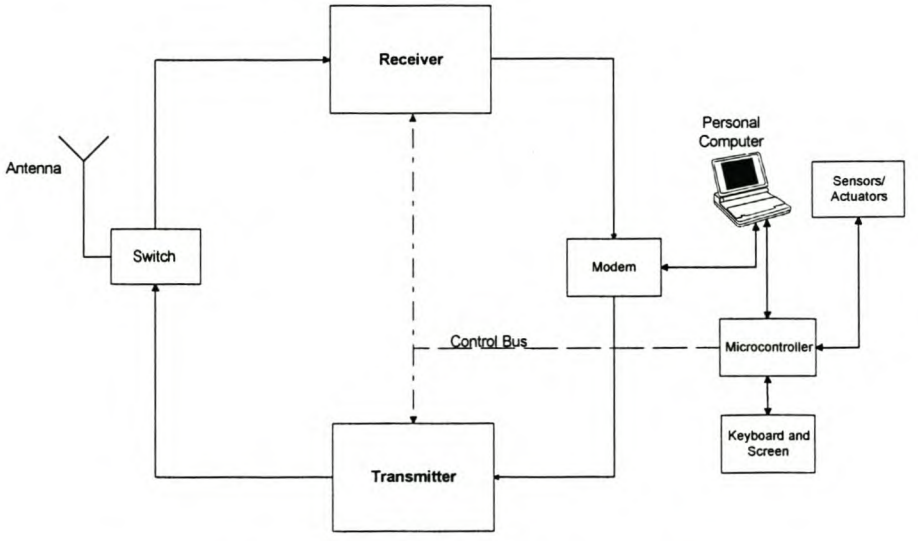

Figure 4-2 Field station Block diagram

The radio frequency (RF) signal that is received at the antenna is fed through a switching system that controls the flow of signals to and from the antenna. The received signal will be demodulated by the receiver and fed to the modem which will convert the audio frequency (AF) signals to discrete digital data that can be fed to the computer. The communication protocol is implemented in the computer.

Data from the computer will be converted to AF signals by the modem and to RF signals by the transmitter. After sufficient amplification to allow it to travel the distance to the satellite, the signal is fed to the antenna for transmission. No reception is possible while transmitting (simplex operation).

Besides controlling the frequencies to which the transmitter and receiver are tuned, the microprocessor has the ability to communicate with a personal computer via a RS232 serial port, to monitor sensors and to control elementary actuators. In this manner, a field station for the needs of a specific customer can easily be developed once the basic system has been designed.

4.4. Proposed Specifications

The proposed specifications have, to a large extend, been modelled on that of the VHF receivers and transmitters on board the ***SUNSAT***[2] microsatellite.

4.4.1. Receiver Specifications

The proposed specifications for the field station receiver are represented in *Table 4-1*. Some of the specifications will be discussed further in the following sections.

Table 4-1 Proposed Receiver Specifications

Frequency	144-146MHz (Narrow band FM – 3kHz dev)
Type	Double conversion superhetorodyne
Intermediate frequencies	10.7MHz 455kHz
Synthesiser resolution	25kHz
Audio Bandwidth	3kHz
IF bandwidth	12kHz
Sensitivity	-117dBm for 12dB SINAD
Image rejection	70dB
Spurious Response	-40dBm
Noise figure	<2dB

Additional features of a field station receiver are a signal-strength indicator, audible output, volume control, squelch trigger and the ability to be easily tuned to the required receiving frequency.

4.4.1.1. Type

Heterodyne receivers accomplish the conversion of the received VHF signal to the required intermediate frequency (IF) by mixing it with a local oscillator signal that differs from the wanted received signal by exactly the IF frequency. The output of the nonlinear mixer can be filtered to produce the wanted sum or difference frequency to be used in the IF stage. The number of conversion stages used until the audio output distinguish between single-, double- or triple conversion receivers.

The usage of the typical IF frequencies for FM radio receivers (10.7MHz and 455kHz) guarantees the availability of parts like filters and quadrature detectors. The first local oscillator has been designed in the form of a frequency synthesiser that can be programmed to enable the receiver to receive the desired signal. The frequency resolution of this synthesiser is 25kHz.

4.4.1.2. IF Bandwidth

The IF bandwidth is defined as the narrowest bandpass filter in the receiving path. Together with the output audio bandpass filter, this filter determines the amount of noise that will be received. By narrowing the IF bandwidth the sensitivity of the receiver can be improved as less noise power is received. On the other hand the IF bandwidth must be sufficient to pass the desired signal without degradation. For AFSK data, the highest frequency tone that will be used will be 2.1kHz and an audio bandwidth of 3kHz will therefore be sufficient.

The IF bandwidth can be determined by Carson's rule which gives the relation between IF Bandwidth, maximum deviation ($\Delta\omega$=3kHz) and the modulating frequency (ω_m=3kHz) as:

$$B = 2(\Delta\omega + \omega_m)$$

The appropriate IF Bandwidth can therefore be calculated as 12kHz.

4.4.1.3. Sensitivity

The sensitivity of a receiver is an indication of the smallest RF signal that the receiver can receive and convert to an audio signal with a given signal to noise ratio. For FM receivers this signal to noise ratio is commonly given as a SINAD measurement (Signal plus Noise and Distortion). This measure of signal quality is defined as[7,8]:

$$SINAD = \frac{Signal + Noise + Distortion}{Noise + Distortion}$$

An audio SINAD level of 12dB corresponds to a signal distortion of 25% or a signal to noise ratio of 4:1 and is a common measure of the sensitivity of FM receivers that will be used throughout the rest of this document.

The sensitivity of the field station receiver will be limited by the noise floor of the surroundings in which the unit will have to operate. The amount of noise received by the receiver is determined by the noise temperature of the surroundings. This figure will be discussed in *Section 4.4.1.6* and is taken as 1000°K. The amount of noise power received is given by the following equation:

$$N_{rec} = kTB \text{ [W]}$$

Where k represents Boltzmans constant, T the noise temperature and B the receiving bandwidth. With a bandwidth of 3kHz the noise floor can therefore be calculated as -133dBm.

4.4.1.4. Image rejection

A mixer produces both the sum and difference of its input frequency sources. This means that, for a fixed local oscillator and IF there will always be two frequencies that the receiver can receive. One of these is the wanted frequency, and the other is the unwanted image frequency. The relative position of these frequencies will vary depending if the LO frequency is higher (high side injection) or lower (low side injection) than the wanted RF frequency as is illustrated in *Figure 4-3*.

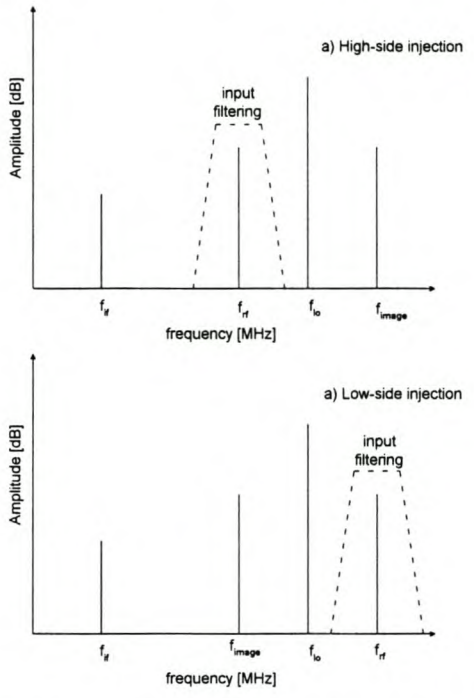

Figure 4-3 Image frequency positions

Filtering around the wanted frequency must be included to avoid interference caused by the reception of signals at the image frequency. Sufficient filtering of the image frequency will cause a 3dB improvement of the received signal-to-noise ratio, due to the fact that noise at the image frequency will no longer be mixed down to the IF.

The difference in the receiver sensitivity for the desired-, and image frequencies is known as the image rejection ratio, and should be at least 70dB to compare with the specifications of commercial VHF receivers.

For the field station low-side-injection will be employed with an IF of 10.7MHz. The possible image frequencies will therefore lie in the band between 122.6MHz and 124.6MHz. These frequencies are used for aeronautical traffic control usually employing low gain omnidirectional antennas.

4.4.1.5. Spurious free response

The image frequency is not the only unwanted frequency that a receiver may receive. A noisy local oscillator may cause the receiver to be unable to distinguish between two signals that are close together. If the input stage of the receiver is subjected to high level signals (in the order of 0dBm) active devices used may display nonlinear behaviour causing the receiver to be sensitive to unwanted signals.

The mixers in superheroterodyne receivers may also mix the higher order harmonics of its applied signals to form the intermediate frequency according to the following equation:

$$f_{IF} = \left| nf_{RF} \pm mf_{LO} \right|$$

The receiver should reject these frequencies. The spurious response refers to the maximum amplitude of unwanted signals that can be applied to the receiver without it losing its sensitivity at the desired frequency. A value of -40dBm is chosen to compare with the ***SUNSAT*** VHF receivers.

4.4.1.6. Noise figure

Any practical two-port will have some degrading effect on any input signal. To quantify this effect, the concept of noise ratio (NR) is defined as the ratio between the input and output signal to noise ratios:

$$NR = \frac{Signal_{in} / Noise_{in}}{Signal_{out} / Noise_{out}}$$

In the above equation $Noise_{in}$ represents the thermal noise generated in the source inpedance, and $Noise_{out}$ represents the sum of the input noise and the noise generated by the two-port multiplied by the relevant gain. The noise figure (F) of a receiver is simply defined as the NR expressed in decibels or:

$$F = 10 \log_{10} NR$$

Another way to describe the effect of a receiver on a received signal is the equivalent noise temperature of a receiver, which is related to the NR by:

$$T_{eq} = T_0 (NR - 1)$$

In this equation, T_0 represents 290°K.

To calculate the equivalent noise temperature of several systems in cascade consider *Figure 4-4*

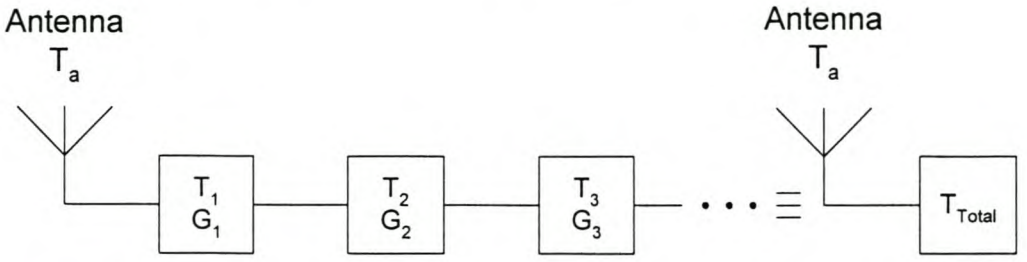

Figure 4-4 The equivalent noise figure of cascaded systems[6]

The equivalent noise temperature or T_{Total} of all the cascaded systems is also dependent on the gain of the various systems, and is given by Friis's formula[6,7] :

$$T_{Total} = T_1 + \frac{T_2}{G_1} + \frac{T_3}{G_1 G_2} + \ldots$$

It is evident that a first stage with a high gain and a low noise figure will ensure that the influence of the following stages on the receiver noise figure will be minimised.

The typical ambient noise temperature received by the antenna, or T_a has been discussed in *Chapter3* and is taken as 1000°K or a noise figure of 6.5dB. Man made noise in an urban environment can raise the ambient noise temperature considerably, but it is not possible to do much about this noise sources, except to try to suppress them at their origin.

For the special case were the ambient temperature of the antenna T_a is equal to T_o = 290°K the noise figure (F) represents the degradation in dB that the signal to noise ratio coming from the antenna will undergo as a result of the receiver. For a practical receiving antenna with $T_a \neq T_o$ the concept of operating- or actual noise ratio (NR') is defined as[6]:

$$NR' = 1 + \frac{T_{Total}}{T_a}$$

T_{Total} represents the equivalent noise temperature of the complete receiving system and by calculating the value of NR' in decibels, the actual degradation in signal to noise ratio for any value of ambient temperature can be calculated. This has been done for T = 30°K, 290°K and 1000°K, and the results have been plotted in *Figure 4-5*.

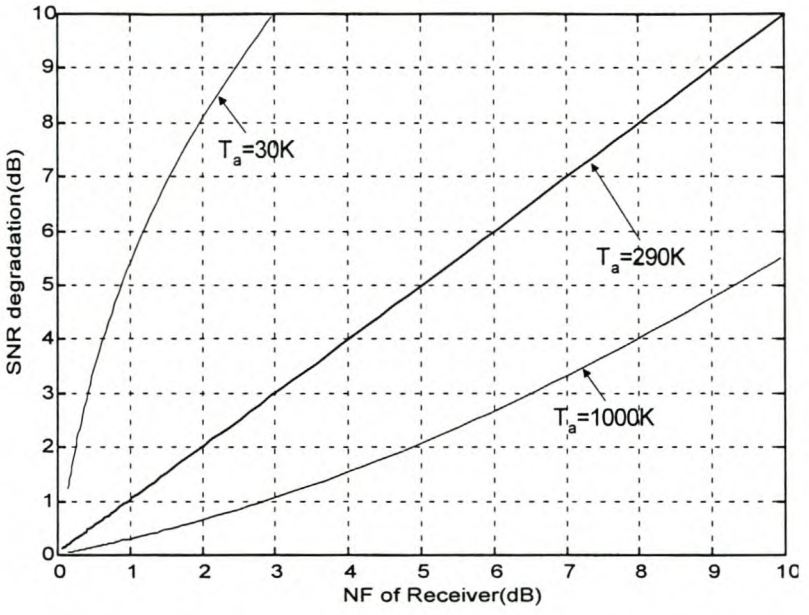

Figure 4-5 Choice of receiver noise figure

The amount of degradation caused in the signal to noise ratio is largely influenced by the ambient noise temperature. The noise figure for a receiver in an area with a T_a of 1000°K can be relatively high (more than 6dB) before it causes a 3dB reduction in the received signal to noise ratio. On the other hand, for an antenna aimed at a relatively noiseless area with a T_a of only 30°K, it will be necessary to ensure a receiver has a noise figure of less than 1dB if serious degradation is to be avoided.

For the field station with its omnidirectional antenna located in areas with high ambient noise temperatures, the added effort and cost of designing a receiver with a noise figure of less than 2dB will therefore not be justified. A narrow bandwidth input filter for the receiver will help to improve its sensitivity by limiting the amount of thermal noise received.

4.4.2. Transmitter Specifications

The specifications for the transmitter are given in *Table 4-2* and will be discussed in more detail in the following sections.

Table 4-2 Transmitter specifications

Frequency	144-146MHz (Narrow band FM – 3kHz dev)
Frequency resolution	25kHz
Sideband rejection	-60dB
RF Power output	5W
Power efficiency	35%
Receive Transmit cycling	15ms

4.4.2.1. Type

The easiest way to build a FM transmitter is to directly modulate a carrier frequency with the correct audio content. The field station transmitter must have a frequency synthesiser with audio injection for this purpose. The synthesiser must be able to span the required frequency band at the specified resolution, and must be designed to have the required harmonic rejection to meet the specifications for spectral purity. This is especially important to ensure that the transmitter will not radiate signals other than the frequency it is operated on. Such signals can cause harmful interference to other users of the radio spectrum and may also be illegal.

4.4.2.2. Power Output

As was seen in *Chapter 3* an output power of 5W should be sufficient to produce a received signal to noise ratio of more than 10dB for more than 90% of an overhead ***SUNSAT*** pass. The power efficiency of the power amplifier will mainly determine the efficiency of the transmitter, and of the whole field station. If the output power amplifier is to be a linear power amplifier module, 40% efficiency is about the maximum that can easily be guaranteed, without excessive costs. For a field station operating in remote locations, the amount of power consumed should be checked carefully if battery operation is desired.

4.4.2.3. Receive transmit Cycling

The time it takes for the field station to switch from receiving to transmitting must be shorter than that required by the communication protocol, and must preferably be as short as possible.

The AX.25 protocol employs variable timing parameters to ensure proper operation. These timers will typically have a value of about 100ms for terrestrial communication

and longer for space communication. The value of 15ms is therefore set as a reasonable specification for the field station transmitter.

4.5. Antennas

The aim of this thesis is not to design complex antenna structures. It was decided to implement the most elementary antenna that would still be able to give the wanted field station performance. Some of the preferred antenna specifications are given in *Table 4-3* and will be discussed in greater detail, and in relation to a few specific antennas in the following sections

Table 4-3 Antenna Specifications

Size	As small as possible
VSWR	<1.5
Type	Omnidirectional
Polarisation	Linear

4.5.1. Size

The size of the chosen antenna will mostly be determined by the wavelength used. Wavelength λ is related to frequency f by the following equation:

$$\lambda = \frac{c}{f}$$

In the above equation, c represents the speed of light in a vacuum. For the Radio Amateur VHF frequencies around 145 MHz the wavelength is around 2.067m. A typical monopole antenna will therefore be $\lambda/4 = 0.52$m long.

4.5.2. Matching

Any antenna can be modelled with a characteristic impedance. To ensure maximum power transfer between the transmitter and the antenna the characteristic impedance of the antenna should be properly matched to that of the transmitter. The voltage standing wave ratio (VSWR) is measure of the quality of matching between the antenna and adjacent systems. A VSWR of 1:1 is ideal, but practically any ratio smaller than 1:1.8 represents a usable antenna.

4.5.3. Antenna gain patterns

Antenna gain patterns give an indication of the gain that can be expected from an antenna in both the horizontal and vertical planes. This gain (usually expressed in

decibels (dB)) can simply be added to the relevant signal strength to get an idea of the resultant signal power after reception or transmission by the antenna.

To be able to use the antenna in a mobile environment it is necessary that it should have an omnidirectional gain pattern in the horizontal plane. The gain pattern in the vertical plane must also be analysed to fully understand the effect of the antenna on the received signal. This effect will now be considered for different omnidirectional antennas

4.5.3.1. Dipole Antenna

The dipole is one of the oldest and most widely used antennas around. It is also frequently used as a reference to measure the performance of other antennas. It is possible to create an effective dipole with each element being $\lambda/4$ in length so that the complete antenna will be $\lambda/2$ long.

According to Van Duzer [4] the gain for a half wavelength dipole antenna can be obtained from the following equation:

$$g_d(\Theta) = 1.64\left[\frac{\cos\left(\frac{\Pi}{2}\cos\Theta\right)}{\sin\Theta}\right]^2$$

When this equation is evaluated for a satellite elevation angle varying from 0° to 180° and a vertically mounted antenna, the pattern of *Figure 4-6* is obtained.

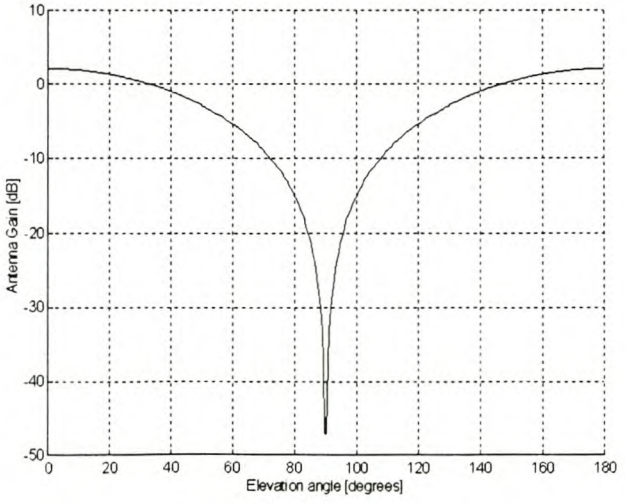

Figure 4-6 Dipole radiation pattern

It is evident that the gain of the dipole degrades significantly as the elevation angle of the satellite approaches 90°. This is because the effective area of the antenna facing the satellite gets smaller as the elevation angle increases. The effect of this characteristic is eased a little because the satellite also gets physically closer to the groundstation for high elevation angles, but it does cause a momentarily loss in signal for the field station employing a vertical dipole on a direct overhead pass. The signal only gets smaller than the receiver sensitivity for elevation angles bigger than 80° (*Chapter 3)*, and if it is considered that direct overhead passes only occurs infrequently in Southern Africa, this proves the usefulness of the dipole for a LEO field station.

The dipole is a linearly polarised antenna, and will therefore cause a constant 3dB signal attenuation when receiving a circularly polarised signal.

4.5.3.2. Monopole Antenna

The Monopole has a similar gain pattern and characteristics to the dipole, but the presence of a ground plane of conducting material obliviates the necessity of one of the elements. When the Monopole antenna is analysed using the method of images[4], it can be seen that the ground plane effectively creates an image of the missing element of the antenna. This means that an antenna with a total length of $\lambda/4$ can be realised should a ground plane be available. As a rule of thumb, the ground plane should extend at least a distance of $\lambda/4$ all around the driving element as the quality and size of the ground plane can influence the gain patterns of the antenna to a large extend.

The Monopole is especially popular for use with motorcars, as the metallic roof of the vehicle can be used as a ground plane for the antenna.

4.5.3.3. J-pole antenna

The J-pole antenna was designed by radio amateurs, and is a type of folded dipole. It consists of a $\lambda/2$ section (L_1) on top of a $\lambda/4$ tuning stub (L_2) as shown in *Figure 4-7.* Matching is done by adjusting the height of the feeding cable attachment (L_3).

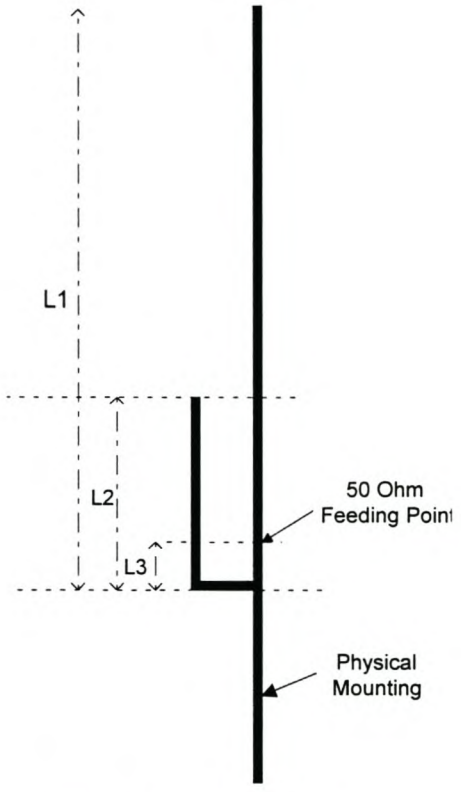

Figure 4-7 J-Pole antenna

The advantage of this antenna it is that it does not require a ground plane, can be fully self-supporting, and is easier to feed directly from a 50Ω coaxial cable than a dipole antenna. The gain pattern is very much like that of a monopole, and it also is a linearly polarised antenna causing a constant 3dB signal attenuation when receiving a circularly polarised signal.

4.5.3.4. Circularly polarised antennas

Antennas with circular polarisation and omnidirectional horizontal gain patterns do exist. The quadrifilar helix antennas and the Amateur Radio "eggbeater" antennas are examples of this. These antennas also generally have smoother vertical gain patterns that are desirable for field station operation added to the fact that they have a constant gain advantage over a linearly polarised antenna.

Problems with this kind of antenna are that they are more complex to manufacture, and generally have a more fragile physical design.

4.6. References

1. F. Grobler, *The design and implementation of a store and forward communication system on the SUNSAT microsatellite*, Thesis for masters in Engineering (Electronic) at University of Stellenbosch, January 1994
2. P van der Westhuizen, *A VHF and UHF receiver for the SUNSAT microsatellite (Afrikaans)*, Thesis for masters in Engineering (Electronic) at University of Stellenbosch, January 1994
3. Mostert & Milne, SUNSAT: Solutions for store and forward communication
4. Ramo, Whinnery & Van Duzer, *Fields and waves in communication electronics*, Johan Wiley and Sons, Third Edition, 1994
5. F. White, *A miniature Crystal controlled FM transmitter (Afrikaans)*, Thesis for masters in Engineering (Electronic) at University of Stellenbosch, Oct 1992
6. J.J Roux, *The design of a VHF and UHF Receiver Front-end for the SUNSAT micro satellite,* Thesis for masters in Engineering (Electronic) at University of Stellenbosch, January 1998
7. Paul H. Young, *Electronic Communication Techniques*, Prentice Hall International Edition, 1994
8. M. Gruber, *QST Product Reviews: A look behind the scenes*, QST-Magazine, October 1994

5. Receiver design

5.1. Block diagram

A block diagram of the field station receiver is presented in *Figure 5-1*.

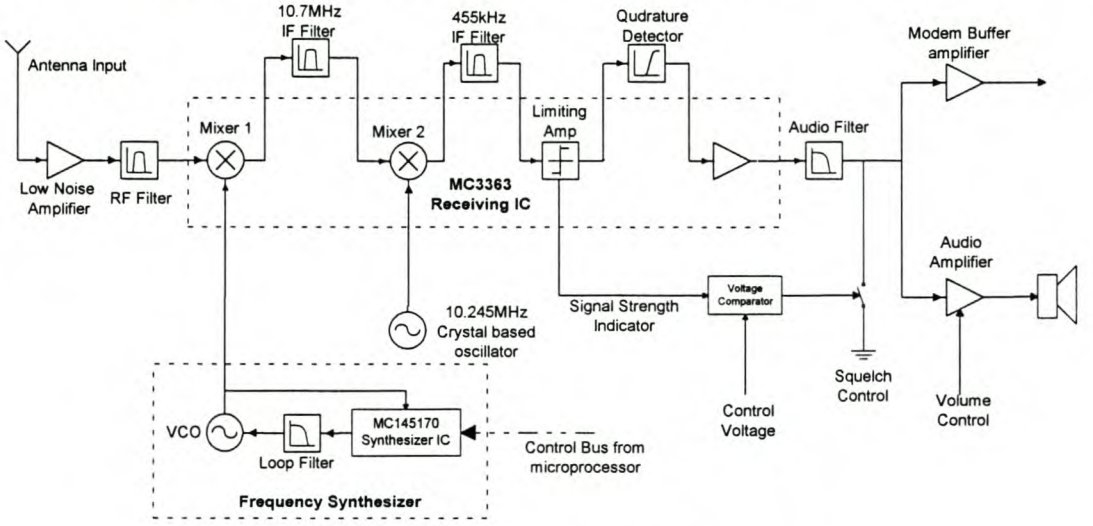

Figure 5-1 Receiver Block diagram

The received radio frequency (RF) signal from the antenna is fed through a switching system that controls the flow of signals to and from the antenna. The received signal travels through a low noise amplifier (LNA) to amplify it, while adding as little noise as possible. The LNA also has some frequency selective properties to reject unwanted signals. Next the signal is fed through a RF filter. This filter improves the selectivity of the receiver by rejecting unwanted out of band signals, as well as attenuating the image frequency of the mixer. The signal is next fed to the ***Motorola*** MC3363 receiving integrated circuit (IC). This IC comprises a complete dual conversion, narrowband, FM receiver with two mixers, a voltage controlled oscillator, limiting amplifier and a received signal strength indicator (RSSI). The audio output of the receiver is fed through an appropriate audio filter and amplifier to the modem. A voltage controlled squelch trigger and a RSSI output is also part of the design.

The 1st LO used by the MC3363 consists of a phase locked loop (PLL) frequency synthesiser that enables the receiver to tune to the wanted frequency under the control of the microcontroller.

The design of the different subsystems of the receiver will now be discussed in greater detail.

5.2. Low noise amplifier (LNA)

A noise figure of 2dB has been specified for the receiver in *Chapter 4*. To be able to reach this specification the LNA will need a noise figure of less than 2dB and also sufficient gain to minimise the influence of the next stage of the receiver which is the passive RF filter with a noise figure of about 4dB. If the gain of the LNA is too high, it will limit the dynamic range of the receiver.

The BF981 dual gate MOSFET transistor has been used as the LNA active device. These devices were also used successfully in the ***SUNSAT*** VHF preamplifiers[1], are inexpensive and are capable of a 1dB noise figure at VHF frequencies.

The data sheet for the BF981 gives the transistors Y-parameters for the following conditions (V_{DS}=10V, I_D=10mA, V_{G2S}=4V, T_{amb}=25°C). Although this differs a little from the current design, these values will be used in the next sections.

5.2.1. Biasing

The drain current (I_D) was chosen as 5mA, and 5V is used as the drain source voltage (V_{DS}), supplied through the drain matching inductor. This means that the LNA will consume 25mW of power equating to 11% of the maximum rating on the data sheet[2]. The lower bias current will improve the stability of the device by lowering the LNA gain.

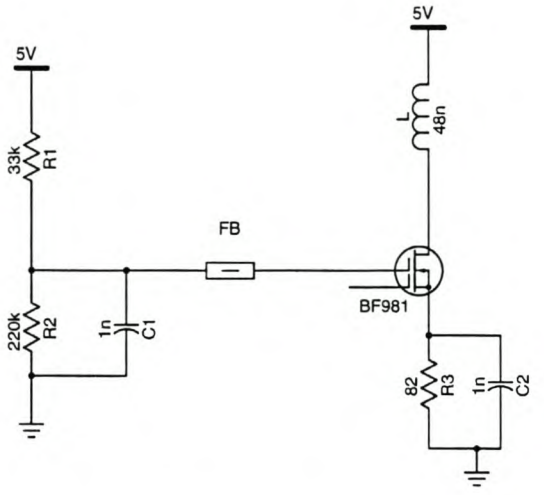

Figure 5-2 LNA Biasing Circuit

The bias voltage at the gate one (V_{G1S}) of the BF981 for I_D=5mA is given as –0.4V. This means that the source voltage needs to be 0.4V higher than ground. The voltage at gate one is 0V as it is grounded through an inductor that forms part of the input matching circuit. To achieve the wanted source voltage with an I_D of 5mA, the value of the Source resistance (R_3) is given by:

$$R_S = \frac{0.4V}{5mA} = 80\Omega .$$

A value of 82Ω is chosen for the practical resistor. In order to ensure avoid loss of gain, the source of the BF981 is AC grounded by a 1nF capacitor.

The bias voltage at the gate two (V_{G2S}) of the BF981 for I_D=5mA is given as 4V. If the bias current is chosen as 20μA, the values of the two biasing resistors can be calculated as follows:

$$R_1 = \frac{1V}{20\mu A} = 50k\Omega \text{ and } R_2 = \frac{4V}{20\mu A} = 200k\Omega .$$

The practical resistor values of 33kΩ for R_1 and 220kΩ for R_2 gives rise to a biasing current of 19.7μA and a V_{G2S} of 4.3V.

Feedback current between gate 2 and the source of the transistor can cause voltages across any impedance that might exist between these points. To prevent unwanted oscillations, these two points will therefore be short circuited for AC with two 1nF

capacitors (C_1 and C_2) with short leads. A ferrite bead is also inserted between C_1 and gate 2 to damp possible resonances, and to help prevent unwanted UHF oscillations.

5.2.2. Input Matching

The input load of the transistor determines its noise figure. This means that the input matching circuit needs to match the 50Ω load of the antenna to the input impedance required by the transistor in order to achieve the minimum noise figure. By designing the input matching to be frequency selective, the receiver's spurious response can be improved.

The datasheet[2] specifies a source impedance with a 1.6kΩ resistor in parallel with a 500Ω inductor to achieve the minimum noise figure of 0.6dB at 145MHz. This value differs from the required input impedance for maximum gain (9kΩ in parallel with a 500Ω inductor).

The inductance necessary to generate a 500Ω impedance at 145MHz can be calculated as:

$$L = \frac{X_L}{2\Pi f} = 548nH$$

This relative large value of inductance can be difficult to realise, and therefor a 500Ω capacitor is included in parallel with this inductor to reduce the required inductance to 274nH. By using a variable capacitance, the circuit can be tuned for the optimum noise figure. The required capacitance is given by:

$$C = \frac{1}{2\Pi f X_C} = 2.2pF,$$

and a variable capacitor of 5pF will give the wanted result.

A tapped inductor circuit has been used to transform the 50Ω antenna impedance to the high impedance required by the BF981 and to make the input matching frequency selective. When the coupling coefficient between the two coils is close to unity, the relation between the input and output resistances is given by:

$$\frac{R_1}{R_2} = \left(\frac{n_1}{n_2}\right)^2$$

For the sake of a high quality factor it was decided to use an air core inductor. This means that the coupling coefficient would be very low, and that the above equation would not be valid. If the exact coupling is known, the graphs in the book by Kraus, Bostian and Raab[3] can be used, but instead the transforming effect has been measured on a ***Hewlett Packard*** HP8753C network analyser to design the circuit correctly.

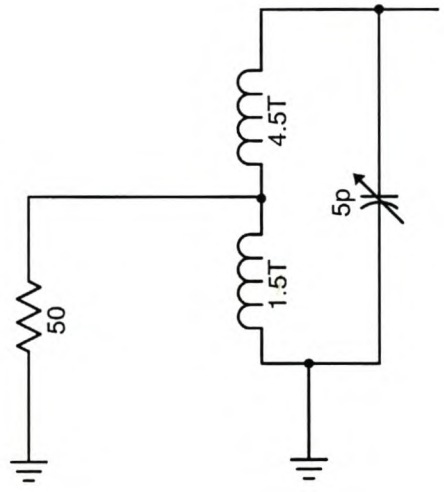

Figure 5-3 LNA Input Matching

With 5 turns of 1.68mm diameter tinned copper wire wound on a 13mm diameter former and tapped at 1.5 turns to R_1 (a 50Ω termination) the network analyser measured an output serial impedance of 48Ω+j227Ω at 145MHz. This gives rise to a quality factor of $Q_S = \frac{227\Omega}{48\Omega} = 4.73$. The equivalent parallel resistance and inductance are given as[3]

$$R_{PE} = R_S(1+Q_S^2) = 1121\Omega \text{ and}$$

$$L_{PE} = L_S\left(\frac{1+Q_S^2}{Q_S^2}\right) = 261nH \text{ respectively.}$$

When these values are plotted on the noise circles of the BF918 at 145MHz with a parallel capacitor that is varied from 1 to 5pF the results of the dark line on *Figure 5-4* are obtained.

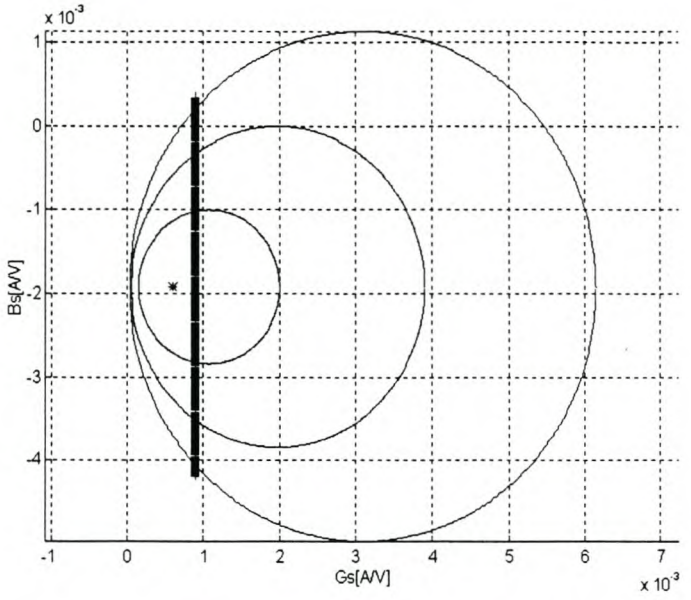

Figure 5-4 Input Matching

It is important that the input matching network has little insertion loss, as this loss will be representing the noise figure of the first system after the antenna. The total noise figure of the LNA with a reasonable amount of gain will be $N_{LNA}=N_{MATCH}+N_{BF981}$. This insertion loss is related to the ratio between the loaded and unloaded quality factor of the input inductor as follows:

$$L_{in} = 20\log_{10}(1-\frac{Q_L}{Q_U})$$

The quality factor refers to the ratio between the resistive and reactive elements in an inductor or capacitor. It can be defined for the parallel or the serial case as follows:

$$Q_S = \frac{X_S}{R_S} \text{ and } Q_P = \frac{X_P}{R_P}$$

Q_L refers to the resultant quality factor when the loading effect of the circuit in which it will be used is taken into account. The loading resistance will be the transformed resistance of 1.1kΩ in parallel with the input impedance of the BF981 of 9.1kΩ. This value of 998Ω gives rise to a Q_L of 4.2. Q_U refers to the measured quality factor when the element is measured with high impedance apparatus. The value for Q_U for the input inductor was measured with a ***Marconi*** inductance meter to be 150. The insertion loss of the input matching circuit is therefore 0.24dB, and the noise figure of the LNA can be tuned to be less than 1.5dB.

5.2.3. LNA input protection

The LNA should be protected against high input voltages to prevent the breakdown of the BF981 active device. To this end the BF981 is equipped with integrated back-to-back diodes between its gates and source. The antenna switching network presented in *Chapter 6* gives further protection.

5.2.4. Gain

The ac equivalent circuit of the biased LNA is given in *Figure 5-5*[12]. The dotted lines represent the boundary to the internal model of the BF981, showing that it can be considered a voltage controlled current source.

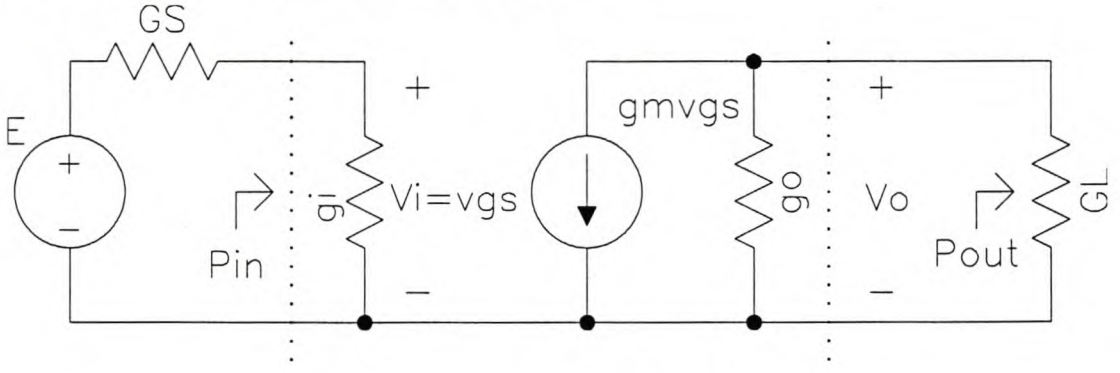

Figure 5-5 LNA – AC equivalent Circuit

The values of the characteristic input- and output conductance (g_i and g_o) of the BF981 are given in the datasheet[2]. This impedance consists of both real and reactive parts, but the latter are cancelled by the input and output matching circuits. For the calculations of this section only the real part of the conductance will be considered (g_i=0.109mS and g_o=55µS).

The transducer power gain of the circuit is defined as[3]:

$$G_T = \frac{P_{Delivered.to.load}}{P_{Availeable}} = \frac{4g_m^2 G_S G_L}{(g_i + G_s)^2 (g_o + G_L)^2}$$

The transconductance (g_m) of the BF981 are given as 11mS for an I_D of 5mA. The output matching circuit will transform the 50Ω load of the LNA to 680Ω to produce a load conductance G_L of 1/680Ω. When the output drain resistor is considered in parallel with the output resistance of the transistor ($g_o = \frac{1}{18.2k\Omega} + \frac{1}{680\Omega} = 15.3\text{mS}$)

and the input resistance of 1.1kΩ is used to calculate the source conductance (G_S), the gain can be computed as 18.4dB.

5.2.5. Output Matching

The Y-parameters in the datasheet[2] indicate that the BF981 is unconditionally stable at 145MHz. The 680Ω output resistor is included to ensure that the LNA will also be stable when no input loading is present[1].

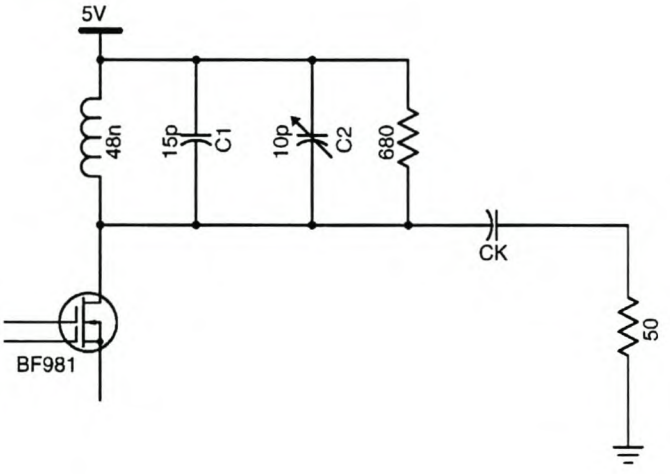

Figure 5-6 LNA Output Matching

The output reactance of the BF981 is a capacitance of 960μS (about 1pF at VHF). To resonate this capacitance with a single inductor would be difficult, as the required inductor would be quite large (1.2mH at 145MHz). Instead a practical inductor is inserted, and then enough capacitance is added in parallel to resonate (together with the internal capacitance) with this component.

The insertion loss of the output matching circuit should be kept as small as possible (while still retaining some frequency selectivity) and is given by:

$$L_{in} = 20\log_{10}(1-\frac{Q_L}{Q_U})$$

The Q_U obtainable with a small air core inductor is in the order of 140. To limit the tuned circuit loss to less than 1dB, Q_L should therefore be at least 10 times smaller resulting in an insertion loss of 0.91dB.

The wanted inductor can be calculated from the value of the output resistor and this quality factor as:

$$Z_P = \frac{R_P}{Q_L} = 45\Omega = 48nH$$

Five turns of 0.76mm diameter copper wire wound on a 4mm former gave rise to an inductance of 46nH, with a Q_U of 138.

The 24pF of capacitance required to resonate with this inductance at 145MHz are provided by the two capacitors (C_1 and C_2), the internal capacitance of the BF981(1pF) and the effect of the coupling capacitor C_K as shown in *Figure 5-6.*

The effect of the coupling capacitor C_K is to transform the 50Ω impedance of the measuring equipment or the next stage of the receiver to a resistance in parallel with a capacitance. This capacitance can be accommodated for by detuning the 10pF variable capacitor C_2, and the resistance should be as close as possible to 680Ω to ensure maximum power transfer between the LNA and the 50Ω stage.

The parallel equivalent resistor for C_K and the 50Ω resistor are given by[3]:

$$R_{PE} = R_S\left(1+Q_S^2\right)$$

This equation can be rewritten (with R_{PE}=680Ω and R_S=50Ω) to find the wanted quality factor:

$$Q_S = \sqrt{\frac{R_{PE}}{R_S} - 1} = 3.55$$

The impedance wanted from the capacitor can now be calculated as:

$$X_S = R_S.Q_S = 177.5\Omega$$

This gives rise to a 6.18pF capacitor at 145MHz which can be realised by a practical value of 5.6pF. The parallel equivalent capacitor is given by[3]:

$$X_{PE} = X_S\left(\frac{Q_S^2+1}{Q_S^2}\right) = 191.5\Omega$$

This effect can therefore be accommodated for by detuning the 10pF variable capacitor C_3 by 5.7pF.

5.2.6. Physical construction

The high Q air-core inductor that is used for the input and output matching circuits of the LNA is very sensitive to disturbances in their respective magnetic fields. It is necessary to shield these components, and therefore the completed LNA has been housed in a grounded metal box.

5.3. RF Filter

The field station receiver needs to operate in the amateur frequency band (144-146MHz) that is flanked by frequencies used by other applications as is shown in *Figure 5-7*[12]. The omnidirectional antennas used, will receive a lot of these signals together with the desired signal from the satellite. Signals arriving at the receiver therefore need to be filtered to suppress unwanted reception of other frequency sources. Although the LNA has some frequency selective characteristics, these alone are not sufficient, and additional filtering is required.

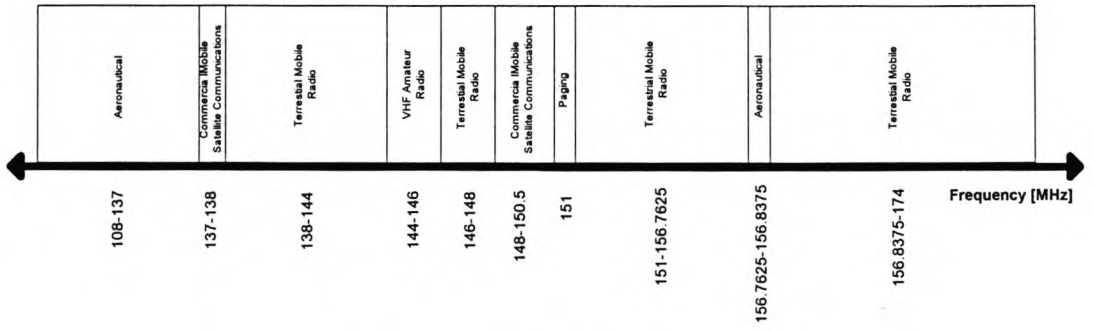

Figure 5-7 The VHF spectrum

A commercial helical filter unit from ***Toko*** was used as RF filter. The unit was measured on the ***Hewlett Packard*** HP8753C network analyser and its S_{21} response is shown in *Figure 5-8.*

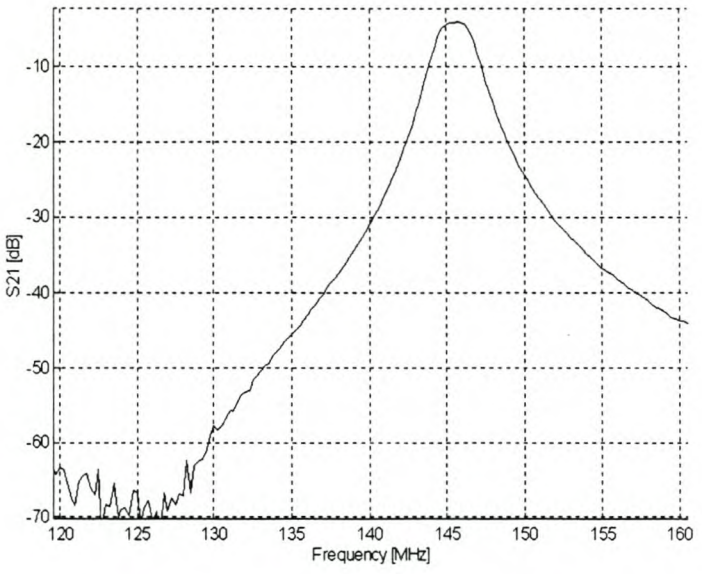

Figure 5-8 RF Filter - Frequency response

As can be seen, this unit has the wanted sharp frequency response giving more than 60dB attenuation at the image frequency of 123.6MHz. Signals in the commercial mobile radio band surrounding the amateur band are attenuated by more than 20dB. The insertion loss for the filter in its 2MHz passband around 145MHz is 4.2dB.

The input and output of the filter have been tapped to provide convenient 50Ω input and output impedance to the rest of the receiver.

5.4. Synthesised 1st Local oscillator *

The aim of a frequency synthesiser is to provide a programmable frequency source for mixing down the received signal to the intermediate frequency. A block diagram of the system is given in *Figure 5-9*. The main components of the system are a crystal reference, a phase comparator, a loop filter; a voltage controlled oscillator (VCO) and a programmable counter.

* For more general detail about the design of frequency synthesisers please refer to *Appendix B*.

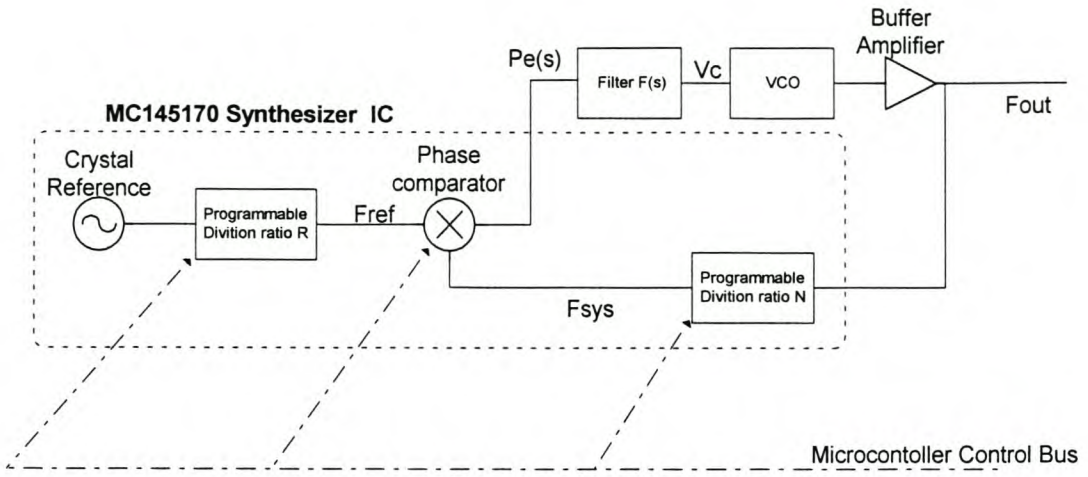

Figure 5-9 Synthesised Oscillator

A crystal oscillator with a high quality factor is used as a reference. The output of the crystal oscillator is divided to a convenient reference frequency. The phase of the reference signal is compared with that of the VCO in the phase comparator, generating a phase error signal $P_e(s)$. This signal is fed through the loop filter to the control voltage of the VCO. The output of the VCO is buffered to the IF-mixer, but is also used to feed a programmable counter. Depending on the division value loaded in this counter the synthesiser output will be an integer multiple of the reference frequency making the synthesiser tuneable with a resolution of the reference frequency.

$$f_{out} = N * f_{ref}$$

The different subsystems of the synthesiser will now be discussed in more detail.

5.4.1. Synthesiser IC (MC145170)

The *Motorola* MC145170 is a single chip frequency synthesiser that can be used directly for VHF frequencies. Included on the chip are a crystal based reference oscillator, two phase detectors and two digital counters[4]. The first of these divides the reference oscillator to the wanted reference frequency, while the second is used as the loop divider to provide the output frequency as a multiple of the reference. The circuit diagram of the MC145170 implementation is shown in *Figure 5-10.*

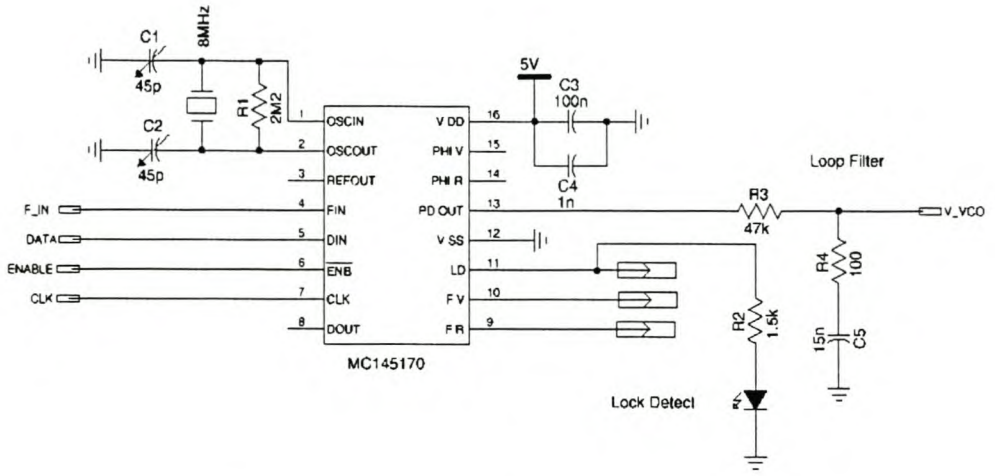

Figure 5-10 MC145170 Circuit diagram

5.4.1.1. Crystal Phase reference

An 8MHz Crystal is used to drive the reference oscillator. Changing the oscillator frequency will change the final synthesiser output, and this can be used to fine-tune the output frequency using a variable capacitor to slightly change the reference frequency.

To achieve the frequency reference of 25kHz the 8MHz oscillator needs to be divided by 320. This value will be loaded into the R-counter of the MC145170.

5.4.1.2. Phase comparator

The MC145170 gives the designer the option of two independent phase comparators with linear transfer functions. The comparator with a single phase-error output will be used, and for this case the comparator gain is given by the MC145170 data sheet[4] as:

$$K_P = \frac{V_{DD}}{4\Pi} = \frac{5V}{4\Pi} = 0.398\left[{}^{V}/_{\text{radian}}\right]$$

5.4.1.3. Control by microcontroller

The MC145170 operates on three data lines carrying serial data and is very easy to control from a microcontroller. A novel design feature enables it to count the number of bits received, and thereby decide for which of its three internal registers the data are destined. In this manner the two counters can be loaded to their respective recount values, and the control register can be programmed to operate the chip as desired. The control register specifies which phase comparator is used and which output pins are

active. The lock detect output is used to drive a LED to indicate that the synthesiser is locked and operating as required, while the other output pins are deactivated.

The recount value of the second divider needs to be changed as the receiver is tuned to different frequencies in the reception band of 144MHz to 146MHz. For this range the VCO needs to be tuned between 133.3MHz and 135.3MHz, the frequency difference being the value of the first IF. The corresponding range for the N-counter (with a 25kHz reference frequency) is therefore 5332 to 5412 with an average value of 5372. The microcontroller will be programmed to preset the receiver to this value (a receiving frequency of 145MHz) and will enable the user to program the synthesiser to any frequency within the receiving range.

5.4.2. VCO

The internal VCO of the MC3363 is used as loop oscillator as can be seen in *Figure 5-11.*

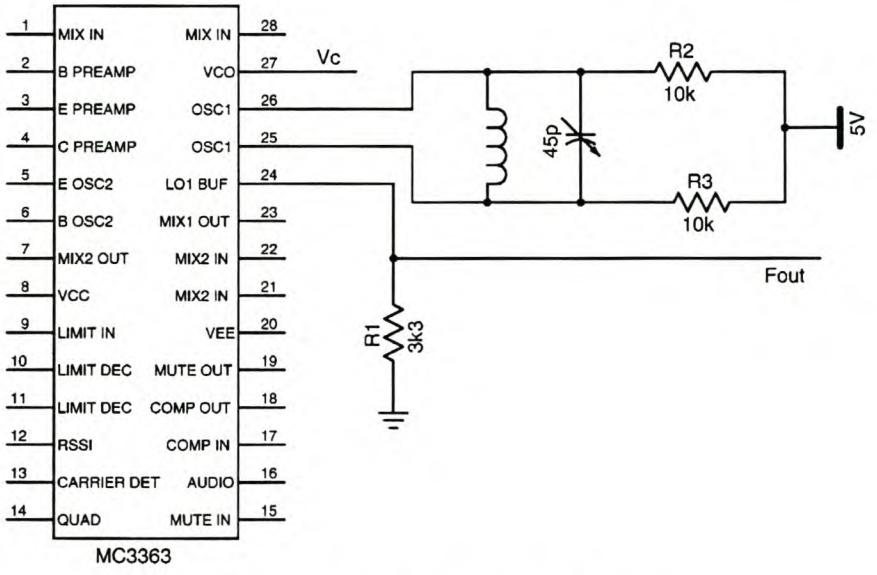

Figure 5-11 Receiver VCO

The inductor and capacitor act in parallel with the internal structure of the MC3363 to resonate at the wanted oscillator frequency. The two pull-up resistors (R_2 and R_3) are used to inject current into the circuit to ensure stable oscillations. The inductor is formed by 8 turns of 0.39mm copper wire wound on a TO-25 toroidal core for mechanical stability (giving rise to an inductance of about 30nH). The 45pF variable

capacitance is used to move the linear part of the VCO response to the wanted frequency band.

The voltage over pin 27 controls the reverse bias over the MC3363's two internal varacter diodes. The capacitance of these two diodes can be controlled between 10pF and 25pF[5], but the control voltage should not be lower than 0.7V, as this can cause the oscillator to stop functioning. The output resistor, R_1 is included for signal shaping as recommended in the application note[5].

To determine the characteristics of the VCO a variable voltage between one and five volts was applied to the control input at pin 27, and the output measured obtaining the results of *Figure 5-12*.

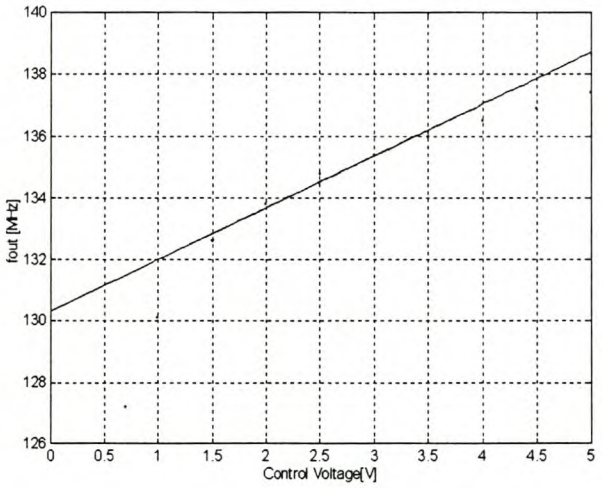

Figure 5-12 VCO Characteristics

As can be seen the VCO behaves linearly between 136MHz and 132.6MHz for an input voltage varying between 3.5V and 1.5V. These values can be used to compute the VCO gain as follows:

$$K_o = \frac{2\Pi(f_f - f_2)}{V_1 - V_2} = 1.0681*10^7 \text{ [rad/s/V]}$$

Although the VCO span is adequate to cover the 2MHz receiving bandwidth, changing component values brought about by ageing or extreme temperature variations may cause it to be unable to cover the receiving bandwidth.

The amplitude of the output signal has been measured as 170mVpp in 50Ω at 135MHz.

5.4.3. Buffer Amplifier

The MC145170 synthesiser IC requires at least 500mVpp in 50Ω of input signal amplitude to drive the loop divider at VHF frequencies[4]. As was seen in the previous section the MC3363 was only capable of delivering 170mVpp in 50Ω and the simple buffer amplifier of *Figure 5-13* has therefore been included in the design to amplify the VCO output to the required voltage levels.

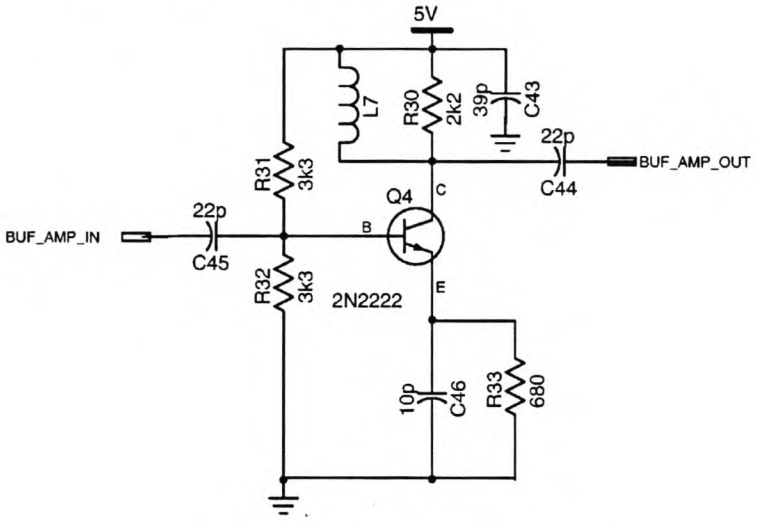

Figure 5-13 Buffer Amplifier

The amplifier has a 4 time voltage gain at the required frequencies delivering 625mV in 50Ω to drive the MC145170.

5.4.4. Loop Filter

The wanted specifications for the receiver synthesiser are given in *Table 5-1*

Table 5-1 Synthesiser specifications

Damping (ζ)	0.7
Maximum error	5%
Settling time (t_s)	10ms
Sideband rejection	>55dB

The damping ratio, maximum error and settling time specify the transient response of the loop. A damping ratio of 0.7 will result in a damped system without excessive overshoot, and the settling time is shorter than typical human reaction time, to allow for quick frequency changes while tuning the receiver. The sideband rejection refers

to the spectral purity of the oscillator, and is the difference in output level between the main frequency component, and the reference sidebands around it.

A passive loop filter with a single pole and zero like the one in *Figure 5-14* is used to give the wanted loop characteristics. If the loop does not satisfy the sideband rejection specification set to it, an extra capacitor may be inserted in parallel with the serial combination of R_2 and C. If this capacitor is chosen to have a frequency roll-off significantly higher than the loop filter frequencies, it will have only a minimal influence on the loop response while attenuating the reference sidebands.

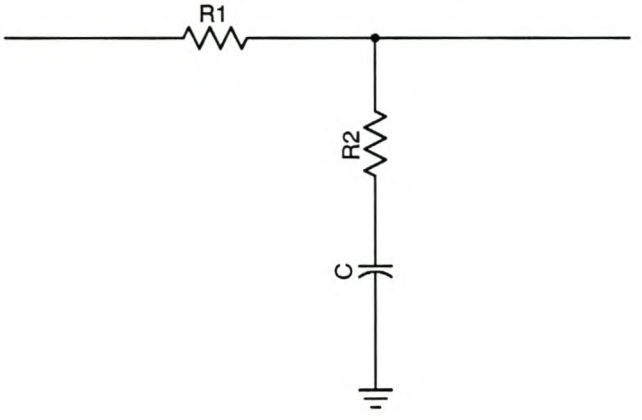

Figure 5-14 Synthesiser Loop filter

The transfer function of the filter is given by

$$F(s) = \frac{1+\tau_2 s}{1+\tau_1 s} \text{ (with } \tau_2 = R_2 C \text{ and } \tau_1 = (R_1 + R_2)C\text{).}$$

When this is inserted in the synthesiser, it can be shown that the natural frequency ω_n is given by

$$\omega_n = \sqrt{\frac{K_v}{N\tau_1}},$$

and the damping ratio ζ is given by:

$$\zeta = \frac{N + K_v\tau_2}{2\omega_n N\tau_1} = 0.5\omega_n(\tau_2 + \frac{N}{K_v})$$

To determine the natural frequency from the settling time, the relationships shown in *Figure 5-15* are used.

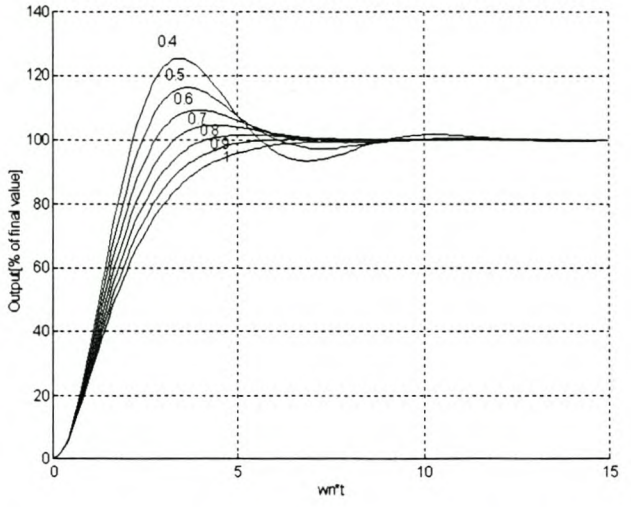

Figure 5-15 Normalised output relationships

From the figure it can be seen that a loop with a damping ratio of 0.7 will settle to less than 5% for $\omega_n t=10$. From the required lock up time the natural frequency can now be found as $\omega_n=1000$[rad/s]. Kv is simply the product of the phase detector and VCO gains: $Kv=Kp*Ko=0.398*1.0681*10^7=4.25*10^6[s^{-1}]$. From this value and the average value of the N-counter (5372) the value of τ_1 and τ_2 can be calculated as $7.91*10^{-4}$ and $1.363*10^{-4}$ respectively.

When a filter capacitor of 15nF is used together with the definition of τ_1 and τ_2 the values of R_1 and R_2 can be computed as 43.7kΩ and 9.063kΩ respectively. For the practical design a R_1 of 168kΩ and R_2=150kΩ have been used giving rise to a damping ratio of 0.69 and a ω_n of 497rad/s. When the loop step response with these values is plotted, the result of *Figure 5-16* is obtained.

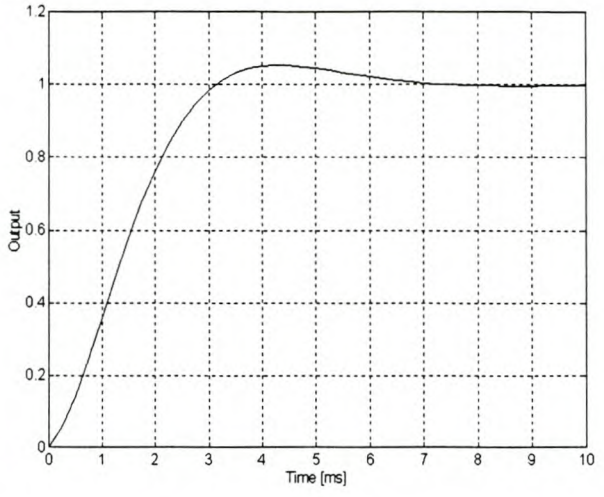

Figure 5-16 System step response

As can be seen the loop settles to its 5% of its final value in less than 10ms as was specified.

5.5. Receiver system (MC3363)

5.5.1. Mixer input matching

The mixer input of the MC3363 needs to be matched to 50Ω to achieve optimum performance. The mixer input impedance was measured to be 12Ω in series with a 49Ω capacitor with a ***Hewlett Packard*** HP8753C Network analyser. The input power of the network analyser was set to a level of -40dBm to ensure that the mixer was not measured over a nonlinear part of its frequency response.

The measured impedance can be transformed to a parallel equivalent of 213Ω in parallel with a 52Ω capacitor. A conventional two-element matching network was used as can be seen in *Figure 5-17*. The quality factor of such a network can be found from:

$$Q_S = \sqrt{\frac{R_P}{R_S} - 1} = 1.8 .$$

This gives rise to a parallel inductance $X_P=R_P/Q$ = 118Ω and a serial capacitance of $X_S=Q*R_S=90\Omega$. The capacitance equates to 12.3pF at 145MHZ and can be realised with the 20pF variable capacitor shown in *Figure 5-17*.

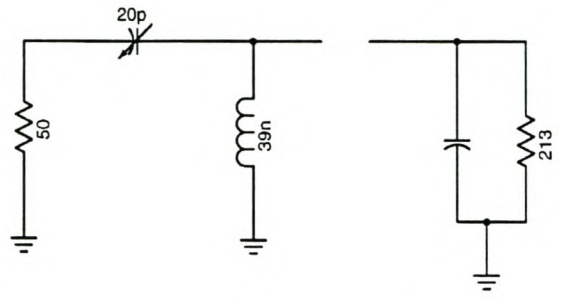

Figure 5-17 Mixer Input matching

To calculate the final value of inductance needed in the matching network, it should be remembered that the input of the mixer represents a 52Ω capacitor. A 52Ω inductance is needed to resonate with this capacitance, in parallel with the 118Ω calculated above. These two values give rise to a 36Ω inductance that equates to a 39nH inductor at 145MHz.

5.5.2. MC3363 1st Mixer

The first mixer is a double balanced unit that provides about 18dB of signal gain at the 10.7MHz. The isolation characteristics of the mixer are shown in *Table 5-2*. The strong isolation of 41dB between the LO signals at the mixer input (RF) port means that very little power from the LO will be fed back to the LNA and the antenna.

Table 5-2 First Mixer Isolation [5]

Signal	LO	Output (IF)	Input (RF)
LO	0	-17	-41
RF	-16	-9	0
IF	-29	0	<-40

The output of the mixer is impedance matched to 330Ω to allow direct insertion of ceramic filters of this impedance.

5.5.3. 1st IF Filter

The first IF Filter is a ***Murata*** unit (SFE10.7MS2) with a 3dB bandwidth of 230kHz and a 20dB bandwidth of 660kHz. The filter has an input- and output impedance of 330Ω and an insertion loss of 4dB. Signal outside the -40dB filter passband are suppressed by at least 40dB.

5.5.4. Second mixer and crystal oscillator

A 10.245MHz crystal is used in a parallel resonant crystal oscillator. When this frequency is mixed with the first IF of 10.7MHz, the second IF (455kHz) is produced as a difference frequency. The other products of the mixing operation are filtered out by the second IF filter. The mixer has a gain of 25dB, and is matched to the filter impedance of 1500Ω

5.5.5. 2nd IF Filter

The second IF Filter is a ***Murata*** unit (SFGM455C) with a 6dB bandwidth of 12.5kHz, an insertion loss of 6dB and input- and output impedance of 1500Ω. Signals outside the filter passband will be suppressed by at least 25dB.

5.5.6. Limiting amplifier and Quadrature detector

A block diagram of the receiver circuitry following the second IF filter is shown in *Figure 5-18.*

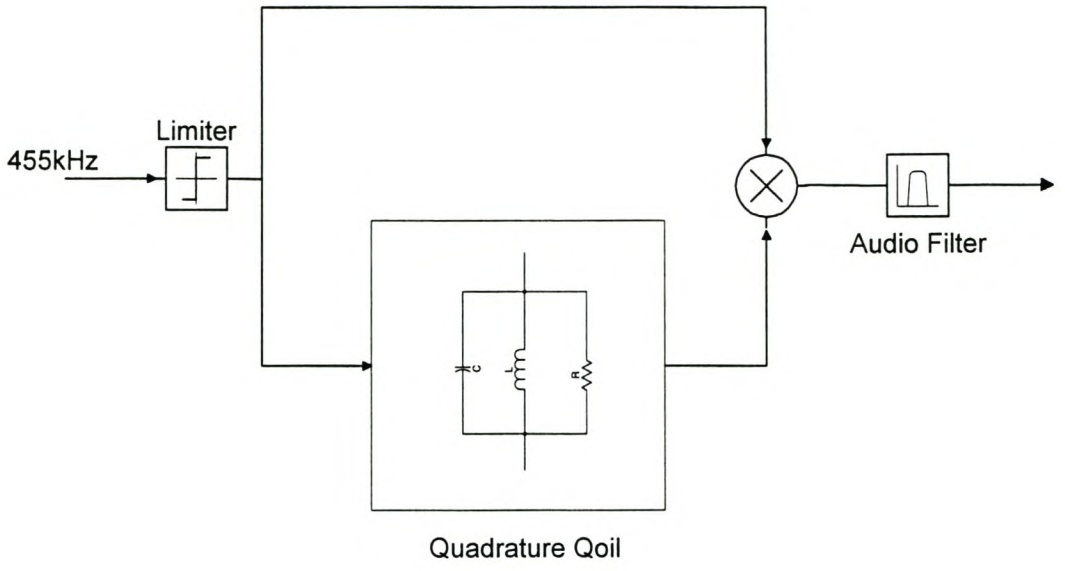

Figure 5-18 Limiter and qaudrature detector

The limiting amplifier also has a 1500Ω input impedance for easy matching to the IF filter. The limiting amplifier prevents unwanted effects caused by variations in the amplitude of the received signal by amplifying the signal until only the frequency and phase information are left in it.

An integrated package from ***Toko*** (RMC2A6597[4,5]) is used as the resonant part of the detector. This package consists of a parallel combination of capacitance and inductance, which (together with an external resistor)form the equivalent circuit shown in *Figure 5-18*. The resultant frequency response of the package and a parallel resistor has been plotted in *Figure 5-19*.

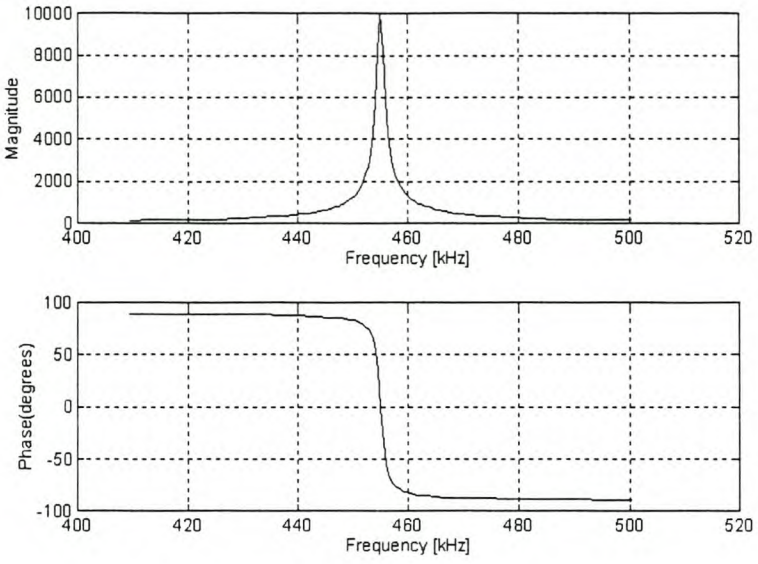

Figure 5-19 Quadrature coil – Frequency Response

The values of the inductor and capacitance determine the position of the resonant peak in the amplitude response. The resistor provides damping, and the bigger its value, the higher the amplitude peak, and the steeper the linear part of the phase response. The quadrature coil has very little influence on the amplitude of the demodulated signal as this signal has already been amplitude limited.

When the output from this coil is multiplied with the unmodified limiter output, and the result low pass filtered, the original modulating signal is received as a difference product from the frequency multiplication[6].

5.5.7. RSSI output

The RSSI output of the MC3363 is a current that varies from 5μA to 12μA (for a RF input varying between –120dBm and –50dBm) depending on the amount of limiting that takes place in the limiting amplifier[4]. The MC3363 application notes[5] recommends a specific op-amp buffer circuit to convert this current linearly to a voltage that can be used as an indication of the received signal strength. This circuit has been used unaltered as can be seen in *Figure 5-20.*

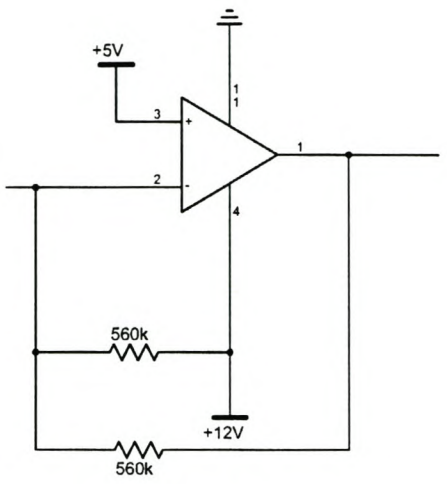

Figure 5-20 RSSI Buffer[5]

5.5.8. Squelch trigger

The squelch trigger allows the user to set a level of received signal power below which no audible output will be given. Besides easing the strain on operators who has to listen to audio noise, this feature also ensures that the modem will give no data output when no signal is received. The circuit that drives the squelch switch is shown in *Figure 5-21*.

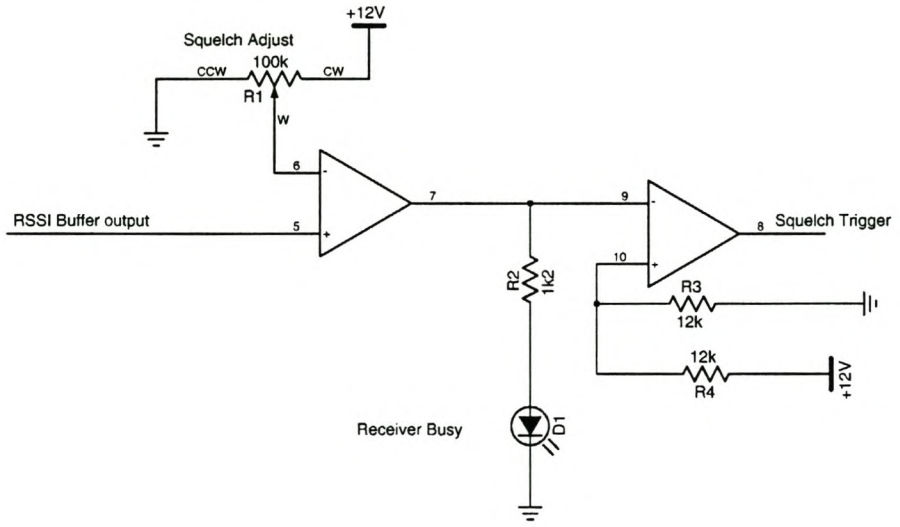

Figure 5-21 Squelch circuit

The voltage output of the RSSI buffer is compared to a variable voltage with a op-amp voltage comparator. The output of this open loop system is used to drive a led

that indicates the current status of the squelch trigger. The second op-amp is used to invert the signal to drive the FET squelch switch.

5.5.9. Audio Filter

The audio output is filtered by a simple RC filter (with R=5.6k and C=10nF) like the one shown in *Figure 5-22*

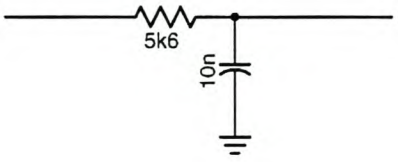

Figure 5-22 Audio output filter

The above values gives rise to a 3dB audio bandwidth of 2.8kHz.

5.5.10. Audio amplifiers

The receiver audio amplifiers are illustrated in *Figure 5-23* .

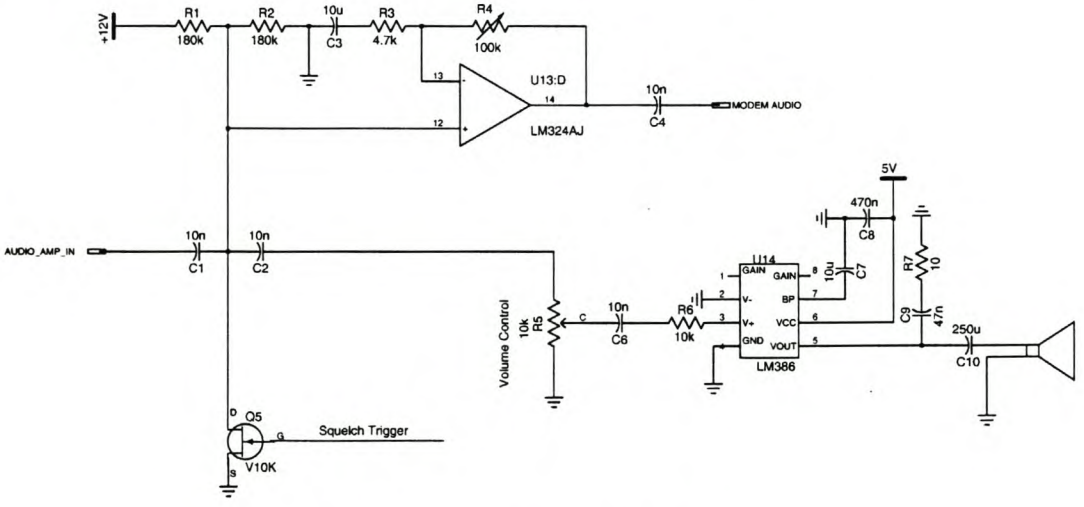

Figure 5-23 Audio Amplifiers

The audio output from the audio filter is fed to a V10K MOSFET[11] transistor that switches the audio signal to ground when no RF signal is received by the receiver. The operation of the squelch circuitry has been discussed in *Section 5.5.8.*

Two independent amplifier systems are included in the design to amplify the audio output of the receiver. The op-amp buffer amplifier is included to present the audio input of the modem with the correct voltage levels (0.3V). It is done by means of a

non-inverting operational amplifier with variable gain. Capacitor C_1 is included to limit the gain of the amplifier at DC to prevent it from amplifying the bias voltage supplied by resistors R_3 and R_4.

A ***National Semiconductor*** LM386 audio amplifier has been included to drive a loudspeaker to provide an audible output to the received signal. The circuit used follows that represented in the LM386 datasheet[7].

Special care has to be taken to decouple the audio amplifier power supply, as this is the part of the receiver that draws the most current when high audio output levels are required. Variations in the power supply can have an adverse effect on the synthesiser stability.

5.6. Power Supply

With the exception of the 12V supply required by the quad op-amp package used for the RSSI buffer, and the squelch circuitry, the complete receiver system has been designed to operate from a 5V supply. A linear voltage regulator (LM3805) was used to supply the different parts of the receiver with the required voltage. Decoupling capacitors have been included in the circuit to limit unwanted oscillations on the power supply lines. The power supply circuitry used is shown in *Figure 5-24*

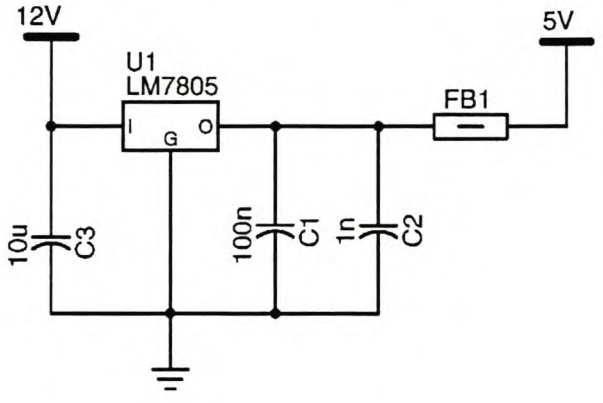

Figure 5-24 Power supply Circuitry

5.7. References

1. J.J Roux, *The design of a VHF and UHF Receiver Front-end for the SUNSAT micro satellite,* Thesis for masters in Engineering (Electronic) at University of Stellenbosch, January 1998
2. Phillips Inc, *Field effect transistors*, Phillips databook, January 1981, July 1985 and July 1987
3. H.L. Krauss, C.L. Bostian & F.L. Raab, *Solid State radio engineering*, John Wiley and Sons Inc., 1980
4. Motorola Inc *Motorola Communication Devices*, Motorola databook , 1995
5. Motorola Inc, *VHF Narrowband FM Receiver Design,* Motorola Application Note AN980, 1988
6. Paul H. Young, *Electronic Communication Techniques*, Prentice Hall International Edition, 1994
7. National semiconductor, *National Operational Amplifiers Databook*, National Databook, 1995
8. *Phase-Locked Loop design fundamentals,* Motorola Application Note AN535, Motorola Inc, 1988
9. *The MC145170 in basic HF and VHF Oscillators,* Motorola Application Note AN1207, Motorola Inc, 1988
10. Murata LDT, *90' Murata Products*, Murata databook, 1980
11. Supertex Inc, *VN10K N-Channel enhancement-mode vertical DMOS FET's datasheet*, 1995
12. South African Telecommunications Regulatory authority (SATRA), *RSA Frequency Allocations*, CSIR, March 1998

6. Transmitter design

6.1. Block diagram

The transmitter block diagram is represented in Figure 6-1.

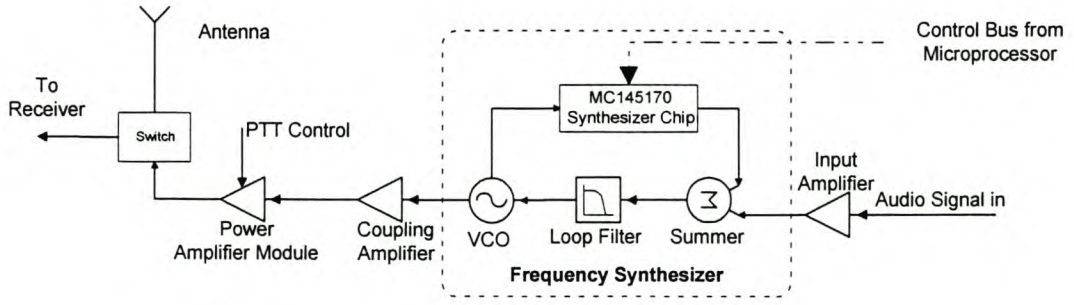

Figure 6-1 Transmitter Block Diagram

The heart of the transmitter is the frequency synthesiser that will provide a stable source at the carrier frequency. It is controlled by the microcontroller, to enable the user to easily change the transmit frequency. To add information to this carrier, it is modulated by an audio signal originating from the modem.

The FM modulated output of the synthesiser is fed to a power amplifier module, which amplifies the signal to supply up to 5W of RF power, and is activated by the push-to-talk (PTT) control. The switching unit connects the antenna to the receiver by default, but will route the output of the power amplifier to the antenna whenever it is activated.

6.2. Frequency synthesiser*

6.2.1. Modulating the Filter output

For the case where the modulating audio signal is added to the phase locked loop at the input to the VCO, the closed loop bandwidth of the synthesiser must be smaller than the lowest audio frequency used. If this is not done, the loop will try to filter out the audio signals.

---

* For more general information regarding the design of frequency synthesisers, please refer to *Appendix B*

6.2.2. Synthesiser IC (MC145170)

The block diagram for the transmitter synthesiser is shown in *Figure 6-2*. The main components of the system are the crystal reference, the phase comparator, the loop filter, the VCO, programmable counters and a summing circuit for adding the modulating audio signal to the loop.

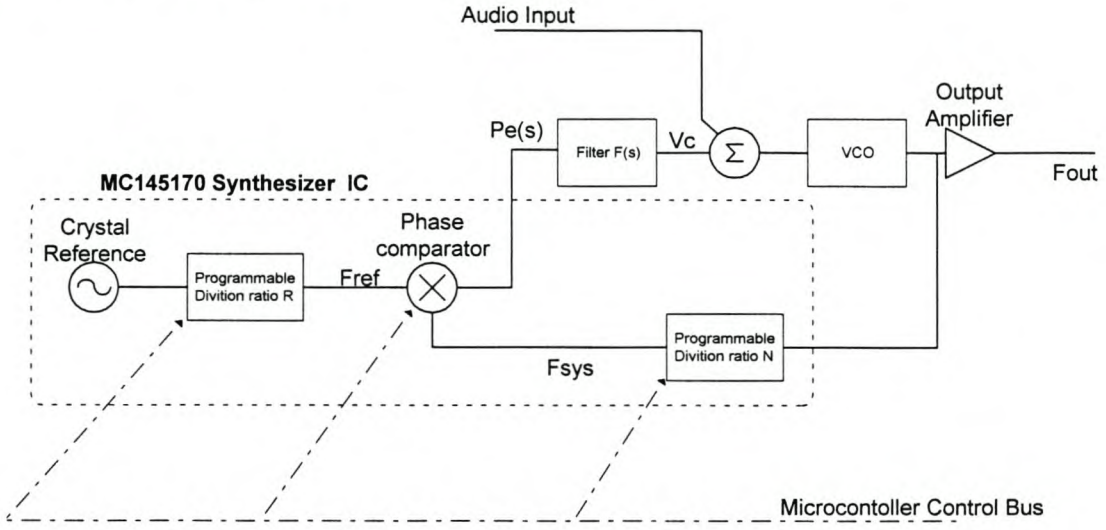

Figure 6-2 Transmitter Synthesiser

The same ***Motorola*** integrated circuit (MC145170) used for the receiver has been utilised for the transmitter[1,2,3]. The crystal reference oscillator is driven by an 8MHz crystal, leading to a value of 320 for the recount value of the first digital divider in order to provide a 25kHz synthesiser resolution.

The output frequency will be varied between 144 and 145MHz, resulting in a range of 5760 to 5840 for the recount value of the second divider. For the default transmitter frequency of 145MHz the counter should be set to 5800.

The comparator with a single phase-error output has been used, and for this case the comparator gain is given by the MC145170 data sheet[1] as:

$$K_P = \frac{V_{DD}}{4\Pi} = \frac{5V}{4\Pi} = 0.398\left[{}^{V}/_{\text{radian}}\right]$$

6.2.3. VCO

An independent voltage controlled oscillator (VCO) has been designed for the field station transmitter as illustrated in *Figure 6-3*.

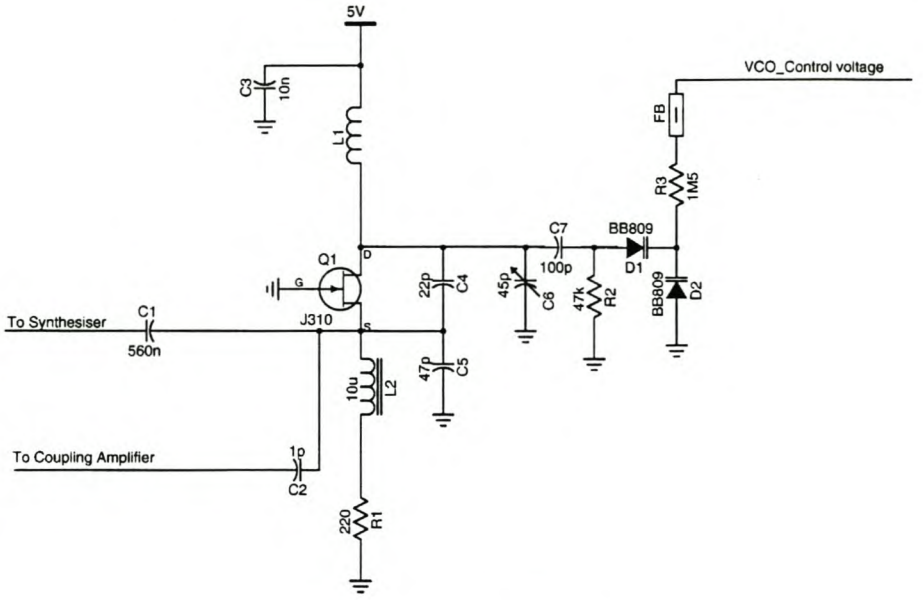

Figure 6-3 VCO Circuit

6.2.3.1. Tuned Circuit

The control voltage that forms the output of the loop filter and the modulating summer is applied to two BB809 varacter diodes (D_1 and D_2). These diodes have the property that their equivalent capacitance is controlled by the magnitude of their applied reverse voltage. (Resistor R_2 is used to reverse bias diode D_1.) This characteristic can be seen in *Figure 6-4*[4]. The dotted line represents the capacitance curve for the case where two diodes are used in parallel to make the voltage response more linear.

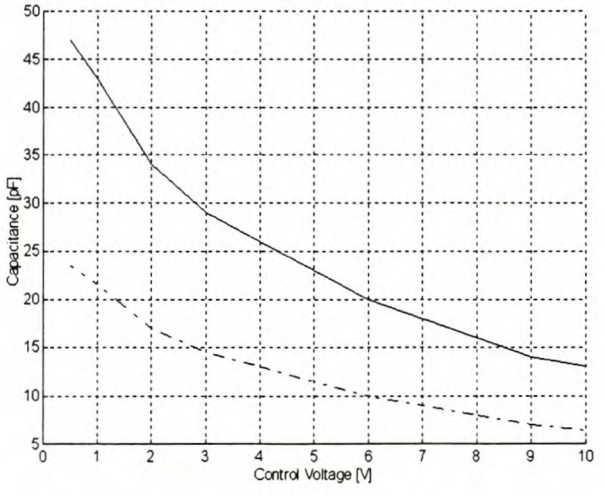

Figure 6-4 BB809 Characteristics

The equivalent capacitance of D_1 and D_2 will vary between 23pF and 11.5pF as the control voltage is varied between 0 and 5V. The capacitance of the diodes is

connected in parallel with variable capacitor C_6, the series combination of C_4 and C_5, and inductor L_1 to form the resonant circuit of the VCO. Inductor L1 is formed by three turns of 0.39mm diameter wire on a TO-25 toroidal core, resulting in an inductance of 18nH. The ratio between C_4 and C_5 determines the stability of the oscillation, and has been set to 0.46.

6.2.3.2. Biasing

A J310 N-channel depletion field effect transistor (FET)[5] is used as the active device for the VCO, and is connected in a common gate configuration. The drain-source voltage V_{DS} has been chosen as 3.5V, and resistor R_1 biases the FET at a drain current I_D of approximately 5.6mA. Decoupling capacitor C_3 and RF choke L_2 ensure a stable voltage supply.

6.2.3.3. Output Circuit

Capacitor C_1 couples the VCO to the MC145170 synthesiser IC. The value of 560nF was chosen to represent a very low impedance to a signal at 145MHz. Capacitor C_2 is used to supply the coupling amplifier with the VCO output and have been chosen as 1pF to present the VCO with a much higher impedance and to load it as little as possible.

6.2.3.4. Measured results

When the VCO was measured for a control voltage varying between 0 and 5V, the results of *Figure 6-5* were obtained.

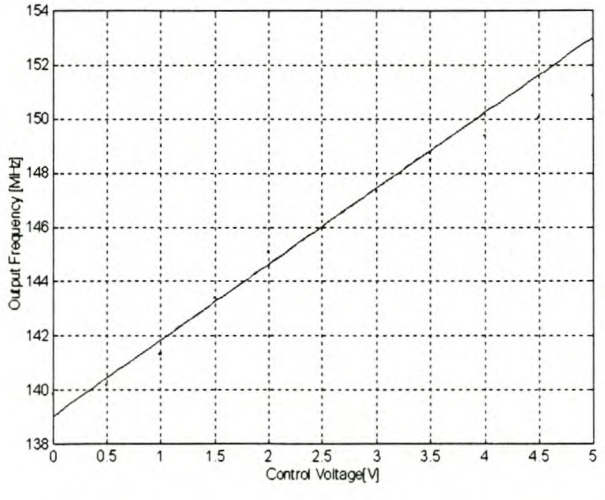

Figure 6-5 VCO characteristics

The VCO behaves linearly between 141.3MHz and 148.5MHz for an input voltage varying between 1V and 3.5V. This is adequate to cover the 2MHz transmitting band. These values have been used to compute the VCO gain as follows:

$$K_o = \frac{2\Pi(f_f - f_2)}{V_1 - V_2} = 1.7945 * 10^7 \text{ [rad/s/V]}$$

6.2.4. Loop Filter

The wanted characteristics for the transmitter synthesiser are given in *Table 6-1.*

Table 6-1 Synthesiser specifications

Closed loop bandwidth	100Hz
Maximum overshoot	>5%
Settling time (t_s)	10ms
Sideband rejection	60dB

The closed loop bandwidth of the synthesiser must be smaller than the minimum audio frequency content used to modulate the loop. The minimum frequency used by the 1200baud modem is 1.1kHz, and the closed loop bandwidth is therefore chosen more than 10 times smaller than this value at 100Hz.

A passive loop filter with a single pole and zero like the one in *Figure 6-6* and similar to the loop filter used for the receiver synthesiser is used to give the wanted loop characteristics.

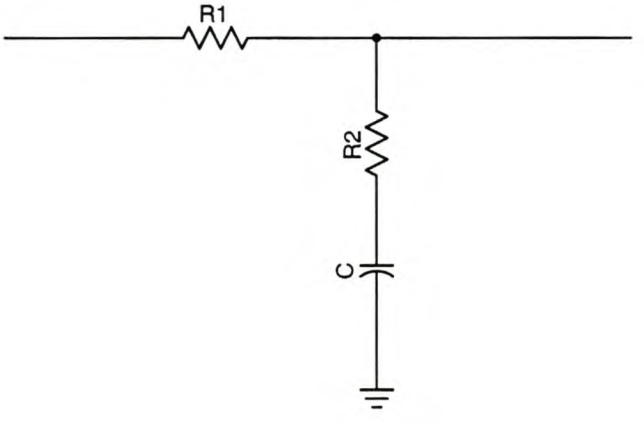

Figure 6-6 Synthesiser Loop filter

The loop gain K_v is defined as the product of the phase detector and VCO gains: $Kv=Kp*Ko = 0.398*1.7945*10^7 = 7.1421*10^6$ [s^{-1}]. With the natural frequency fixed at 630rad/s the normalised relationships shown in *Figure 6-7* are used to determine the combination of damping ratio and settling time.

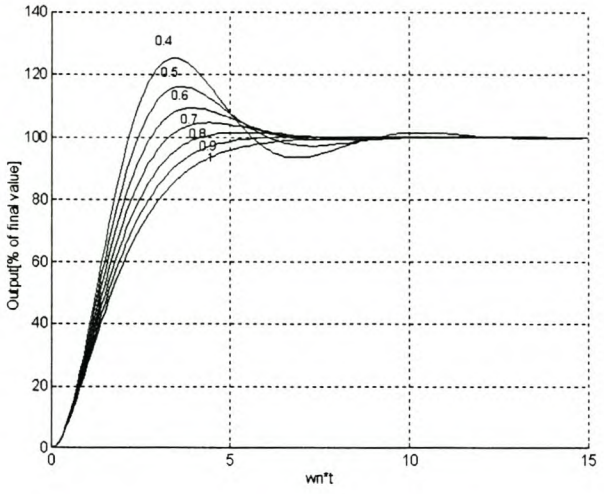

Figure 6-7 Normalised Loop parameters

If a settling time of 10ms is specified, the product $\omega_n * t_s$ will give 6.3. From the figure it can be seen that a loop with a damping ratio of 0.9 will settle to less than 5% for $\omega_n t=5$. To limit the loop overshoot at the expense of a slower settling time, it was decided to design a critically damped loop with a damping factor of 1.

From these values and the average value of the N-counter (5800) the value of τ_1 and τ_2 can be calculated as $3.1*10^{-3}$ and $2.4*10^{-3}$ respectively.

These values, together with the definition of τ_1 and τ_2 and a 330nF capacitor, lead to values of 2.21kΩ and 7.1kΩ for R_1 and R_2 respectively. When practical values of 3.9kΩ and 10kΩ are used, a natural frequency of 82.4Hz, and a damping ratio of 1.06 are observed leading to the step response of *Figure 6-8*.

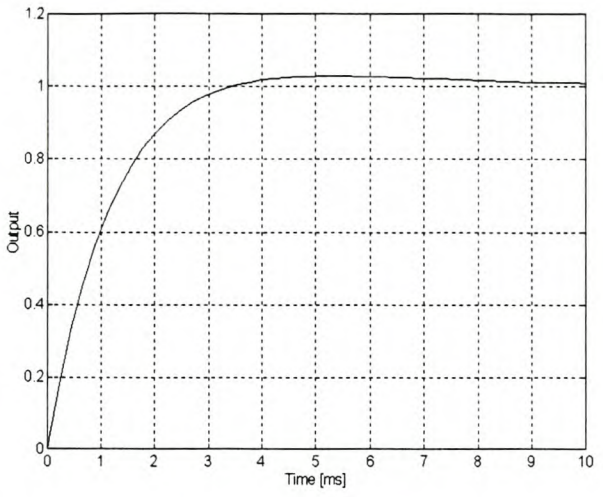

Figure 6-8 System Step response

As can be seen the system have settled to a value very near to its final value at a time of 10ms after a step response has been applied.

6.2.5. Summing amplifier

A LM358 operational amplifier from ***National Semiconductor***[6] has been used to buffer the audio input of the synthesiser.

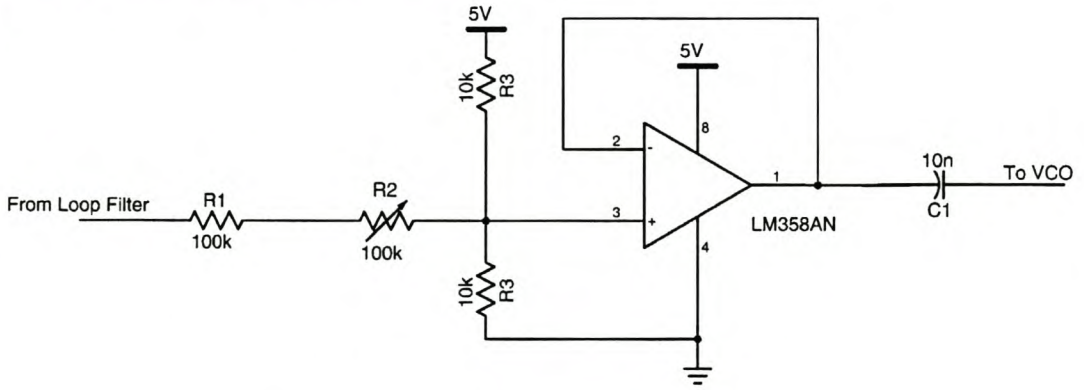

Figure 6-9 Audio input buffer

The variable resistor R2 is included to adjust the amplitude of the signal to ensure a maximum frequency deviation of 3kHz.

6.2.6. Output Amplifier

A MAR-6 amplifier is used to step up the output of the synthesiser to levels needed by the power amplifier module as is illustrated in *Figure 6-10*. The module has output and input impedance of 50Ω and a maximum gain of 20dB at 145MHz[8].

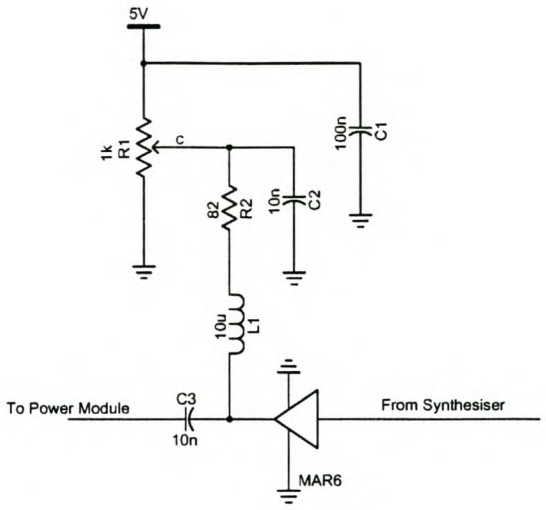

Figure 6-10 Coupling Amplifier

The amount of amplification of the MAR-6 is controlled by the bias current applied to it. Variable resistor R_1 can be used to control this current, and resistor R_2 is included to limit the current to a maximum of 50mA

Capacitors C_1 and C_2 are included to decouple the supply voltage, while capacitor C_3 couples the coupling amplifier to the power amplifier module. Inductor L_1 is included to limit interference to the amplifier voltage source.

6.3. RF Power Amplifier Module

A ***Mitsubishi*** linear power amplifier module (M67755L)[9] is used to provide the necessary output power.

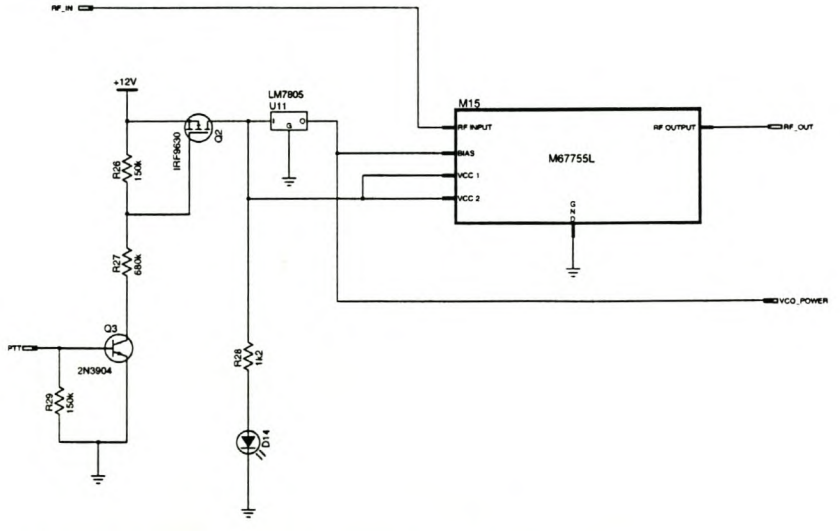

Figure 6-11 Power amplifier module

The module has been designed with an input and output impedance of 50Ω, and can therefore be connected directly to the coupling amplifier. The output power will depend on the amount of input power applied and will vary linearly between 0 and 7W for an input power varying between -10dBm and 5dBm.

A MOSFET switch is used to supply the M67755L module and the transmitter VCO with power when the push to talk (PTT) line is taken to 0V. A LM7805 voltage regulator is included to provide the power module with 5V of bias voltage and to supply power to the synthesiser VCO.

6.4. Transmit receive switching

The receiver is left connected to the antenna by default. Whenever the PTT control of the transmitter is activated, the power amplifier delivers RF power that is routed to the antenna. The receiver must be protected against this signals, as the high power levels will cause the LNA to saturate, and can even damage it. The 1N4148 signal diodes that are connected in parallel with the receiver input in *Figure 6-12* limit the voltage applied to the receiver to 0.7V, thereby protecting it. Received signals will typically be very small and will not be bigger than the 0.7V needed to reach the output of the power amplifier.

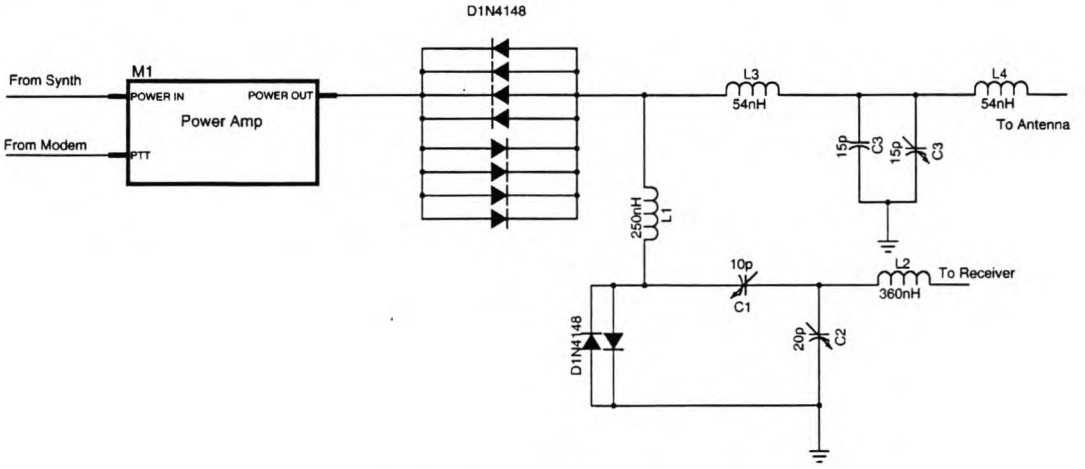

Figure 6-12 Antenna Switch

The purpose of the matching inductors L_1, L_2 and capacitors C_1, C_2 are to match the 50Ω antenna input to 50Ω as seen by the receiver input.

The output power of the amplifier will generate a much bigger voltage than 0.7V into the 50Ω antenna easily forward biasing the serial signal diodes to reach the antenna.

To combat distortion introduced into the output signal of the power amplifier by the signal diodes, inductors L_3 and L_4 (formed by 4 turns of 1.68mm copper wire on a 7mm air-core former) form a simple low pass filter together with capacitor C_3. The filter was designed by matching the 50Ω power amplifier output to a 100Ω load (giving a Q of 1) and matching this load to a 50Ω antenna impedance. The filter response was measured on a ***Hewlett Packard*** HP8753C network analyser and its S_{21} response is shown in *Figure 6-13*.

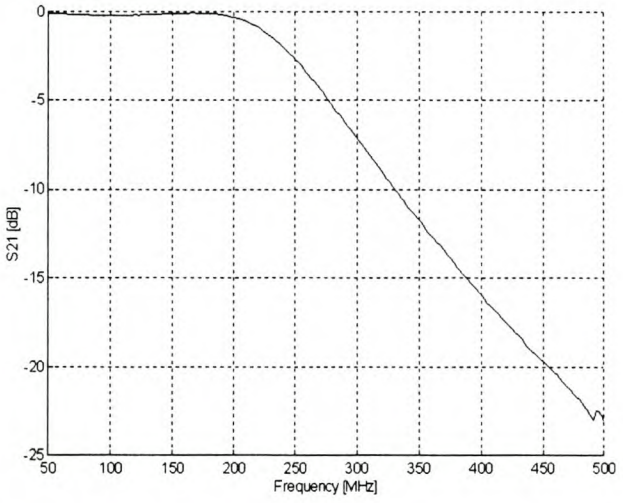

Figure 6-13 Output Filter - Frequency Response

As can be seen the filter provides 6dB of attenuation at 290MHz, and more than 18dB at 435MHz. The loss at 145MHz was measured to be less than 0.5dB.

6.5. Power Supply

With the exception of the 12V supply required by power amplifier, the complete transmitter system has been designed to operate from a 5V supply. Linear voltage regulators (LM3805) have been used to supply the receiver with the required supply voltage and decoupling capacitors have been included in the circuit to limit unwanted oscillations on the power supply lines. The power supply circuitry used is shown in *Figure 6-14*.

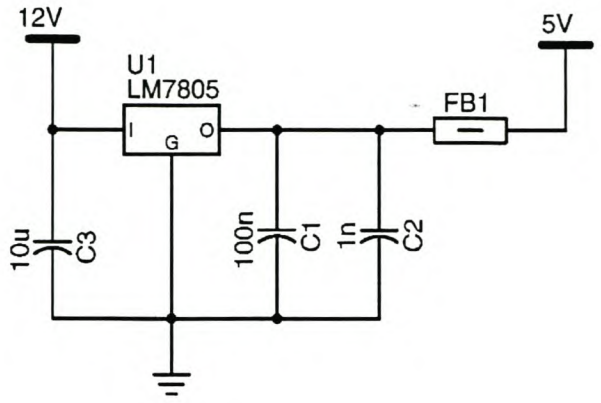

Figure 6-14 Power supply Circuitry

The 12V source supplying the transmitter must be able to deliver at least 4A of current if it is to be used at full RF output.

6.6. References

1. Motorola Inc *Motorola Communication Devices*, Motorola databook , 1995
2. *Phase-Locked Loop design fundamentals,* Motorola Application Note AN535, Motorola Inc, 1988
3. *The MC145170 in basic HF and VHF Oscillators,* Motorola Application Note AN1207, Motorola Inc, 1988
4. *BB809 VHF variable capacitance diode Data sheet*, Phillips semiconductors, May 1996
5. Motorola Inc, *Small signal transistors, FET's and diodes device data,* Motorola databook
6. National semiconductor, *National Operational Amplifiers Databook*, National Databook, 1995
7. *1N4148 High conductance Fast Diode - Data Sheet*, Fairchild Semiconductor, 1997
8. Mini Circuits, *RF Designer's Handbook*, Mini Circuits Data book, 1993

7. Data communications

The international standards organisation (ISO) has developed the reference model illustrated in *Figure 7-1* for the interconnection of different protocol layers[1,3] in a data communication network.

Layer	Function
7	Application
6	Presentation
5	Session
4	Transport
3	Network
2	Data Link
1	Physical

Figure 7-1 ISO protocol model

A data communication network will not necessarily contain all of the layers, and sometimes the layers are not clearly defined, but the model does help to understand the variety of available communication protocols better. The interpretation given in the following sections therefore, does not represent the only possible way to apply the ISO model to the field station, and is largely based on the defining document of the AX.25 link layer protocol[2].

For the basic field station, only the data link layer is necessary to interconnect the physical layer (the radio transmitter and receiver) with the application layer that gives the user access to the system. Some form of network layer protocol (like TCP/IP) may also be included, but is not strictly necessary.

A block diagram illustrating data communication in the field station is presented in *Figure 7-2*.

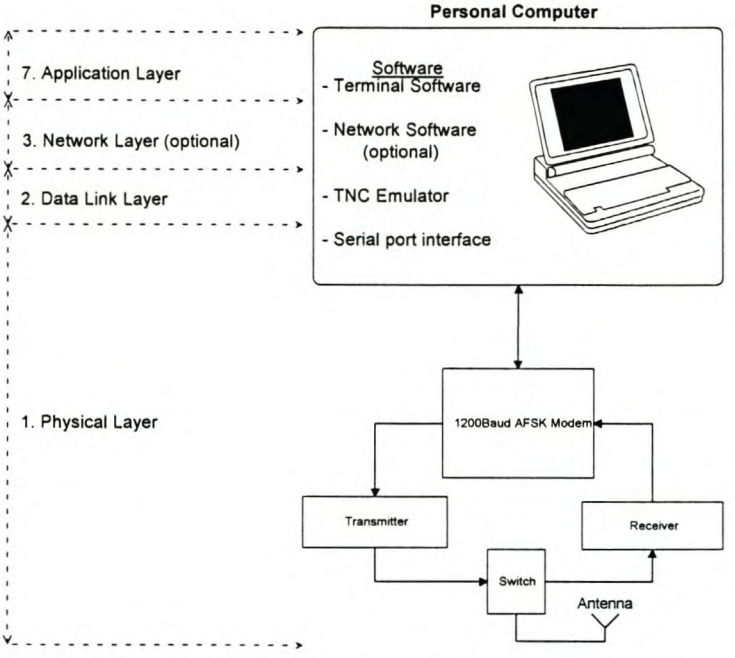

Figure 7-2 Field Station data communications

For the initial development of the field station, a personal computer will be needed to implement the higher level data protocols, and to connect to the hardware discussed in the previous chapters.

7.1. AFSK modem

Together with the receiver and transmitter, the modem forms the physical layer in the ISO model of *Figure 7-1*. The ***Texas Instruments*** TCM3105[4] is a single chip frequency-shift-keying (FSK) modem, capable of 1200baud data communication over a voiceband channel (limited to 3kHz bandwidth). The modem can be set up to function in either the Bell-202 or the CCITT-V23 standards as summarised in *Table 7-1* and shown in *Figure 7-3*.

Table 7-1 AFSK Modem Frequencies

	Bell-202	**CCITT-V23**
Mark frequency (1)	1200Hz	1300Hz
Space frequency (0)	2200Hz	2100Hz

The transmitting circuit provides one of two output frequencies, depending on the data applied to the digital input pin. The receiving circuitry converts the received analogue frequency tones to digital data. According to the data sheet [4], a 0.3Vpp input voltage

is recommended on the analogue input from the field station receiver, and a 1.9V voltage will be supplied to the field station transmitter.

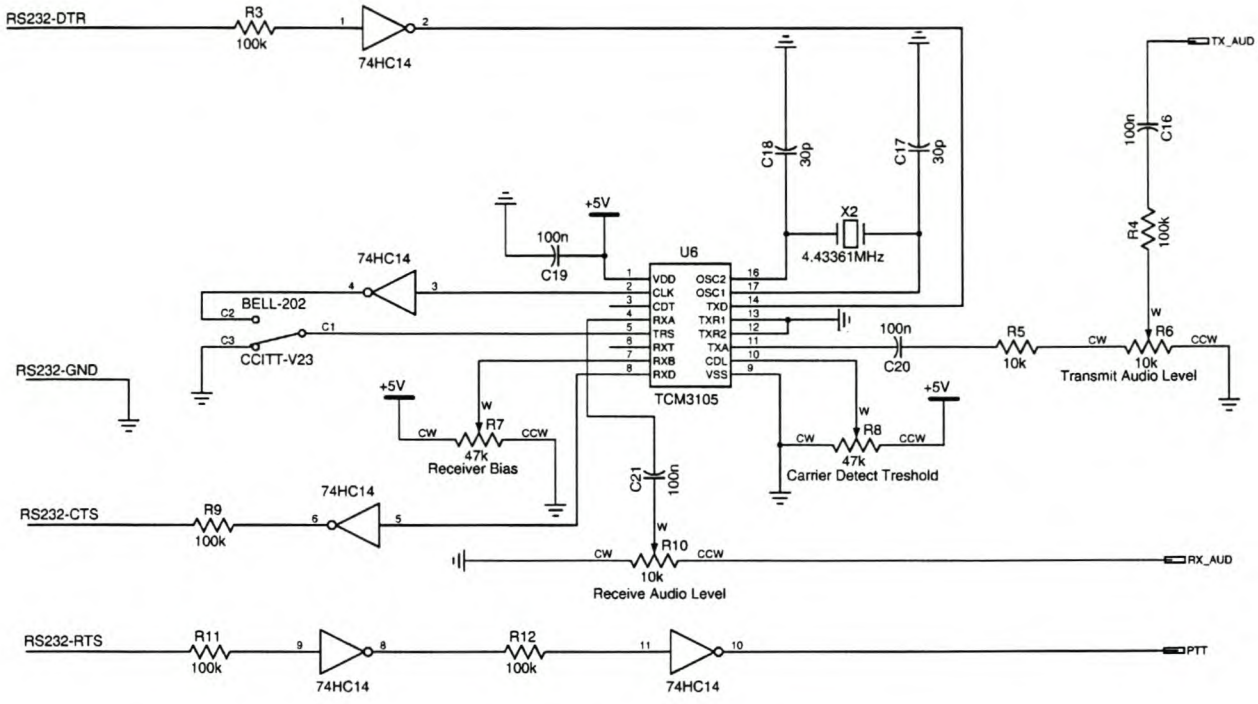

Figure 7-3 Modem Schematics

A 74HC14 inverter package will be used to convert the digital input and output of the TCM3105 to correct levels for use by the driver software running on the field station computer.

The modem baud rate is programmed to 1200baud by grounding pins 12 and 13. By switching pin 5 of the TCM3105 between ground and an inverted clock signal, the modem can be set up to operate in the CCITT-V23 or Bell-202 modes respectively with the corresponding FSK frequencies as indicated in *Table 7-1*.

The variable voltage applied to pin 7 of the TCM3105 adjusts the carrier level detection circuitry, and this value should be set between 0.6 and 0.8 times the supply voltage. A variable voltage at pin 7 of the TCM3105 sets the decision threshold of the final comparator of the receiver, and also influences the bias distortion of the output data. To adjust the voltage level to its optimum point, a continuos mark frequency must first be applied to the RXA input for a minimum of 11ms. Thereafter a continuous sequence of alternating mark and space frequencies must be applied, and

the resistor adjusted to give a digital output with a 50% duty cycle. The voltage value should be between 0.45 and 0.65 times the modem supply voltage.

7.2. Data link layer protocols

Data communication is not complete once the modem has converted between digital and analogue signals. In the unpredictable mobile satellite environment the use of a packet type protocol means that temporary loss of signal will result only in retransmission of a part of, rather than the complete message. Communication protocols are also necessary where multiple stations try to simultaneously access the same channel resources.

7.2.1. AX.25 Protocol

The amateur X.25 (AX.25[2]) data link layer protocol has been implemented on ***SUNSAT***, thereby giving radio amateurs across the world access to ***SUNSAT's*** store-and-forward services. The implementation of AX.25 on ***SUNSAT*** uses a first-in-first-out (FIFO) queue for reception and transmission. AX.25 users will therefore compete for the same channel and retransmissions will occur in the case of collisions.

7.2.1.1. Protocol definition

Serial modem data are converted to packets of data or frames, which are in turn made up by fields. The fields contain addressing, error-checking, control information and the data to be communicated. Three general types of frames are defined, as illustrated in *Figure 7-4*[2]. The supervisory frame (S-frame) contains link control information such as reception acknowledgements, or retransmission requests. The unnumbered frames (U-frame) are used to send additional control information, but can also be used to broadcast information to multiple recipients without the normal flow control. In this mode no provision is made for error correction. Information frames (I-frame) are used to convey user data, and are the only type of frame that carry a sequence number, to make requests for the retransmission of a specific frame possible.

Flag	Address	Control	Info	FCS	Flag
01111110	112/224 Bits	8/16 Bits	N*8 Bits	16 Bits	01111110

U and S frame construction.

Flag	Address	Control	PID	Info	FCS	Flag
01111110	112/224 Bits	8/16 Bits	8 Bits	N*8 Bits	16 Bits	01111110

Information frame construction.

Figure 7-4 AX.25 Frames

At the start and end of each frame are **flag fields**, which define frame boundaries. Bit stuffing is used to alter any other fields that may have the flag value (7E Hex) ensuring frame integrity.

The **address field** identifies the six-character radio callsigns of the sender and receiver, as well as any secondary station identifiers (SSID) that may be in use. Provision is also made for the routing from source to destination through relay stations or digipeaters.

The **protocol identifier (PID) field** defines the network layer protocol, if such a protocol is used.

The **information fields** are used to convey the user data between stations. The number of information fields in a frame can vary from 1 to 256.

The **frame check sequence (FCS) field** is a 16 bit number calculated with an algorithm published in the ISO3309(HDLC) document. The receiving station calculates this number according to the data received, and a matching FCS field will ensure error free data transmission.

7.2.1.2. Terminal node controllers (TNC's)

Terminal node controllers (TNC's) are devices that implement the AX.25 protocol, as shown in *Figure 7-5*.

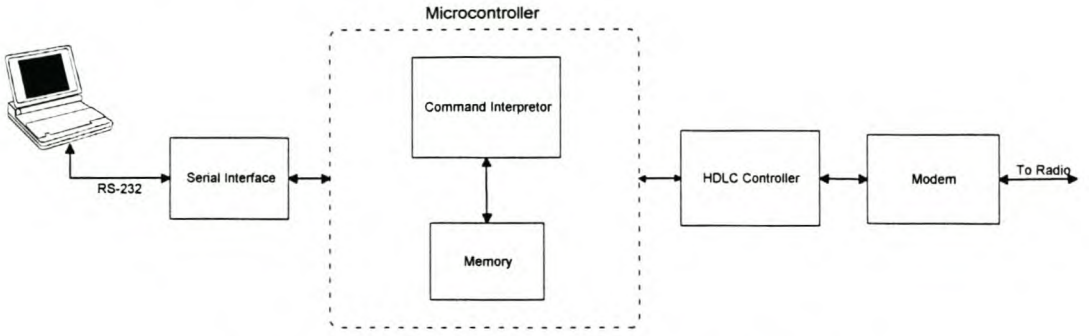

Figure 7-5 Terminal Node controller (TNC)

Serial RS-232 data are converted to logical voltage levels by the serial interface. The command interpreter handles user commands. The high level data link control (HDLC) unit handles the assembly and disassembly of the frames, and also computes the FCS field. The modem handles the conversion of the data to analogue voltages, which can be transmitted over the medium.

In the prototype field station only the TNC modem have been implemented in hardware, with the rest of the TNC functionality contained in software on a personal computer.

7.2.2. Future SRMA Services

The split-channel-reservation-multiple-access (SRMA)[7] protocol has been designed to maximise efficient data transfer between a single LEO satellite and multiple ground stations. Its has been designed specifically with the application of store-and-forwarding messaging via a satellite network in mind.

A satellite employing SRMA will send a continuous polling signal, inviting field stations to apply to upload relevant data. Responding field stations will be placed in a priority queue depending on the satellite movement, and their position in the footprint. Once at the top of the queue, the field station will be assigned the full channel bandwidth for a limited time.

Communication from the SRMA field stations will have a smaller number of collisions, and less protocol overhead. Throughput therefore should be greater, compared to AX.25. The software to implement SRMA exists, but it still needs to be

implemented on ***SUNSAT*** before it can be evaluated between the field station and the satellite.

7.3. Field Station software *

7.3.1. Terminal software

The terminal software provides the user interface for sending and receiving messages. Any one of several popular terminal packages like those used by radio amateurs can be used for the field station.

7.3.2. TNC emulator software

Software drivers that emulate the working of a TNC are freely available, and are employed in the field station. This software implements a basic TNC using the resources of the personal computer, and making extra hardware unnecessary. The modem found in a conventional TNC must still be provided, but this can easily be done with a serial interface like that discussed in *Section 7.1.*

The drivers that need to be loaded to emulate the TNC are *TFPCX.exe* and *TNCDED.exe* and are supplied in the diskette under the *TPK* subdirectory.

7.3.3. Frequency control software

Simple software to control the receiving and transmitting frequencies of the field station has been developed using the ***Pascal*** programming language[8]. This software is not critical for the field station operation, but gives the user instant readouts of the transmitting and receiving frequencies, as well as the ability to instantly program the field station synthesisers to new values.

7.3.4. Microcontroller software

Software for the ***Atmel*** 89c2051 microcontroller for controlling the field station synthesisers has been written in the 89c2051's assembly language according to the data sheets[9]. The microcontroller is also set up to display the selected frequencies on a small liquid crystal display (LCD) screen, to monitor a simple keyboard and to

---

* All the software developed for, and used by the prototype version of the fieldstation are listed in *Appendix C* and supplied on a 3.5" diskette with this document.

communicate with the frequency control software on the computer via a RS-232 serial interface.

7.4. References

1. Andrew S. Tenenbaum, *Modern operating Systems*, Prentice Hall International, 1992
2. Beech, Nielson, Taylor, *AX.25 Link Access Protocol for Amateur Packet Radio - Version 2.2* , ARRL, November 1997
3. American radio and Relay League, *The ARRL Handbook 68th Edition*, ARRL 1991
4. Texas Instruments, *TCM3105 FSK Modem Data Sheet*, 1994
5. Ben van der Merwe, *The AX.25 and SatFTP protocols: Design and Implementation*, Documentation for Honours project (Computer Science) at University of Stellenbosch, February 1998
6. Stan Horzepa, *Your Gateway to Packet radio*, ARRL,
7. F. Grobler, *The design and implementation of a store and forward communication system on the SUNSAT microsatellite*, Thesis for masters in Engineering (Electronic) at University of Stellenbosch, January 1994
8. Borland, *Turbo Pascal 6 - Library Reference*, Borland International, 1990
9. ATMEL, *AT89C2051 Data sheet*, ATMEL semiconductor, 1994

8. Measurements and Results

Measurements were used to compare the achieved field station performance with the specifications set out in *Chapter 4*.

8.1. Receiver Measurements

8.1.1. LNA performance

To determine the relationship between input and output power, the LNA was fed with a ***Hewlett Packard*** HP8647A signal generator, while the output spectrum was measured on a HP8590L spectrum analyser. The graph of *Figure 8-1* was obtained as a result of the measurement.

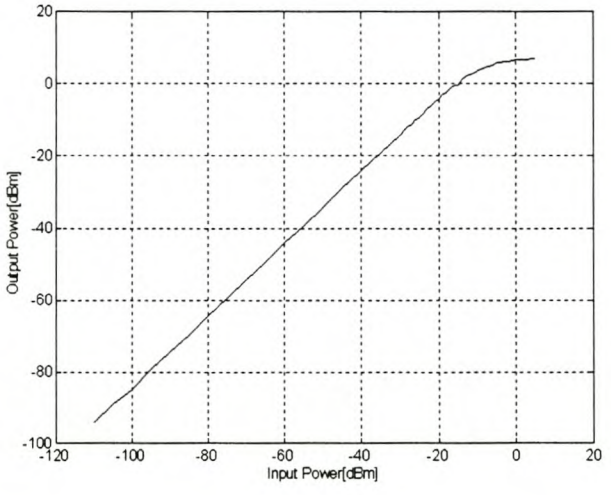

Figure 8-1 Input/output power relationship

The 1dB input compression point of the LNA was found to be around -14dBm.

To obtain the wideband frequency response of the LNA, it was measured on a ***Hewlett Packard*** HP8753C network analyser after a full two-port calibration and with -40dBm power input. The resultant S_{21} measurement is represented in *Figure 8-2*.

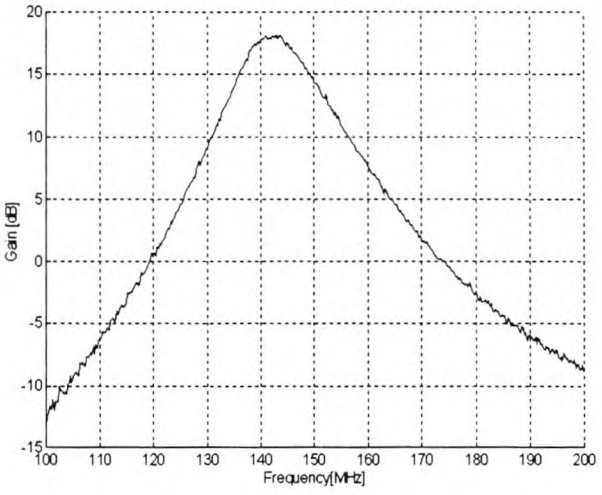

Figure 8-2 LNA - S_{21} response

The gain measured is higher than with the spectrum analyser at around 17.8dB. This value compares well with the computed gain of 18.4dB as was stated in *Chapter 5*. It is evident that the selectivity of the LNA alone will not give sufficient suppression of the image- and other unwanted frequencies to satisfy the spurious- response specification.

8.1.2. Sensitivity and spurious response

To measure the receiver's rejection of signals at unwanted frequencies, the setup shown in *Figure 8-3* was used[3].

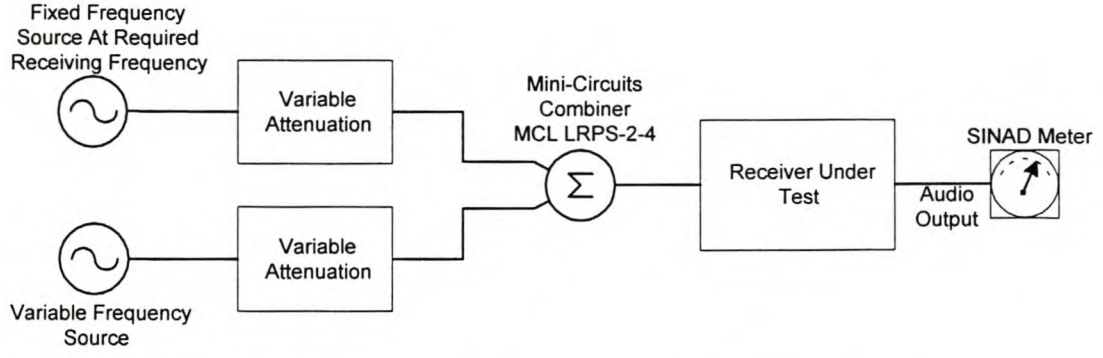

Figure 8-3 Setup for Spurious response Measurement

The fixed frequency source at the required frequency is applied to the receiver tuned to that frequency, and the attenuation adjusted to find the minimum signal strength that can be demodulated by the receiver to give a 12dB SINAD audio output. The applied signal strength, with the combiner loss taken into account, represents the receiver sensitivity. The variable frequency source is then also applied at a power

level equal to that specified for the spurious free response of the receiver. By sweeping the variable frequency source, frequencies can be identified where the second signal generator will degrade the sensitivity of the receiver. After the spurious frequencies have been identified, the sweep generator can be tuned to these frequencies, and its input power reduced to find the level where the degrading effect stops.

To measure the spurious response of the field station the variable generator was swept between 100MHz and 200MHz with a power level of -40dBm, and a 400Hz modulating signal, to distinguish it from the 1kHz signal modulating the fixed oscillator. In both cases a 3kHz deviation was used.

The first measurement was done with the signals feeding the receiver IC directly, and the results of *Figure 8-4* were obtained taking the attenuation caused by the combiner and cables into account.

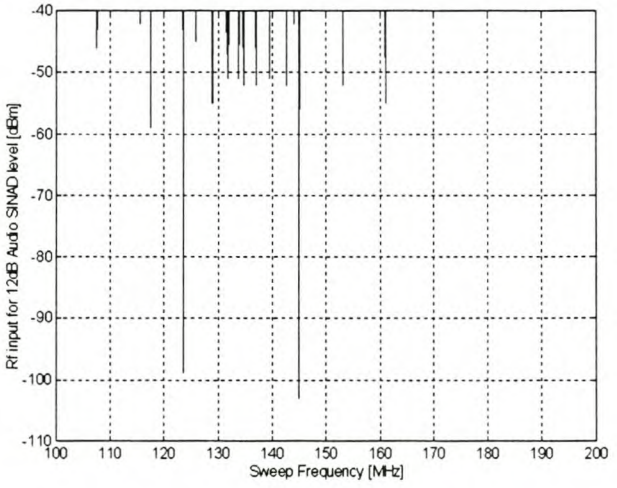

Figure 8-4 Spurious response - Receiver IC only

The sensitivity of the receiver IC alone can be seen to be -102dBm for a 12dB SINAD audio output. It is evident that the receiver alone offers very little attenuation of the image frequency at 123.6MHz with any signal bigger than -99dBm causing a degradation in the received audio level. Various other spurious frequencies can also be seen.

The next measurement was taken with the LNA and the input filter connected to the receiving circuit. The rest of the measurement setup stayed the same to be able to accurately compare the results.

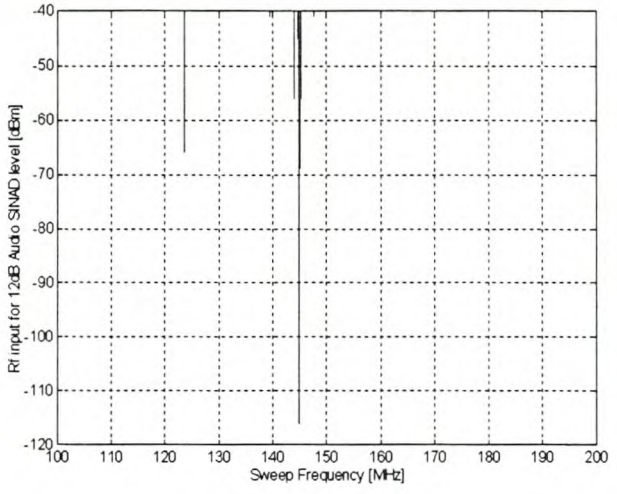

Figure 8-5 Spurious Response - complete field station receiver

The sensitivity of the receiver has been improved to -116dBm for 12dB SINAD audio output. The image rejection at 123.6MHz is 45dB. This does not fully satisfy the spurious response specifications.

A few other frequencies where an interference signal bigger than -40dBm would cause degradation of the wanted received signal were also measured, but these frequencies all fell within the passband of the input filter, and therefore in the frequency band allocated to amateur radio use.

Despite the above spurious frequencies where the field station receiver does not meet its specification, it continued to function satisfactory in an environment filled with very strong interference signals.

8.1.3. Synthesiser Sideband rejection

The VCO of the LO synthesiser does not have a RF output, but feeds the buffer amplifier directly, as was discussed in *Chapter 5*. To get an indication of the performance of the receiver synthesiser, it was therefore measured with an inductive probe connected to a ***Hewlett Packard*** HP8590L spectrum analyser. The results of *Figure 8-6* were obtained.

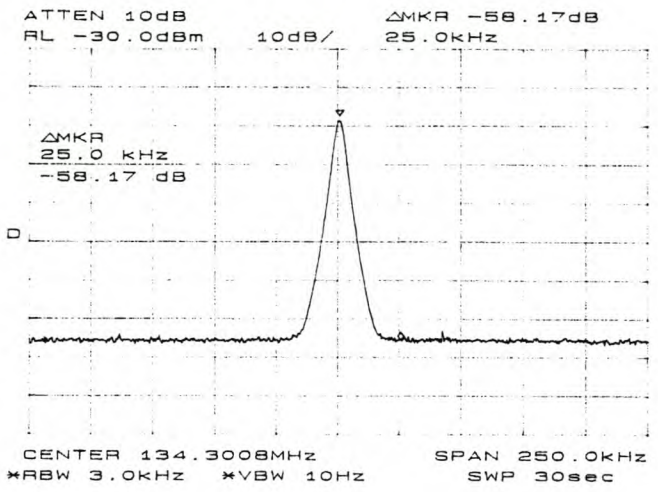

Figure 8-6 Receiver Synth - Sideband rejection

The sidebands were too small to be picked up by the probe, but it is evident from the result that the synthesiser does meet the specification of 50dB with a difference of 58dB between the fundamental frequency and the point 25kHz away.

8.2. Transmitter measurements

8.2.1. Synthesiser Performance

The transmitter synthesiser is critical for the performance of the field station transmitter, and therefore needs to function optimally. The RF output of the coupling MAR-6 amplifier was measured, by coupling it directly with the 50Ω input of a spectrum analyser to obtain the results of *Figure 8-7*.

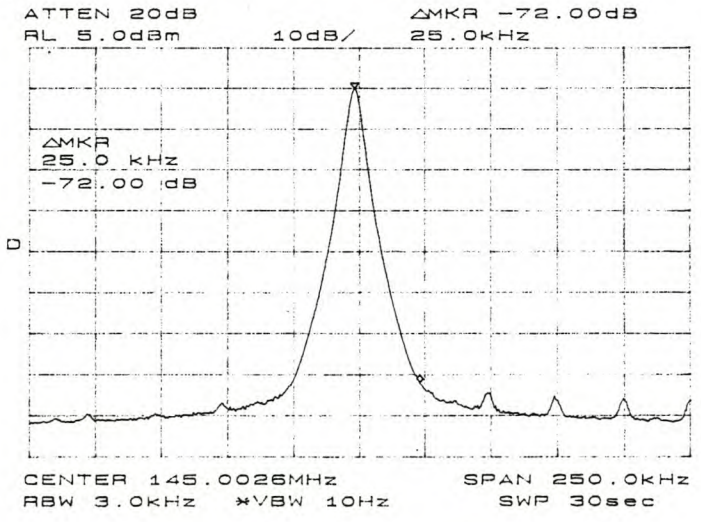

Figure 8-7 Transmitter Synth - Sideband rejection

A difference of 72dB was measured between the fundamental frequency output and the first sideband image 25kHz away, easily satisfying the specification of 60dB.

To get an indication of the phase noise present in the synthesiser output, a measurement was also taken on a narrow frequency span of 25kHz. As can be seen in the result of *Figure 8-8*, there is a 75dB difference in signal power between the fundamental and a point 12.5kHz away.

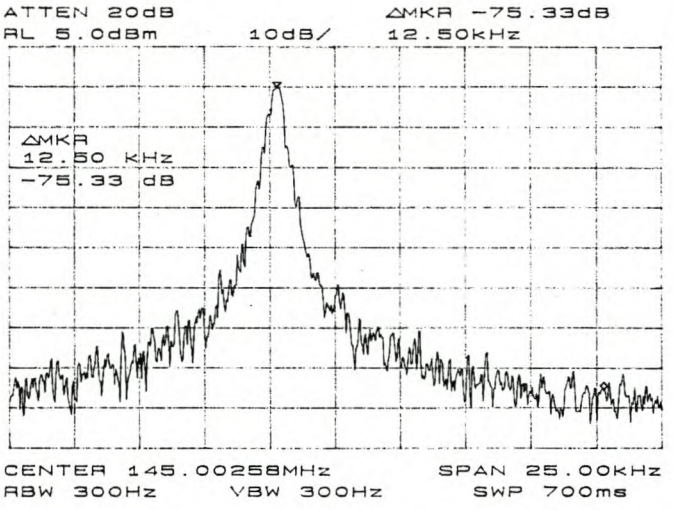

Figure 8-8 Transmitter Synth - Noise performance

The harmonic output of the coupling amplifier and the synthesiser is important because it will be fed directly to the power amplifier module, and high levels might cause damage to this unit. The harmonic output of the coupling amplifier adjusted to its full gain was measured with the spectrum analyser, obtaining the result of *Figure 8-9*.

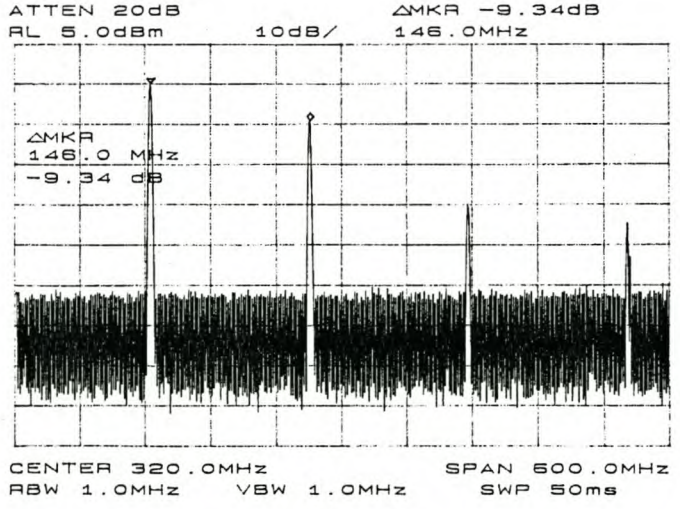

Figure 8-9 Transmitter Synth - Harmonics

There is 9dB power difference to the second harmonic at 290MHz, and more than 30dB to the third and fourth at 435MHz and 580MHz respectively.

8.2.2. Lock Time

The time it takes for the transmitter phase locked loop to acquire lock is very important, as this will be the main limiting factor to decide the delay from the time a push to talk signal is sent to the transmitter, till it produces a modulated RF output.

To measure the synthesiser lock time, a storage oscilloscope was connected to the control voltage of the transmitter VCO and the lock time measured as is shown in *Figure 8-10*.

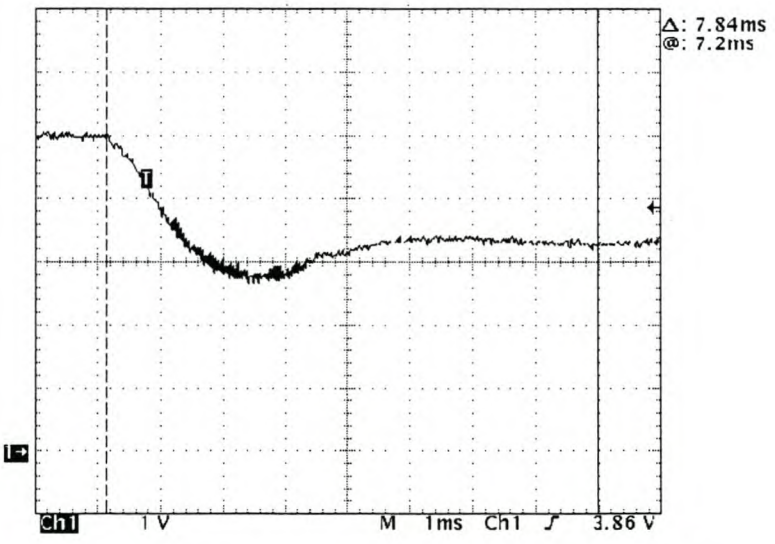

Figure 8-10 Transmitter Synth - Lock Time

The measurement represents a worst case scenario where the synthesiser has to lock at initial VCO switch on, and it is evident that lock is achieved in less than 8ms satisfying the lock specification of 10ms. The fact that more signal overshoot can be seen than the synthesiser has been designed for can be understood when the influence of the oscilloscope input impedance on the loop filter is taken into account.

8.2.3. Power amplifier performance

In order to evaluate the performance of the M67755L power module, it was fed with a signal generator at 145MHz, and its current consumption and output power were measured. The results of the measurement are given in *Figure 8-11* with the solid line representing output power, and the dotted line current consumption.

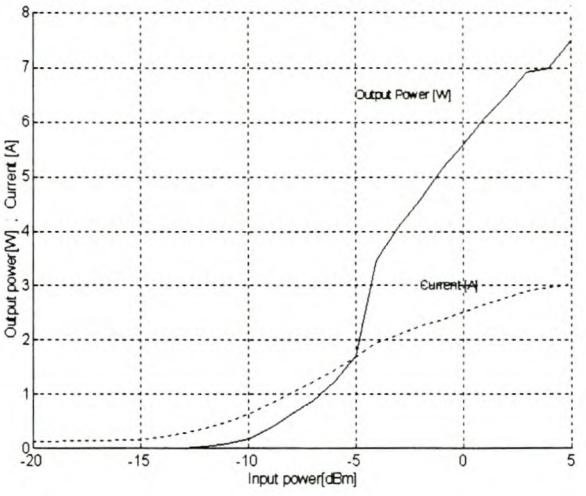

Figure 8-11 Power Amplifier - Amplitude and Current response

It is evident that the power module is capable to generate between 1 and 7W of RF output power for an input power range between -10dBm and 5dBm. The power supply must be capable of supplying 3A if the maximum power output is required. The efficiency of the power amplifier is about 30%.

The harmonic content of the output signal was measured on a ***Hewlett Packard*** HP8590L the result of the measurement is shown in *Figure 8-12*.

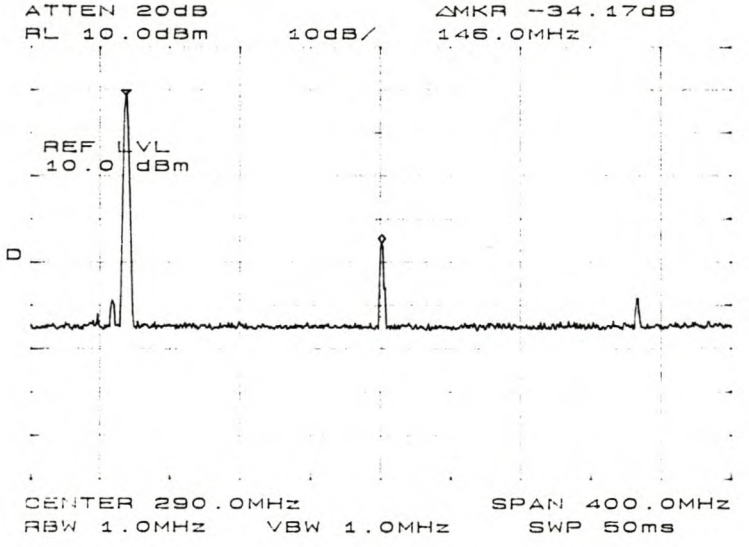

Figure 8-12 Power amplifier - Harmonic content

The difference between the power levels between the fundamental signal at 145MHz, and the second harmonic at 290MHz, is 34dB, while the difference to the third harmonic at 435MHz is about 48dB.

8.3. Data communication performance

The completed field station was used to transmit and receive files between its controlling computer and a remote computer coupled to a TNC and a radio transceiver. While this validated the functionality of the field station, software updates still need to be done to the ***SUNSAT*** flight software before the field station can be used in earth-satellite link.

8.4. References

1. Phase noise measurement of Z-Com VCO's, Application Note AN-109, Z~communications Inc, 1997
2. *M67755L Mitsubishi RF Power Module Data Sheet*, Mitsubishi Inc, November 1997
3. J.J. Roux, *The design of a VHF and UHF Receiver Front-end for the SUNSAT micro satellite,* Thesis for masters in Engineering (Electronic) at University of Stellenbosch, January 1998
4. *The MC145170 in basic HF and VHF Oscillators,* Motorola Application Note AN1207, Motorola Inc, 1988

9. Conclusions and recommendations

9.1. Conclusions

The breadboard design and practical evaluation of a field station for mobile LEO satellite communication has been completed successfully. A study of existing satellite communication systems employing LEO satellites, as well as the physical phenomena, influencing the VHF communication link between earth and such satellites was done. This was used to determine the specifications needed for a functional field station before work on the different units of the field station was started. The design entailed work on a receiver, transmitter and modem unit as well as the writing and testing of the necessary software on a controlling personal computer. VHF frequency synthesisers design was also studied.

The field station design makes use of the VHF Amateur Radio frequencies (144-146MHz) and the AX.25 Amateur Radio link layer protocol, making it compatible with the ***SUNSAT*** microsatellite.

It was proved that it is possible to build a field station that satisfies the requirements for LEO satellite communication for less than R1000. This makes it possible to fulfil the potential for economically viable store-and-forward type data communications through ***SUNSAT*** or similar satellites.

Table 9-1 presents a summary of the performance of the field station.

Table 9-1 Field Station Performance

Receiver	
Frequency Range	144-146MHz
Sensitivity	-115dBm for 12dB SINAD
Modulation	NBFM (3kHz deviation)
Spurious Response	-40dBm
Image rejection	45db
Power consumption	440mW
Transmitter	
Frequency Range	144-146MHz
Power Output	5W
Modulation	NBFM (3kHz deviation)
Transmit Cycling	10ms
Sideband rejection	72dB

Power consumption	75mW (Standby)
	1 to 40W (Transmitting
Data Communication	
Data Rate	1200 Baud
Modulation Type	AFSK
Link Layer Protocol	A.X. 25

9.2. Cost Breakdown

A breakdown of the cost of the components of the field station is given in *Table 9-2*.

Table 9-2 Field Station - Cost Breakdown

Description	Price [R]
M677551 Power amplifier mudule	390
MC145170 Synthesiser IC	20
MC3363 Receiver IC	30
Toko RF Filter	50
LM386 Audio Amplifier	5
TCM3105 Modem IC	40
Mar 6 – RF amplifier	15
Keypad	15
Powertip 16*2 Display Unit	50
Atmel 89c2051 microcontroller	12
Other Components	200
Total	847

These values are given only as a rough estimate and may vary over time, especially as the actual values may depend on foreign exchange rates.

9.3. Recommendations

In the design of the field station several modular building blocks were completed. Some of the components used in the building blocks are on the verge of replacement by newer technology. This newer technology will have to be implemented in the field station before a final commercial version thereof can be developed.

9.3.1. Obsolete Technology

9.3.1.1. BF981 Dual Gate MOSFET

The BF981 dual gate MOSFET is very difficult to obtain and will therefore not be a good choice for use in a final version of the field station. Several replacement MOSFET transistors exist that can be used as the active device in a LNA for the field station receiver. An example of this is the BF991 manufactured by ***Philips***.

9.3.1.2. TCM3105 AFSK Data modem

The TCM3105 Data modem from ***TEXAS Instruments*** is obsolete, but still remains available as it was used extensively in a large number of products throughout the world. If a new modem IC is needed for the field station, the FX614 from ***CML Semiconductor Products*** can be investigated.

9.3.1.3. MC3363 Receiver IC

Motorola recently announced the new MC13515/6 range of receiver IC's to replace the MC3362/3 IC's used in the field station. These newer generation IC's offer improved performance and reduced prices.

9.3.2. Evaluation of New Technology

9.3.2.1. M67755L - Power Amplifier module

The Power amplifier module functioned satisfactorily and in accordance with its data sheets, providing a convenient way of providing enough RF output power to communicate with a LEO satellite. It is the single most expensive component of the field station and will therefore have a big influence its final price. Similar modules with less gain but at about two thirds the price of the M67755L exist and need to be investigated. The use of such a unit will require a coupling amplifier capable of higher output power to drive the module.

9.4. Further development

9.4.1. Further Receiver Development

The performance of the field station receiver falls slightly short of the specifications set out in *Chapter 4*. Better sensitivity will mean the field station will be able to receive the signals transmitted from the satellite for a bigger part of the pass, making the transfer of bigger amounts of data possible.

Transmissions with high power levels on the spurious frequencies of the receiver may cause it to stop functioning. More attention therefore needs to be given to try and improve the spurious response of the receiver.

9.4.2. Packaging

To create a marketable field station some further work remains to be done. The circuit diagram presented in this document needs to be implemented on a properly designed

printed circuit board (PCB). Packaging of the field station in a suitable container must be completed and some form of lightning protection needs to be implemented before the field station can be deployed with confidence in remote areas.

9.4.3. Software development

The control software for the field station can be improved making it more user friendly, and incorporating all of the drivers necessary for an AX.25 session. Currently some research is also being done to implement the AX.25 protocol in a microcontroller[1]. If this can be done, the field station can be redesigned to function without a personal computer.

9.4.4. Antenna Design

The implementation of an antenna more suitable for satellite communication can greatly improve the performance of the field station. Such an antenna should be capable of circular polarisation, giving a 3dB improvement in received signal power over the current design. A more suitable gain pattern will eliminate the null in the monopole gain pattern for direct overhead passes and also give less gain for low elevation angles. This characteristic will minimise interference by terrestrial sources.

9.4.5. SRMA implementation

A previous study[2] showed that SRMA is a more effective protocol to use between a store and forward satellite and a field station. If this protocol is to be implemented between the field station and the ***SUNSAT*** microsatellite, the necessary software for both ends will need to be written.

9.5. References

1. John Hansen, *PIC-et Radio: How to send AX.25 UI frames using inexpensive PIC Microprocessors*, 17th ARRL and TAPR Digital communications Conference, 1998
2. F. Grobler, *The design and implementation of a store and forward communication system on the SUNSAT microsatellite*, Thesis for masters in Engineering (Electronic) at University of Stellenbosch, January 1994

9.6. Complete set of references

1) *1N4148 High conductance Fast Diode - Data Sheet*, Fairchild Semiconductor, 1997

2) American radio and Relay League, *The ARRL Handbook 68th Edition*, ARRL 1991
3) Andrew S. Tenenbaum, *Modern operating Systems*, Prentice Hall International, 1992
4) ATMEL, *AT89C2051 Data sheet*, ATMEL semiconductor, 1994
5) Barry Millar, *Satellites free the mobile phone*, IEEE Spectrum, March 1998-09-28
6) *BB809 VHF variable capacitance diode Data sheet*, Phillips semiconductors, May 1996
7) Beech, Nielson, Taylor, *AX.25 Link Access Protocol for Amateur Packet Radio - Version 2.2* , ARRL, November 1997
8) Ben van der Merwe, *The AX.25 and SatFTP protocols: Design and Implementation*, Documentation for Honours project (Computer Science) at University of Stellenbosch, February 1998
9) Borland, *Turbo Pascal 6 - Library Reference*, Borland International, 1990
10) D.F. Visser, *A high frequency Phase locked loop stabilised oscillator (Afrikaans)*, Report of final year project for degree in engineering (Electronic) at University of Stellenbosch, November 1994
11) F. Grobler, *The design and implementation of a store and forward communication system on the SUNSAT microsatellite*, Thesis for masters in Engineering (Electronic) at University of Stellenbosch, January 1994
12) F. White, *A miniature Crystal controlled FM transmitter (Afrikaans)*, Thesis for masters in Engineering (Electronic) at University of Stellenbosch, Oct 1992
13) Floyd M. Gardner, *Phaselock techniques - Second Edition*, Wiley and Sons, , 1979
14) Globalstar Web Site, http://www.globalstar.com
15) H.L. Krauss, C.L. Bostian & F.L. Raab, *Solid State radio engineering*, John Wiley and Sons Inc., 1980
16) Hall, Barclay & Hewitt, *Propagation of radiowaves*, The institute of Electrical Engineers, 1996
17) International Telephone and Telegraph Corporation, *Reference data for radio engineers 6th Edition*, Howard W. Sams Co., 1975
18) Iridium Web Site, http://www.iridium.com
19) J. Encinas, *Phase locked loops*, Chapman and Hall, 1993
20) J.J Roux, *The design of a VHF and UHF Receiver Front-end for the SUNSAT micro satellite*, Thesis for masters in Engineering (Electronic) at University of Stellenbosch, January 1998
21) JJ du Plooy, *An agile frequency modulated transmitter using the phase-locked loop*, Thesis for masters in Engineering (Electronic) at University of Stellenbosch, February 1973
22) John Brannegan, *Space radio handbook*, RSGB, 1990
23) John Hansen, *PIC-et Radio: How to send AX.25 UI frames using inexpensive PIC Microprocessors*, 17th ARRL and TAPR Digital communications Conference, 1998
24) M. Gruber, *QST Product Reviews: A look behind the scenes*, QST-Magazine, October 1994
25) *M67755L Mitsubishi RF Power Module Data Sheet*, Mitsubishi Inc, November 1997
26) Martin Davidoff, *The satellite experimenter's handbook - 2nd Edition*, ARRL, 1990
27) Mini Circuits, *RF Designer's Handbook*, Mini Circuits Data book, 1993

28) Mostert & Milne, SUNSAT: Solutions for store and forward communication
29) Mostert, Schoonwinkel & Milne, *Pre-flight performance of the communication payloads on SUNSAT, South Africa's first microsatellite*, 8th Bi-annual Conference & Exhibition on Telecommunications in Southern Africa, 1997
30) Motorola Inc *Motorola Communication Devices*, Motorola databook , 1995
31) Motorola Inc, *Small signal transistors, FET's and diodes device data,* Motorola databook
32) Motorola Inc, *VHF Narrowband FM Receiver Design,* Motorola Application Note AN980, 1988
33) Murata LDT, *90' Murata Products*, Murata databook, 1980
34) N.J.J Bornman, *Design of an antenna system for the VHF communication link of the SUNSAT micro satellite*, Thesis for masters in Engineering (Electronic) at University of Stellenbosch, November 1993
35) National semiconductor, *National Operational Amplifiers Databook*, National Databook, 1995
36) ORBCOMM Global L.P., *ORBCOMM System Overview*, ORBCOMM Document A80TD0008 – Revision B
37) P van der Westhuizen, *A VHF and UHF receiver for the SUNSAT microsatellite (Afrikaans)*, Thesis for masters in Engineering (Electronic) at University of Stellenbosch, January 1994
38) Paul H Young, *Electronic communication techniques– Third edition*, Prentice Hall International edition, 1994
39) Phase noise measurement of Z-Com VCO's, Application Note AN-109, Z~communications Inc, 1997
40) *Phase-Locked Loop design fundamentals,* Motorola Application Note AN535, Motorola Inc, 1988
41) Phillips Inc, *Field effect transistors*, Phillips databook, January 1981, July 1985 and July 1987
42) Ramo, Whinnery & Van Duzer, *Fields and waves in communication electronics*, Johan Wiley and Sons, Third Edition, 1994
43) Robert E. Collin, *Antennas and radiowave propagation*, Mcgraw-Hill international student edition 1985
44) Serway, *Physics for scientists and engineers – Third edition*, Sauders College publishing, 1992
45) South African Telecommunications Regulatory authority (SATRA), *RSA Frequency Allocations*, CSIR, March 1998
46) Stan Horzepa, *Your Gateway to Packet radio*, ARRL,
47) Stephen J. Erst, *Receiving Systems Design*, Artech House Inc, 1985
48) Supertex Inc, *VN10K N-Channel enhancement-mode vertical DMOS FET's datasheet*, 1995
49) Teledesic Web Site, http://www.teledesic.com
50) Texas Instruments, *TCM3105 FSK Modem Data Sheet*, 1994
51) *The MC145170 in basic HF and VHF Oscillators,* Motorola Application Note AN1207, Motorola Inc, 1988
52) William F. Egan , *Frequency Synthesis by phase lock*, Wiley and Sons,1981

Appendix A - MATLAB listing for Link Budget Calculations

A.1. LBUDGET.M

```
%Calculate and plot the combined factors
%    that influence the link budget

clear
%------------
%Constants
%------------
TX=1;
            % TX power in Watt for worst case
TXMax=5;
            % TX power in Watt for best case
TXdBm=10*log10(TX/1e-3);
TXMaxdBm=10*log10(TXMax/1e-3);
fop=145e6;
            %operasional Frequency
%-------------------------------------------------------------
%Determine the losses due to different Phenomena
%-------------------------------------------------------------
Ploss

%-------------------------------------------------
%Determine the respective antenna gains
%-------------------------------------------------
Antgain

%-----------------------------
%Calculate the Total link budget
%-----------------------------
%Power RX = TX power + TX antenna + RX
antenna- pathloss  - 3dB polarization loss

PrecMin = TXdBm+gainRecdB+GainTrans-LossMax;
PrecMax = TXMaxdBm+gainRecdB+GainTrans-
LossMin;

for i = 1:length(elevationdeg)
            REC(i)=-117;
end

%---------------------
%Plot Received Power
%---------------------
clf
grid on
zoom on
hold on

plot(elevationdeg,PrecMax,'b')
plot(elevationdeg,PrecMin,'b:')
plot(elevationdeg,REC,'b--')
text(120,-97,'Best Case')
text(120,-110,'Worst Case')
text(120,-120,'Receiver sensitivity')
```

A.2. PLOSS.M

```
% Calculate the slant range for a satellite pass
% also calculate the pathloss for this slantrange
% owing to the following phenomena:
% - Free Space loss
% - Atmospheric absorbtion
% - Ground Reflection

%-----------------------------
% Enviorenment setup
%-----------------------------
%clear
format compact

%-----------------------------
% Constant setup
%-----------------------------
r = 6378.4;             % earths radius equator (km)
    % space comms systems - R Filip. and E. Muehl.
M = 5.98e24;                    % Mass of earth [kg]
G = 6.6725985e-11;
% Universal gravitational constant [N.m^2/kg^2]
% Physics for scientists and engineers - Serway
satmax    = 850;
            % max altitude of satellite to earth [km]
satmin    = 650;
            % min altitude of satellite to earth [km]
atmos     = 100;
% Distance through buttom part of atmosphere [km]
TXpowerdBm=30;
% Worst case transmitted power of SUNSAT
microsatellite = 1W
c = 2.99792458e8;
            % speed of EM wave in vacum [m/s]
P_Pol=3;
            % polazisation loss [dB]
elevationdeg = linspace(0,180,360);       % elevation
angle
elevation = (pi*(elevationdeg/180));
% convert to radians

%---------------------
% General Calculations
%---------------------
Pathsatmax = 2*pi*(r*1e3+satmax*1e3);
            %[m]
Pathsatmin = 2*pi*(r*1e3+satmin*1e3);
            %[m]
Vsatmax = sqrt(G*M/(r*1e3+satmax*1e3));
            %[m/s]
Vsatmin = sqrt(G*M/(r*1e3+satmin*1e3));
            %[m/s]
Tpathsatmax = Pathsatmax/Vsatmax/60;
            %[min]
Tpathsatmin = Pathsatmin/Vsatmin/60;
            %[min]

%-----------------------------
% Calculation of slantrange [km]
%                       - slantrange^2 + r^2 =
(r+satmax)^2 - Pythagorys
%-----------------------------
% Maximum points

slantrangemax = sqrt(2*r*satmax + satmax^2);
earthanglemax = atan(slantrangemax/r)*180/pi;
Tsatmax=(2*earthanglemax/360)* Tpathsatmax

% Slantrange as a function of elevation angle
% sin(e+90)   sin(satangle)
% --------- = ------------         - sine law
% r+satmax         r
% angle which the slantrange makes with the z-axis
of the satellite
```

```
satanglemax =
asin((r/(r+satmax))*sin(elevation+pi/2));
earthanglemax = pi/2-satanglemax-elevation;
            % angles in a triangle = 180 degrees

% the range to the satellite as it passes overhead

% slantrangemax            r
%--------------     = ------------     - sine law
% sin(earthanglemax)    sin(satanglemax)

slantrangemax =
sin(earthanglemax)*r./(sin(satanglemax));
slantrangemax(1,(length(elevation)/2)) = satmax;
% when satellite is overhead

slantrmax = slantrangemax';

%-----------------------------
% Calculation for new altitude
%-----------------------------
% Maximum points
slantrangemin = sqrt(2*r*satmin + satmin^2);
earthanglemin = atan(slantrangemin/r)*180/pi;
Tsatmin=(2*earthanglemin/360)* Tpathsatmin

satanglemin =
asin((r/(r+satmin))*sin(elevation+pi/2));
earthanglemin = pi/2-satanglemin-elevation;

slantrangemin =
sin(earthanglemin)*r./(sin(satanglemin));
slantrangemin(1,(length(elevation)/2)) = satmin;


%-----------------------------------
% Plot Slant range for both altitudes
%-----------------------------------
clf
grid on
hold on
zoom on
plot(elevationdeg,slantrangemax,'b')
plot(elevationdeg,slantrangemin,'b:')
title('Slant range of satellite')
xlabel('Elevation angle [degrees]')
ylabel('Distance from fieldstation [km]')
lt=['-';':'];
nm=['Apogee ';'Perigee'];
%bglegend(lt,nm)
%adhamlet
pause

%-------------------------------------------------------
% Calculation of distance covered through the
buttom part of atmosphere
%-------------------------------------------------------
satangle_atmos =
asin((r/(r+atmos))*sin(elevation+pi/2));
earthangle_atmos = pi/2-satangle_atmos-elevation;

slantrange_atmos =
sin(earthangle_atmos)*r./(sin(satangle_atmos));
slantrange_atmos(1,(length(elevation)/2)) = atmos;

%-----------------------------------
% Plot results
%-----------------------------------
clf
grid on
zoom on
hold on
%plot(elevationdeg,slantrangemax)
%plot(elevationdeg,slantrangemin)
plot(elevationdeg,slantrange_atmos,'b')
title('Slant range of satellite - lower Atmosphere')
xlabel('Elevation angle [degrees]')
ylabel('Distance through lower atmosphere [km]')
%adhamlet
pause

%-----------------------------------
% Plot satellite angle for min altitude
%-----------------------------------
clf
grid on
zoom on
hold on
satanglemindeg = (180*(satanglemin/pi))';
            %convert to degrees
plot(elevationdeg,satanglemindeg,'b')
title('Satellite angle at perigee')
xlabel('Elevation angle [degrees]')
ylabel('Satellite angle [degrees]')
%adhamlet
pause


%-----------------------------------------
% Calculate free space loss
%-----------------------------------------

%-----------------------------------
%          [4*pi*d]^2    [4*pi*d*f]^2
% P_FS     = [------]   =  [--------]
%          [lamda ]      [   c    ]
%-----------------------------------
P_FSMax = ((4*pi.*slantrangemax*1000*fop)/c).^2;
            % perigee and VHF
P_FSMin = ((4*pi.*slantrangemin*1000*fop)/c).^2;  %
apogee and VHF

P_FSdBMax = 10*log10(P_FSMax);
P_FSdBMin = 10*log10(P_FSMin);

%-----------------------------------
% Plot path loss for both altitudes
%-----------------------------------
clf
grid on
zoom on
hold on
plot(elevationdeg,P_FSdBMax,'b')
plot(elevationdeg,P_FSdBMin,':b');
title('Free space loss')
ylabel('Path Loss (dB)');
xlabel('Elevation angle (degrees)');
lt=['-';':'];
nm=['Apogee ';'Perigee'];
%bglegend(lt,nm)
%adhamlet
pause


%-------------------------------------------------
% Calculate and plot loss due to atmosperic
absorbtion
%-------------------------------------------------
P_AA = 0.005*slantrange_atmos;
            %acording to Collin - Loss=0.005dB/km
clf
grid on
zoom on
hold on
plot(elevationdeg,P_AA)
title('Atmosperic absorbtion - lower Atmosphere')
xlabel('Elevation angle [degrees]')
ylabel('P_loss [dB]')
pause
```

```
%-------------------------------------------------------------
% Calculate and plot loss due to ground reflection
according to Collin
%-------------------------------------------------------------
k=2*pi*c/fop;          %Wave constant
graze=linspace(0.001,5*pi/180);
          %elevation angles for first 5 degrees
height=1;              %Antenna Height above ground
F1=2*abs(sin(k*height*tan(graze)));
%Gain factor for first 5 degrees
F1dB=10*log10(F1);
height=2;              %Antenna Height above ground
F2=2*abs(sin(k*height*tan(graze)));
%Gain factor for first 5 degrees
F2dB=10*log10(F2);
height=5;              %Antenna Height above ground
F5=2*abs(sin(k*height*tan(graze)));
%Gain factor for first 5 degrees
F5dB=10*log10(F5);

%--- Compute vector for final calculation
height=1;              %Antenna Height above ground
Ff=2*abs(sin(k*height*tan(elevation)));
%Gain factor for elevation degrees
FfdB=-10*log10(Ff);
          %create vector with losses within first and
          %last 5 degrees of elevation
for n = 1:length(elevationdeg)+1
          if n < 10 | n> 711
                    P_GR(n)=FfdB(n);
          else
                    P_GR(n)=0;
          end %if
end %for
P_GR(length(elevation))=[];

clf
zoom on
hold on
plot(graze*180/pi,F1dB,'b')
plot(graze*180/pi,F2dB,'b:')
plot(graze*180/pi,F5dB,'b-.')
grid on
Title('Gain factor for small elevation angles')
xlabel('Elevation angle [degrees]')
ylabel('Gain factor [dB]')
lt=['- ';': ';'-.'];
nm=['1m';'2m';'3m'];
pause

clf
hold on
plot(elevationdeg,FfdB)
plot(elevationdeg,P_GR)
grid
pause

%-------------------------------------------------
%   Calculate the maximum total loss
%-------------------------------------------------
LossMax=P_FSdBMax+P_GR+P_AA+P_Pol;
LossMin=P_FSdBMin+P_GR+P_AA+P_Pol;
clf
hold on
plot(elevationdeg,LossMax,'b')
plot(elevationdeg,LossMin,'b:')
title('Total Atmospheric Loss')
ylabel('Total loss [dB]')
xlabel('Elevation [degrees]')
grid
text(140,147,'apogee')
text(140,135,'perigee')
%adhamlet
pause
```

```
%-----------------------------------
%   Calculate the maximum doppler shift
%-----------------------------------
clf
hold on
grid
%satanglemax(361)=0.01;
%satanglemin(361)=0.01;
anglemax=pi/2-satanglemax;
anglemin=pi/2-satanglemin;
Vrelmax=Vsatmax.*cos(anglemax);      %[m/s]
Vrelmin=Vsatmin.*cos(anglemin);      %[m/s]
plot(elevationdeg,Vrelmax)
plot(elevationdeg,Vrelmin)
xlabel('Elevation [Degrees]')
ylabel('V_relative [m/s]')
pause

clf
hold on
grid

Dopmax=(fop/c)*Vrelmax;      %[Hz]
Dopmin=(fop/c)*Vrelmin;      %[Hz]
plot(elevationdeg,Dopmax./1e3,'b')
plot(elevationdeg,Dopmin./1e3,'b:')
title('Doppler Frequency Shift')
xlabel('Elevation [Degrees]')
ylabel('f_doppler [kHz]')
text(151,-2700,'Apogee');
text(151,-3700,'Perigee');
```

A.3. ANTGAIN.M

```
%Calculate/ load the antenna gain patterns
%to be used in the total link budget

%clear
%ploss
clf
%elevationdeg = linspace(0,180,721);
% elevation angle
%elevation = (pi*(elevationdeg/180));
% convert to radians



%-------------------------------------------------------------
% Calculate Monopole radiation pattern - acording to
Ramo, Et Al
%-------------------------------------------------------------
theta = elevation-pi/2;

gain = 1.64*(((cos((pi/2)*cos(theta)))./sin(theta)).^2);

gainmax = 1.64;
gainmaxdB = 10*log10(1.64);

gainRecdB = gainmaxdB+10*log10(gain/gainmax);

%-------------------------------
% Plot Monopole radiation pattern
%-------------------------------
clf
grid on
zoom on
hold on
plot(elevationdeg,gainRecdB,'b')
disp('Monopole gain pattern')
xlabel('Elevation angle [degrees]')
ylabel('Antenna Gain [dB]')
pause

clf
axis('off')
disp('Monopole gain pattern')
%set(axes,'GridLineStyle',':')
polar(elevation,gainRecdB+(-1*min(gainRecdB)))
pause


%-----------------------------------------
% Load simulated data from Sunsat VHF antennas
%-----------------------------------------
load VHF_Data.txt
leer=VHF_Data;
Hoek=leer(:,1);
VHF_Gain=leer(:,2);

%-------------------------------
% Plot SUNSAT VHF radiation pattern
%-------------------------------
clf
set(axes,'GridLineStyle','-')
grid on
zoom on
hold on
plot(Hoek,VHF_Gain)
disp('SUNSAT VHF antenna gain pattern')
xlabel('Angle [degrees]')
ylabel('Antenna Gain [dB]')
pause

%-----------------------------------------------
% Determine Gain pattern for positive elevation
%-----------------------------------------------
clf
Hoek2=Hoek(Hoek<69)
Gain2=VHF_Gain(1:length(Hoek2))
plot(Hoek2,Gain2)
grid
pause
for i = 1:length(Hoek2)
        Gain3(length(Hoek2)-i+1) = Gain2(i);
        Hoek3(length(Hoek2)-i+1) = Hoek2(i);
end  %for
Gain3=Gain3';
Hoek3=Hoek3';
clf
hold on
a=max(Hoek2);
Hoek4=[Hoek3;-1*Hoek2(Hoek2>0)];
Gain4=[Gain3;Gain2];
Gain4(length(Gain4)/2)=[];
plot(Hoek4,Gain4,'*')
[p2,S2] = POLYFIT(Hoek4,Gain4,2);
[p4,S4] = POLYFIT(Hoek4,Gain4,4);
y2 = POLYVAL(p2,Hoek4);
y4 = POLYVAL(p4,Hoek4);
plot(Hoek4,y2,'r')
plot(Hoek4,y4,'g')

satanglemindeg=180*(satanglemin/pi);
GainTrans= POLYVAL(p4,satanglemindeg);
plot(satanglemindeg,GainTrans,'b')
pause

clf
zoom on
plot(elevationdeg,GainTrans,'b')
disp('Transmittor Antenna Gain')
xlabel('Elevation angle [degrees]')
ylabel('Antenna Gain [dB]')
grid
pause

%-----------
% Polar Plot
%-----------
clf
title('SUNSAT VHF antenna gain pattern')
angle = linspace(0,2*pi,length(VHF_Gain                ));
angle = angle+3*pi/2;
set(axes,'GridLineStyle',':')
polar(angle,VHF_Gain'+(-1*min(VHF_Gain)+4))
```

Appendix B - Frequency Synthesiser Design

A very basic requirement of most transceiver systems is a stable frequency source that can either be modulated to form a transmitter or mixed with a received signal in a receiver. The design of such an oscillator often forms a substantial part of the design effort of a product.

An attractive solution is the use of phase locked loop (PLL) frequency synthesisers, which give a very stable frequency reference, with the added advantage that the circuit can be easily programmed to tune the oscillator in discrete steps. However, the design of a phase locked loop system can present a host of its own problems. Several integrated circuits exist that can aid the designer, but a basic understanding of the working of a phase locked loop is still necessary for the proper design thereof.

B.1. Basic system

The basic phase locked loop is represented in *Figure B-1*. The synthesiser is made up out of a few discrete blocks, each with a specific function.

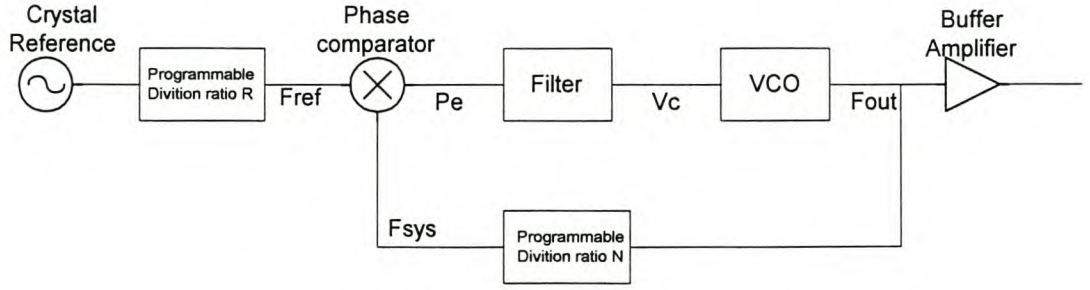

Figure B-1 Basic frequency synthesiser

The basic function of a phase locked loop frequency synthesiser is to lock the phase of a stable frequency source and that of a voltage controlled oscillator (VCO). In doing so the wideband oscillator will gain some of the desirable qualities of the stable frequency source. In a sense the PLL can be seen as a low pass filter that reduces the phase noise of the VCO. Digital dividers make it possible to design a loop with an output frequency that is exactly dividable by the reference frequency.

B.2. Loop components

In the following section the different loop components will each be discussed in more detail.

B.2.1. Crystal Reference

A stable crystal-based oscillator is used as frequency reference for the loop. Because of the high ratio of centre frequency to bandwidth or quality factor of a crystal oscillator, such oscillators are ideally suited for this function.

B.2.2. Reference Divider

A digital divider is used to divide the output of the crystal reference to the desired reference frequency. The frequency formed in this manner and serving as the input to the phase comparator will represent the finest frequency step in which the synthesiser can change its frequency. If the value of the divider is *N*, the output frequency of the synthesiser will be given by:

$$f_{out} = N.f_{reference}$$

Dual mode dividers are sometimes used to generate finer frequency steps.

Any phase jitter present in the reference oscillator will also be multiplied by *N* times, and this is the reason that a stable phase reference is so important for the operation of the PLL.

B.2.3. Phase comparator

The phase comparator will generate a voltage linearly proportional to the difference in phase between the reference and the VCO. Various different kinds of phase detectors can be used, with different characteristics, but for a typical analogue phase detector the output will be given by:

$$V_d = A\sin(P_d)$$

For small values of input phase the output of the phase detector can be represented by a constant gain K_d with the units of [V/rad].

For digital phase detectors it is important to use adequate filtering in the loop to suppress the sidebands that are generated by the typical switching waveforms of digital circuits.

B.2.4. Filter

The loop filter determines the loop characteristics of the PLL. Properties such as bandwidth, rise time and settling time can all be controlled by proper design of the loop filter. In *Section B.3* the effect of various filters on the loop performance will be discussed in more detail.

B.2.5. Voltage controlled oscillator (VCO)

The VCO is central in the operation of the PLL. It must be able to convert changes in voltage to changes in frequency. The characteristics of the VCO are also critical to the overall loop performance.

In the Laplace domain, a VCO is described by a perfect integrator in cascade with a constant gain. To understand why, it is important to remember the relationship between frequency and phase:

$$frequency = \frac{d}{dt}(phase) \qquad phase = \int frequecy.dt$$

The output of the VCO is a sinusoid with the following equation:

$$G(t) = A\sin(P(t))$$

In this equation P(t) describes the instantaneous phase of the signal. The frequency of the VCO is the rate of change of the instantaneous phase or:

$$f_{vco} = \frac{1}{2\Pi}\frac{d}{dt}(P_{vco}(t))$$

This equation gives rise to the following differential equation:

$$dt(P_{vco}(t)) = 2\Pi * f_{vco} * dt$$

which can be integrated to give the relationship between frequency and phase as:

$$P_{vco}(t) = 2\Pi \int f_{vco} dt + P_{vco}(t = 0)$$

For a constant frequency the equation becomes:

$$P_{vco}(t) = 2\Pi * f_{vco} * t + P_{vco}(t = 0)$$

This value can be substituted in the original equation to give:

$$G(t) = A\sin(2\Pi * f_{vco} * t + P_{vco}(t = 0))$$

The VCO is controlled by the control voltage $V_c(t)$. If f_o is defined as the output frequency with $V_c(t)=0$, and with the VCO in the linear part of its operation the output frequency is given by:

$$f_{vco} = f_0 + \frac{K_o V_c(t)}{2\Pi}$$

K_o represents the linear gain of the VCO. When this is substituted in the previous equation it can be seen that the output phase of the VCO is given by :

$$P_{vco}(t) = 2\Pi f_0 t + K_o \int V_c(t)dt + P_{vco}(0)$$

The Laplace transformation of a perfect integrator is given by 1/s, and therefore the frequency domain representation of a VCO is given by:

$$V_{vco}(s) = \frac{K_o}{s}$$

The value of K_o may be determined in a practical VCO by the following equation:

$$K_o = \frac{2\Pi(f_f - f_2)}{V_1 - V_2}$$

The unit of K_o is [rad/V/s].

B.2.6. Loop divider

The loop divider is a digital divider to divide the frequency output of the VCO to that of the frequency reference. For a locked PLL the frequency output of the VCO (f_{vco}) is related to the values of the loop divider and the reference frequency by the following equation:

$$f_{vco} = N * f_{ref}$$

The exact value of N will depend on the desired frequency output of the PLL, and will be programmed digitally. For equations that need the value of N the average value thereof can be used. This average value can be found by:

$$N_{avg} = \frac{f_{vco\_max} + f_{vco\_min}}{2 * f_{ref}}$$

B.3. Mathematical description

A very good way to understand the functioning of a PLL is to consider the Laplace transformation of its components. By using basic control system theory, the designer

can control the exact properties of the PLL. A basic model of the PLL is represented in *Figure B-2.*

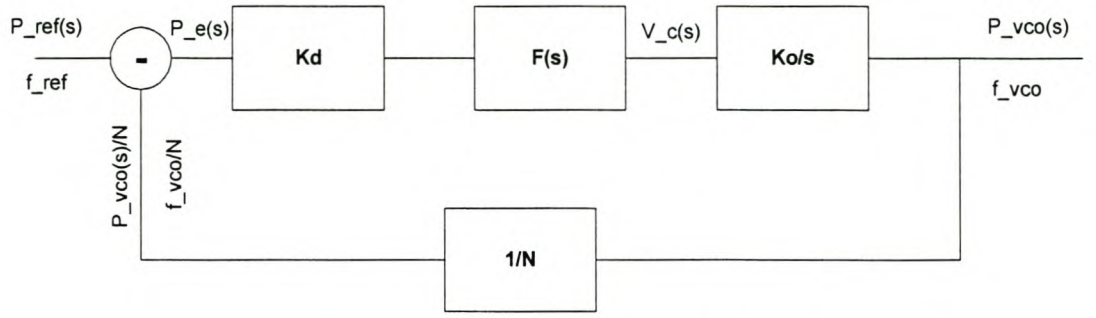

Figure B-2 Mathematical PLL model

The open loop transfer function of this loop is given by: (with $K_v=K_d*K_o$)

$$G(s) = \frac{P_{vco}(s)}{P_{ref(s)}} = \frac{K_v F(s)}{s}$$

The closed loop transfer function is given by :

$$H(s) = \frac{P_{vco}(s)}{P_{ref(s)}} = \frac{K_v F(s)}{s + \frac{K_v F(s)}{N}}$$

The transfer function of the control voltage $V_c(s)$ to the phase of the reference oscillator is given by:

$$\frac{Vc(s)}{P_{ref}(s)} = \frac{sK_d F(s)}{s + \frac{K_v F(s)}{N}} = \frac{s}{K_o} H(s)$$

The phase of the frequency reference, $P_{ref}(s)$, is compared with that of the divided output of the VCO, $P_{vco}(s)$. The resulting signal represents the difference between these two signals and is given by the following equation:

$$P_e(s) = P_{ref}(s) - \frac{P_{vco}(s)}{N}$$

The transfer function from the phase of the frequency reference, $P_{ref}(s)$, to the error output $P_e(s)$ is given by:

$$\frac{P_e(s)}{P_{ref}(s)} = \frac{1}{1 + \frac{K_v F(s)}{sN}} = \frac{s}{K_v F(s)} H(s)$$

For a loop that is locked, i.e. the two frequency sources are in phase, $P_e(s)$ will be a constant voltage. This means that the derivative of phase (frequency) will be zero and that the two oscillators will have exactly the same frequency. This is one of the fundamental characteristics of PLL frequency synthesisers.

By examining the above equations it will be evident that filter transfer function *F(s)* will be responsible for a lot of the loop characteristics of the PLL, and the proper choice of a filter are therefore a big part of the design process. The influence of different filters will now be discussed in detail.

B.3.1. No loop filter

For no loop filter the transfer function of the filter can be replaced by unity and the open- and closed loop transfer functions become

$$G(s) = \frac{F_{vco}(s)}{P_{ref(s)}} = \frac{K_v}{s} \text{ and } H(s) = \frac{F_{vco}(s)}{P_{ref(s)}} = \frac{K_v}{s + \frac{K_v}{N}} \text{ respectively.}$$

The bode diagram for the open loop can be represented by the following graph

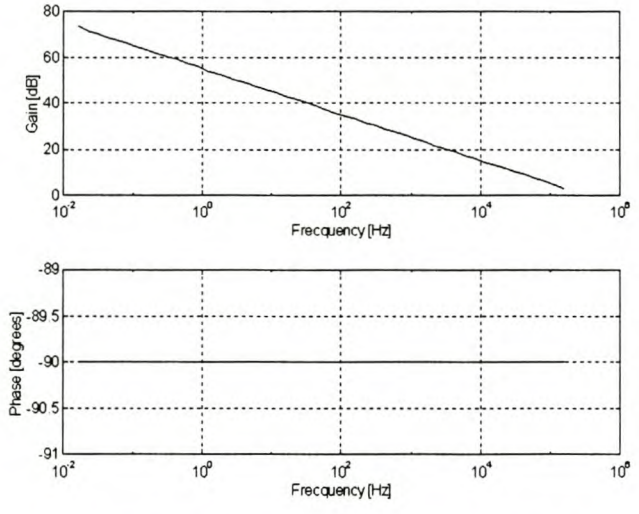

Figure B-3 Open loop – No loop filter

The frequency at which the graph crosses zero is K_v/N. The only way to adjust the bandwidth of this kind of loop would be to adjust the open loop gain K_v. This fact limits the designer to reach criteria for both the bandwidths of the loop and the transient response thereof with the result that this kind of loop is rarely used.

B.3.2. Passive Filter with single pole

The schematic for this type of filter is given in *Figure B-4* and its transfer function is:

$$F(s) = \frac{1}{1+\varpi} \text{ with } \tau=RC$$

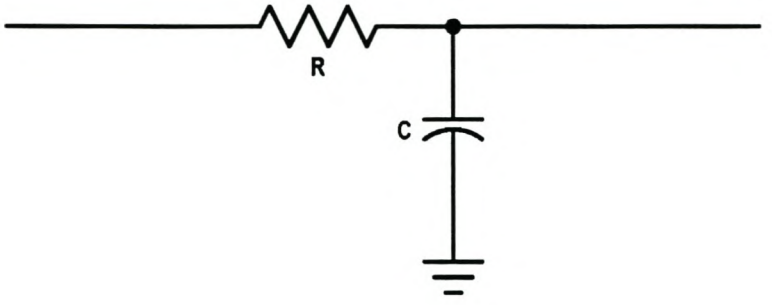

Figure B-4 Circuit diagram – Single pole passive filter

The bode diagram of this filter can be represented by the following graph:

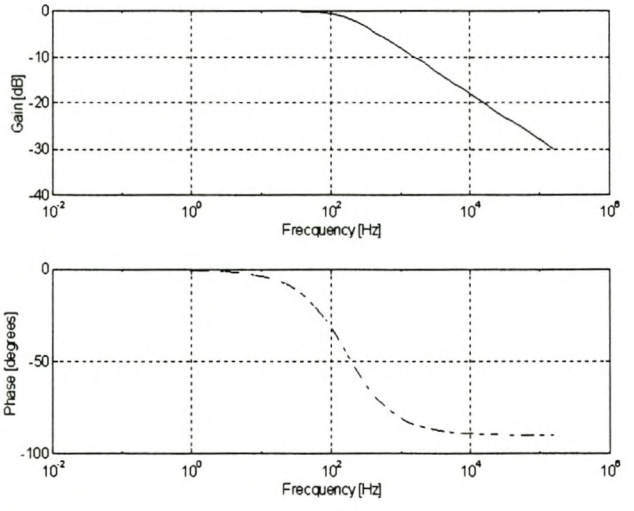

Figure B-5 Bode diagram - Single pole passive filter

The 3dB bandwidth of this circuit is given by $1/\tau$. When this filter is inserted the open and closed loop transfer functions become:

$$G(s) = \frac{F_{vco}(s)}{P_{ref(s)}} = \frac{K_v}{\varpi^2 + s}$$

$$\text{and } H(s) = \frac{F_{vco}(s)}{P_{ref(s)}} = \frac{\frac{K_v}{\tau}}{s^2 + \frac{s}{\tau} + \frac{K_v}{N\tau}} \text{ respectively.}$$

The natural frequency is given by $\omega_n = \sqrt{\frac{K_v}{N\tau}}$ and the damping by $\zeta = \frac{1}{2\omega_n \tau} = \frac{N\omega_n}{2K_v}$.

The transfer function can be written as: $H(s) = \frac{N\omega_n^2}{s^2 + 2\zeta\omega_n + \omega_n^2}$

The open loop bode diagram for the PLL in which the filter has been included is represented in *Figure B-6*.

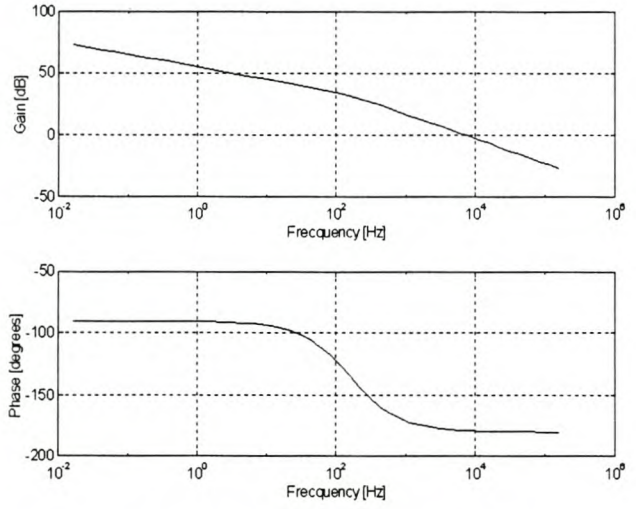

Figure B-6 Open loop bode diagram - Single pole passive filter

Two frequencies is of specific interest namely the 0dB crossing frequency which indicate the bandwidth of the system, and the break frequency at which the effect of the filter causes the amplitude to fall at 40dB per decade. For the case when these two frequencies are equal the damping ratio = 0.5[2]. When the break frequency is less than the bandwidth the damping ratio is less than 0.5 and when the break frequency is more than the bandwidth the damping ratio is more than 0.5.

The closed loop response is represented in *Figure B-7*.

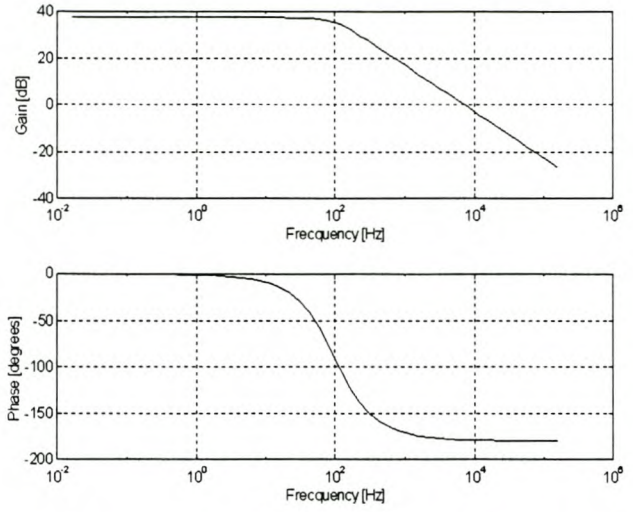

Figure B-7 Closed loop bode diagram - Single pole passive filter

The root locus of the complete system is represented by the following graph:

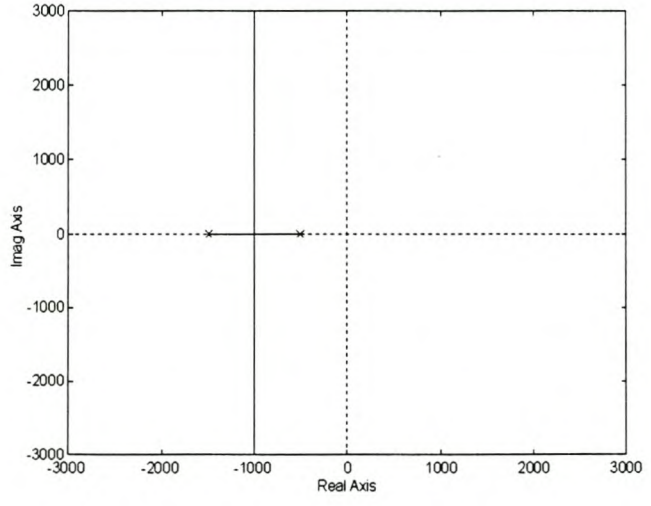

Figure B-8 Root locus - Single pole passive filter

The pole at the origin is caused by the free integrator of the VCO, and the other pole is solely determined by the loop filter. For this type of filter only the position of the pole (τ) and the loop gain (K_V) is under the designers control. Note that increasing the loop gain will move the closed loop roots away from the origin on the root-locus, decreasing the damping in the process. the This can limit the design of a PLL. It will be difficult, for instance, to meet a requirement for narrow bandwidth, without reducing the loop stability.

B.3.3. Passive Filter with single pole and zero

The schematic of this filter is given in *Figure B-9* and its transfer function is given by:

$$F(s) = \frac{1+\tau_2 s}{1+\tau_1 s} \text{ (with } \tau_2 = R_2 C \text{ and } \tau_1 = (R_1 + R_2)C\text{)}$$

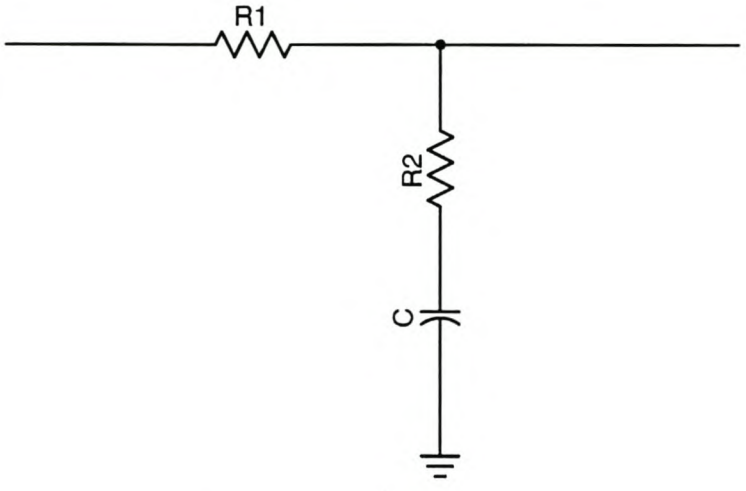

Figure B-9 Circuit Diagram - Passive Filter with single pole and zero

The bode diagram for this filter is represented in the following graph:

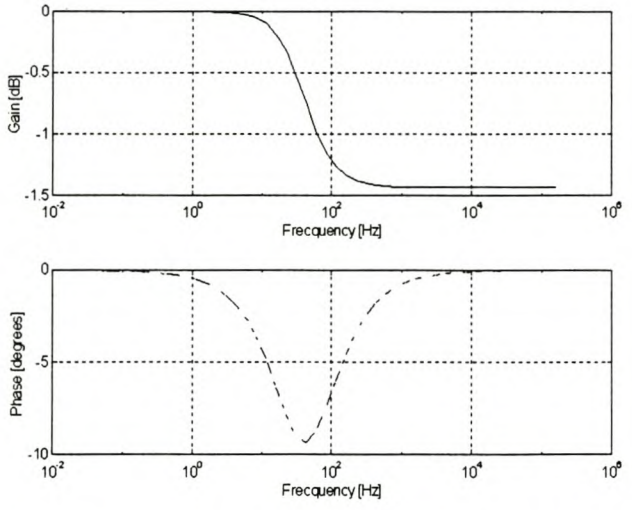

Figure B-10 Bode Diagram - Passive Filter with single pole and zero

The lower frequency break in the amplitude plot is given by $1/\tau_1$ and the higher frequency break by $1/\tau_2$. A possible disadvantage with this kind of filter is that the high frequency response does not fall with 20dB per octave, but stays constant therefore having less effect on unwanted noise or reference harmonics. This problem can be alleviated by putting an extra RC filter (of at least 10 times the loop

bandwidth) in series with the original filter. This will attenuate the unwanted harmonics, while having little effect on the loop characteristics.

When the filter transfer function is inserted the open and closed loop transfer functions become:

$$G(s) = \frac{F_{vco}(s)}{P_{ref(s)}} = \frac{K_v(1+\tau_2 s)}{\tau_1 s^2 + s} \text{ and}$$

$$H(s) = \frac{F_{vco}(s)}{P_{ref(s)}} = \frac{\frac{K_v(1+\tau_2 s)}{\tau_1}}{s^2 + \frac{(N+K_v\tau_2)s}{\tau_1 N} + \frac{K_v}{\tau_1 N}} \text{ respectively.}$$

The natural frequency is given by $\omega_n = \sqrt{\frac{K_v}{N\tau_1}}$ and the damping factor for this kind of loop is $\zeta = \frac{N + K_v\tau_2}{2\omega_n N\tau_1} = 0.5\omega_n(\tau_2 + \frac{N}{K_v})$.

The transfer function can be written as:

$$H(s) = \frac{N(1+\tau_2 s)\omega_n^2}{s^2 + 2\zeta\omega_n + \omega_n^2}$$

The bode diagram for the open loop is represented in *Figure B-11*:

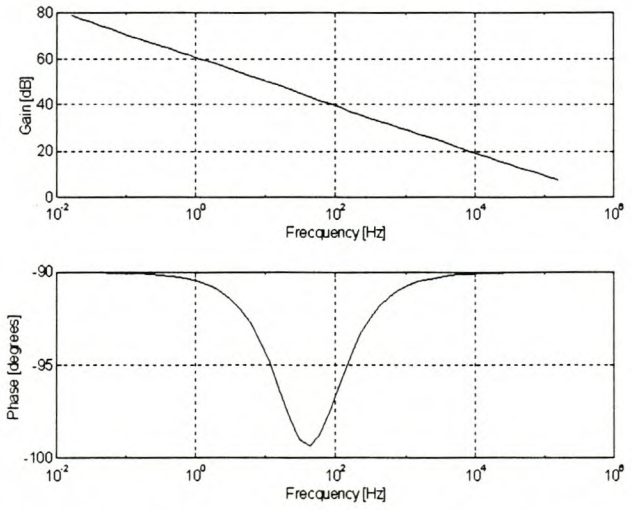

Figure B-11 Open loop Bode Diagram - Passive Filter with single pole and zero

The first breakpoint is located at the frequency value of pole at $1/\tau_1$ and that of the second at the zero at $1/\tau_2$. The closed loop response is represented in *Figure B-12*:

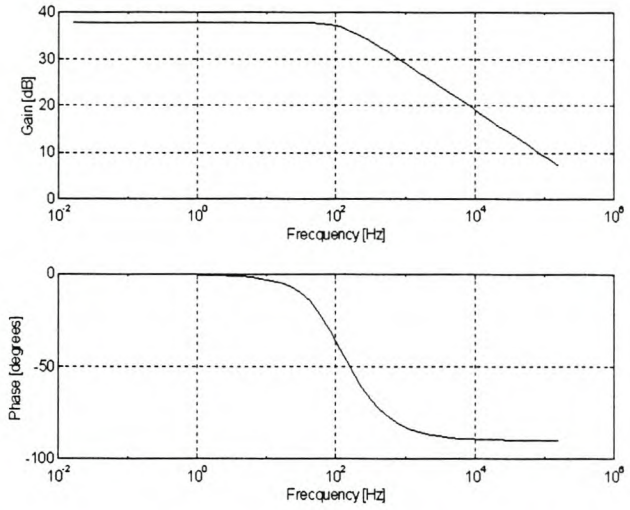

Figure B-12 Closed loop bode Diagram - Passive Filter with single pole and zero

The root locus of the complete system can be represented in Figure B-13:

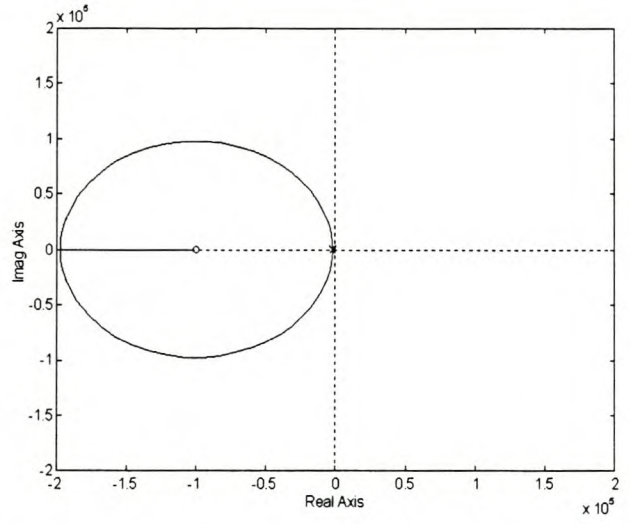

Figure B-13 Root locus diagram - Passive Filter with single pole and zero

The pole caused by the VCO is at the origin with the pole at $1/\tau_1$ also clearly visible. By changing the position of this pole and the zero at $1/\tau_2$ it is possible to obtain the wanted loop response. Increasing the loop gain will never decrease the damping below some minimum. The component values required by the prescribed loop specifications can sometimes be difficult to realise, and in such cases an active filter can be used.

B.3.4. Active filter with single pole and zero.

The schematic of this filter is given in *Figure B-14* and its transfer function (for the case where the open loop gain of the amplifier is very large) is given by:

$$F(s) = \frac{1+\tau_2 s}{\tau_1 s} \text{ (with } \tau_2 = R_2 C \text{ and } \tau_1 = R_1 C)$$

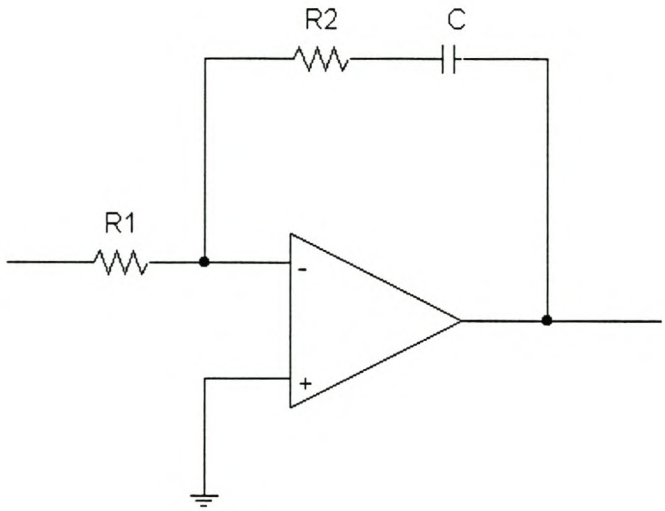

Figure B-14 Circuit diagram - Active filter

The bode diagram for this filter is represented in *Figure B-15*:

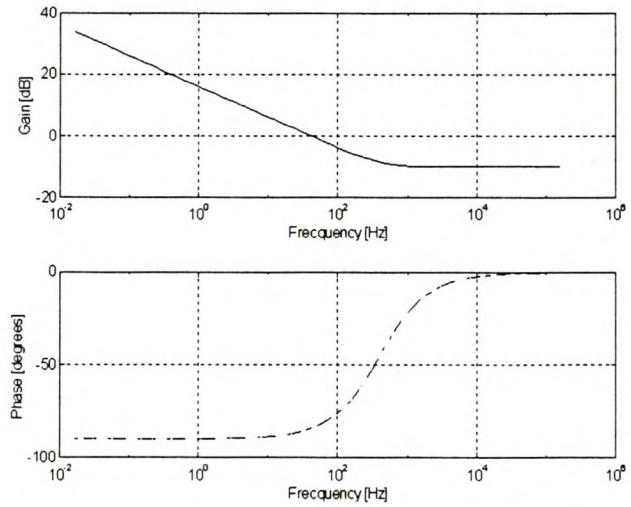

Figure B-15 Bode diagram - Active filter

A possible disadvantage with this kind of filter is that the high frequency response does not fall with 20dB per octave, but stays constant therefore having less effect on unwanted noise or reference harmonics. This problem can be alleviated by putting an extra RC filter of at least 10 times the loop bandwidth in series with it.

When filter transfer function is inserted the open and closed loop transfer functions become:

$$G(s) = \frac{F_{vco}(s)}{P_{ref(s)}} = \frac{K_v(1+\tau_2)}{\tau_1 s^2} \text{ and}$$

$$H(s) = \frac{F_{vco}(s)}{P_{ref(s)}} = \frac{\dfrac{K_v(1+\tau_2 s)}{\tau_1}}{s^2 + \dfrac{K_v \tau s}{N\tau_1} + \dfrac{K_v}{N\tau_1}} \text{ respectively.}$$

The natural frequency is given by $\omega_n = \sqrt{\frac{K_v}{N\tau_1}}$. The damping factor for this kind of loop is $\zeta = \frac{K_v \tau_2}{2\omega_n N\tau_1} = 0.5\omega_n \tau_2$. The transfer function can be written as:

$$\tau H(s) = \frac{N(1+\tau_2 s)\omega_n^2}{s^2 + 2\zeta\omega_n + \omega_n^2}$$

The bode diagram for the open loop is represented in *Figure B-16*:

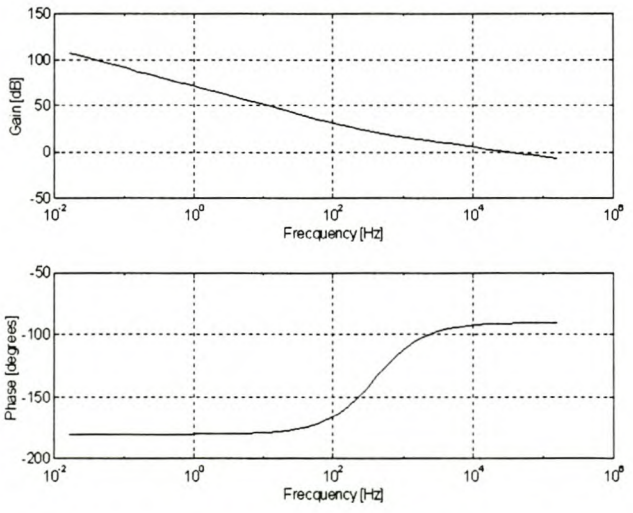

Figure B-16 Open loop bode diagram - Active filter

As can be seen the amplitude response initially falls at 40dB/decade (due to the two poles at the origin), but flattens out to 20dB/decade above the zero frequency of $1/\tau_2$. The closed loop response is given in *Figure B-17*:

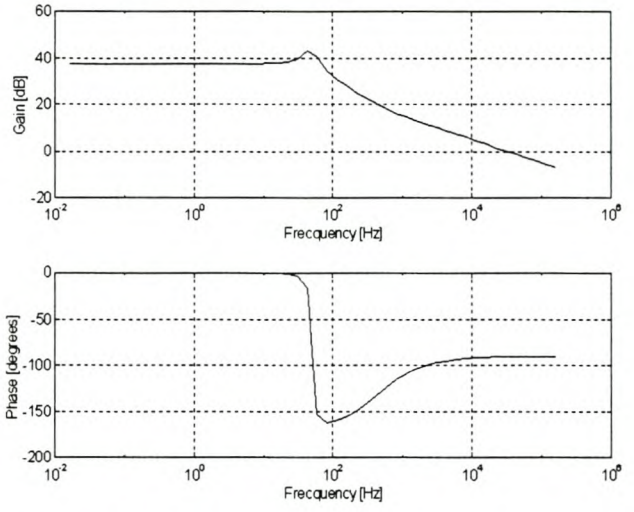

Figure B-17 Closed loop bode diagram - Active filter

The root locus of the complete system is represented by the graph in Figure B-18:

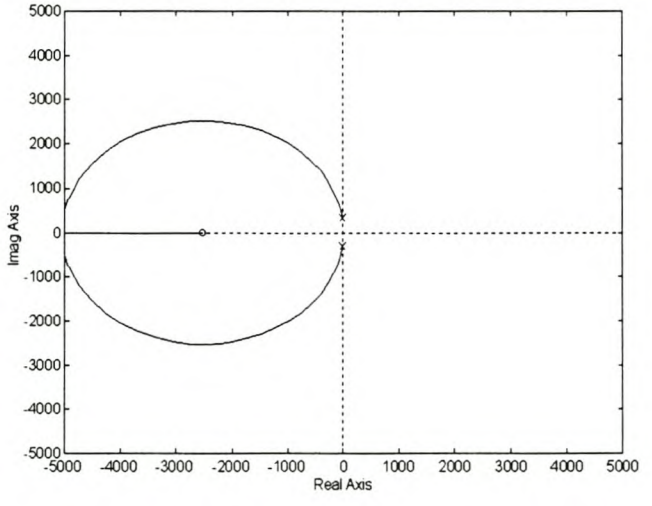

Figure B-18 Root locus diagram - Active filter

The pole caused by the VCO is at the origin with the pole at $1/\tau_1$ also clearly visible. By changing the position of this pole and the zero at $1/\tau_2$ it is possible to obtain the wanted loop response. The active filter generally gives rise to better tracking performance[5].

B.4. Design Guidelines

B.4.1. Specifications

The required design specifications will greatly determine the design of the synthesiser. The characteristics of the VCO and phase detector should first be measured accurately to design the loop filter according to the specifications.

B.4.1.1. Harmonic rejection

Sideband rejection refers to the difference in the synthesiser output between the fundamental frequency and the sideband frequencies removed by multiples of the reference frequencies from it. At least 60dB difference is usually required for a frequency synthesiser.

B.4.1.2. Lock Time

The lock time is the time it takes for the PLL to acquire positive lock. For the worst case this value can be taken as the time from switch-on to PLL lock witch will be longer than the time taken to lock when the N-counter is changed from one value to another.

B.4.1.3. Loop bandwidth

As was already seen in the previous sections, the PLL behaves like a low pass filter rejecting frequencies higher than a certain bandwidth. The closed loop bandwidth ω_n is an important parameter in the correct design of the loop.

B.4.1.4. Overshoot and Damping Ratio

The maximum percentage of overshoot in the loop step response before it settles to its final value is defined as the loop overshoot. The damping ratio gives an indication of the lock time and overshoot of the system, and will usually be specified as 0.7.

B.4.2. Choice of filter

The influence of different types of filters have already been discussed in *Section B.3*. The PLL is rarely used without a loop filter and a filter with at least one pole and zero are usually used. Extra filtering can also be employed to meet the harmonic rejection requirements.

To determine the values of the filter components it is first necessary determine the loop parameters from the specifications given. For this use it is convenient to draw a normalised step response for different values of damping ratio like that given in *Figure B-19*.

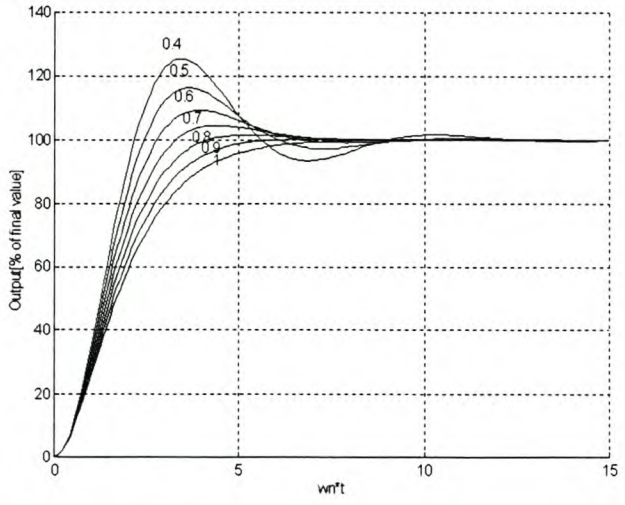

Figure B-19 Normalised Step response

Using the correct normalised step response the designer can determine the required loop parameters from those specified, and choose filter component values to satisfy the specifications

B.5. Frequency Modulating a Synthesiser

The frequency synthesiser can be modulated directly with audio frequencies signal to generate a frequency modulated (FM) output. Two possible configurations of injecting the audio in the loop will now be discussed.

B.5.1. Modulating the Crystal reference

If the crystal reference is designed as a voltage controlled crystal oscillator (VCXO), the modulating signal can be applied at its input to generate the desired FM modulated signal. The relationship of the output frequency to the reference frequency and the loop divider must be kept in mind to design the VCO correctly.

$$f_{out} = f_{ref} * N$$

In order to build a transmitter with a peak frequency deviation of 3kHz on the output frequency (f_{out}), the modulation of the reference must be limited to 3kHz/N. The filter

of the synthesiser must be designed, so that the closed loop bandwidth of the PLL is bigger than the maximum audio frequency that will be used to modulate the loop.

B.5.2. Modulating the Filter output

Any noise source in the synthesiser loop will tend to have the effect of modulating the VCO and create sidebands in the frequency output. This can also be used to create a FM modulator, by intentionally adding the modulating signal in the loop before the VCO.

In this case the closed loop bandwidth of the synthesiser must be smaller than the lowest audio frequency used to modulate the VCO. If this is not done, the loop will try to filter out the audio signals.

B.6. Reference

1. Paul H Young, *Electronic communication techniques– Third edition*, Prentice Hall International edition, 1994
2. J. Encinas, *Phase locked loops*, Chapman and Hall, 1993
3. JJ du Plooy, *An agile frequency modulated transmitter using the phase-locked loop*, Thesis for masters in Engineering (Electronic) at University of Stellenbosch, February 1973
4. William F. Egan , *Frequency Synthesis by phase lock*, Wiley and Sons,1981
5. Floyd M. Gardner, *Phaselock techniques - Second Edition*, Wiley and Sons, , 1979
6. *Phase-Locked Loop design fundamentals,* Motorola Application Note AN535, Motorola Inc, 1988
7. *The MC145170 in basic HF and VHF Oscillators,* Motorola Application Note AN1207, Motorola Inc, 1988
8. D.F. Visser, *A high frequency Phase locked loop stabilised oscillator (Afrikaans)*, Report of final year project for degree in engineering (Electronic) at University of Stellenbosch, November 1994

Appendix C - Schematic Diagrams

The schematic diagrams for the complete fieldstation are presented on the following pages.

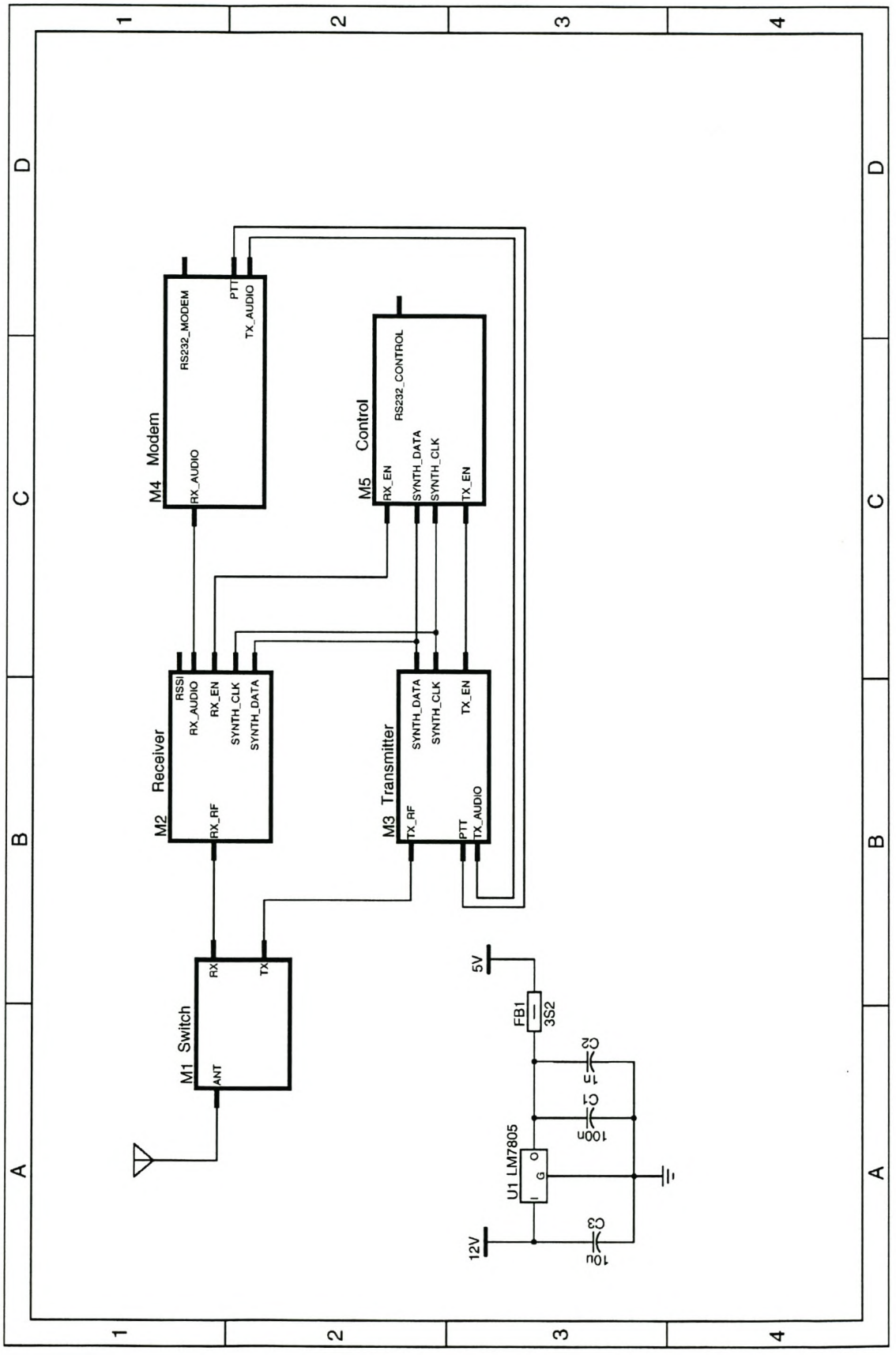

Figure C-1 Complete Fieldstation Diagram

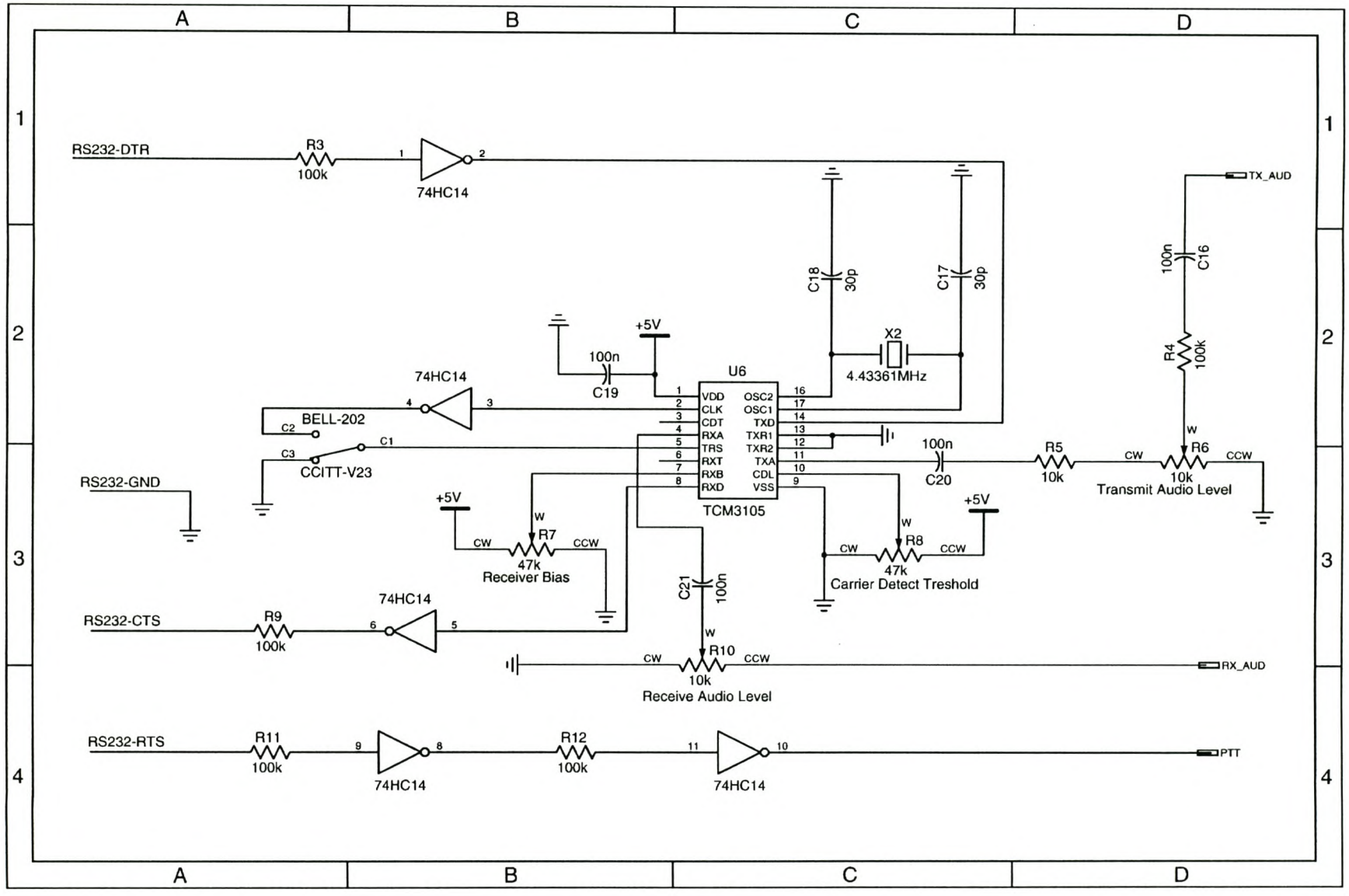

Figure C-2 Modem Schematics

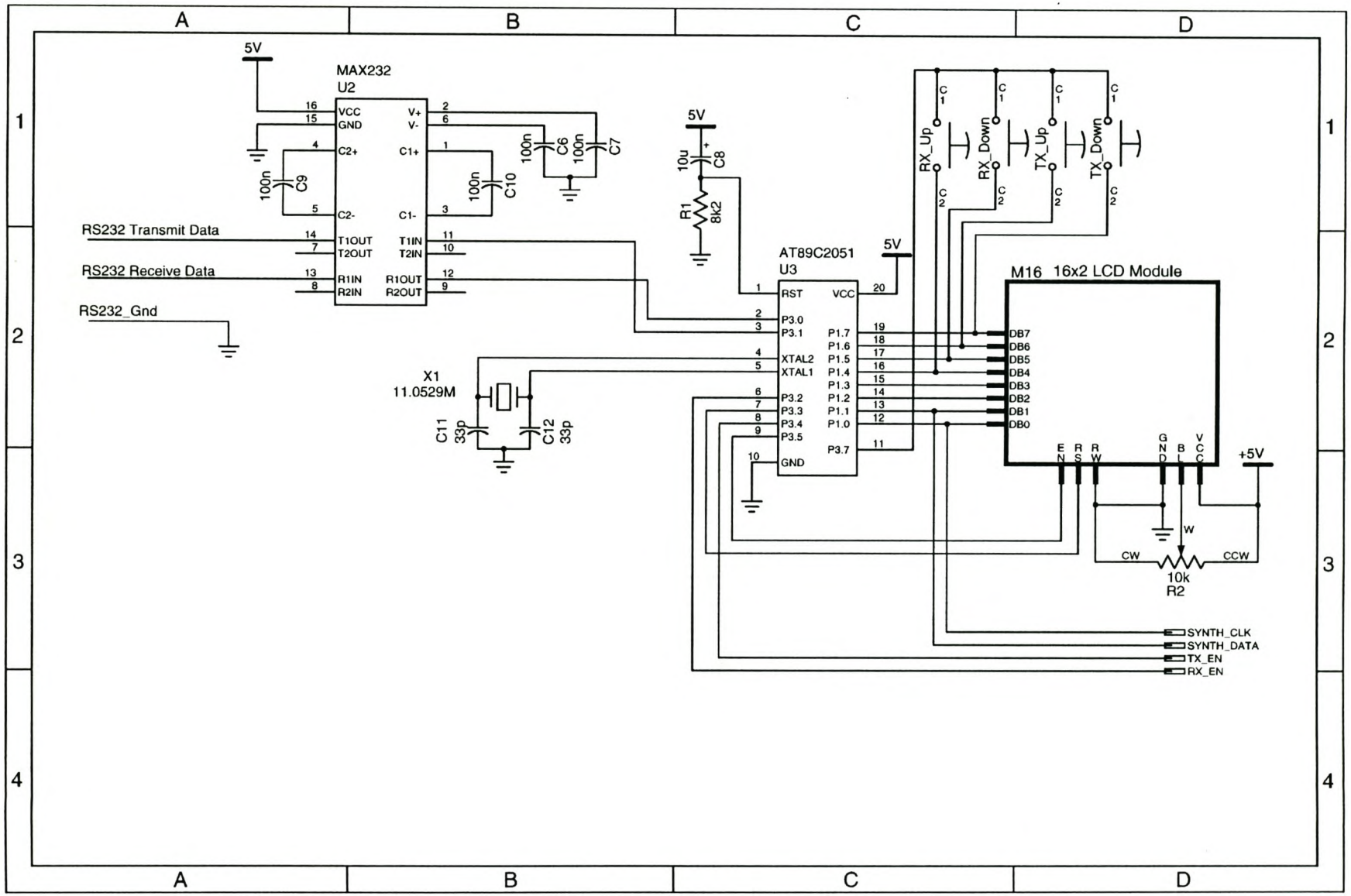

Figure C-3 Controlling Circuit

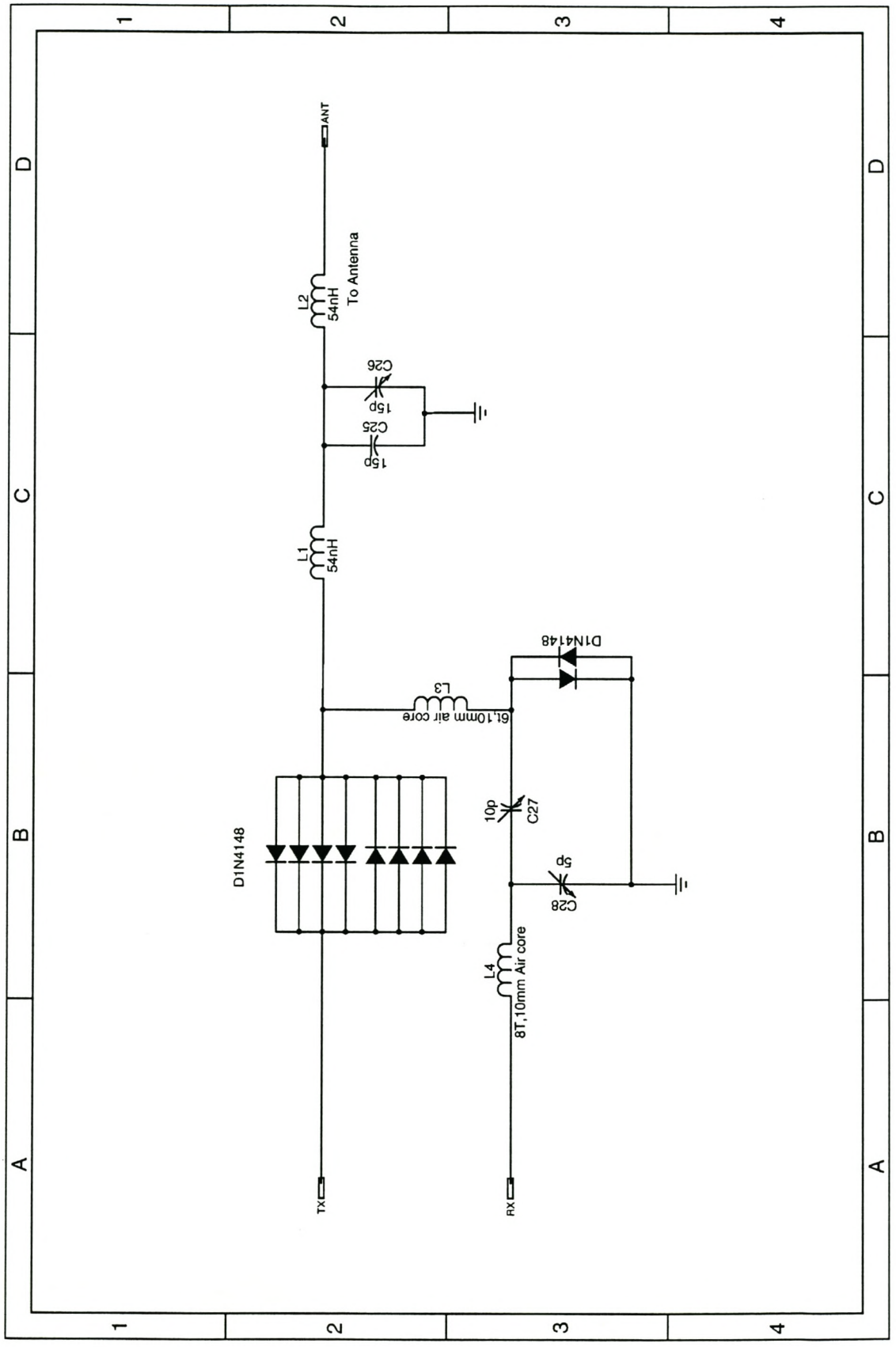

Figure C-4 Transmit Receive Switch

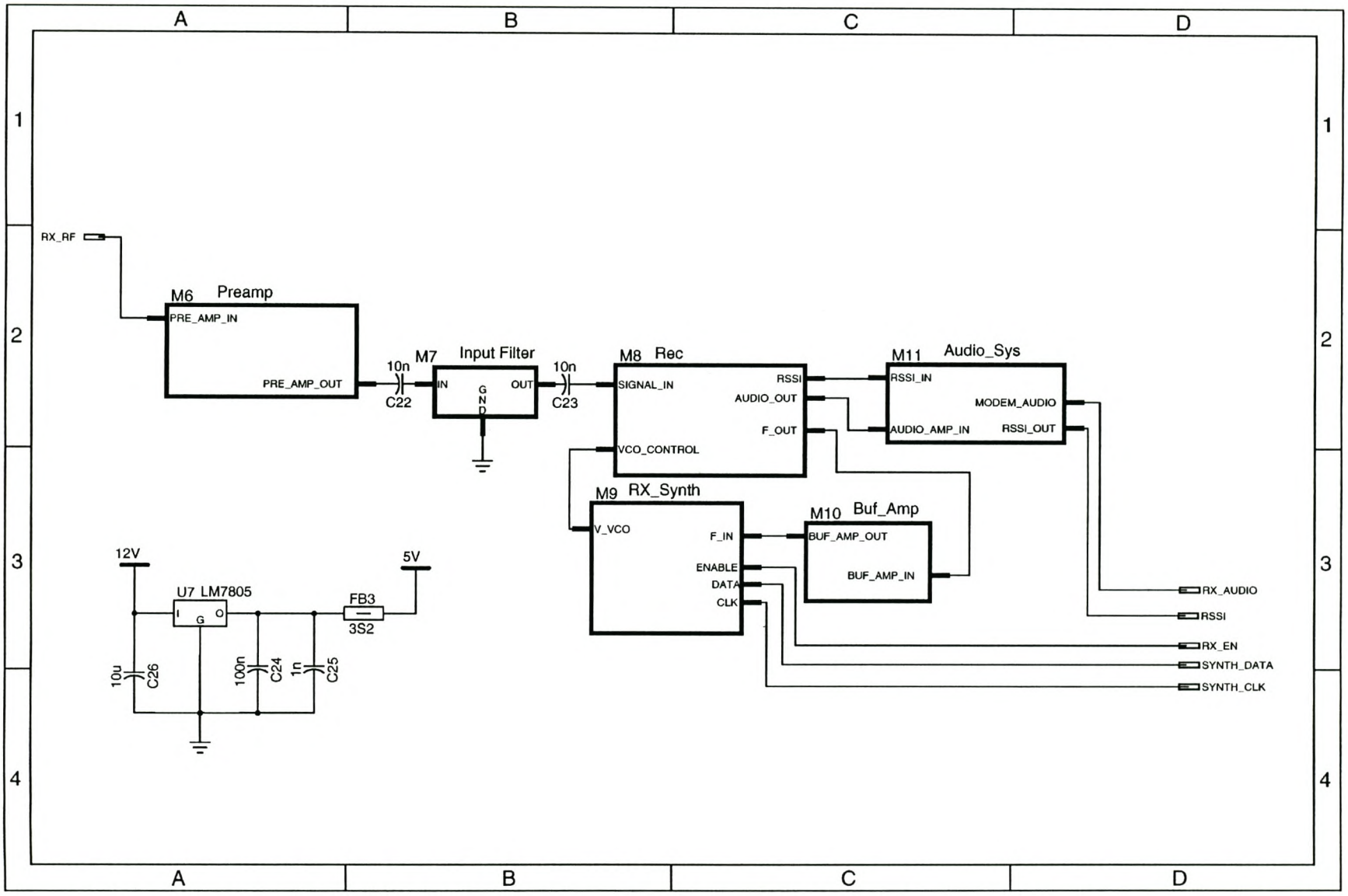

Figure C-5 Receiver Schematic diagram

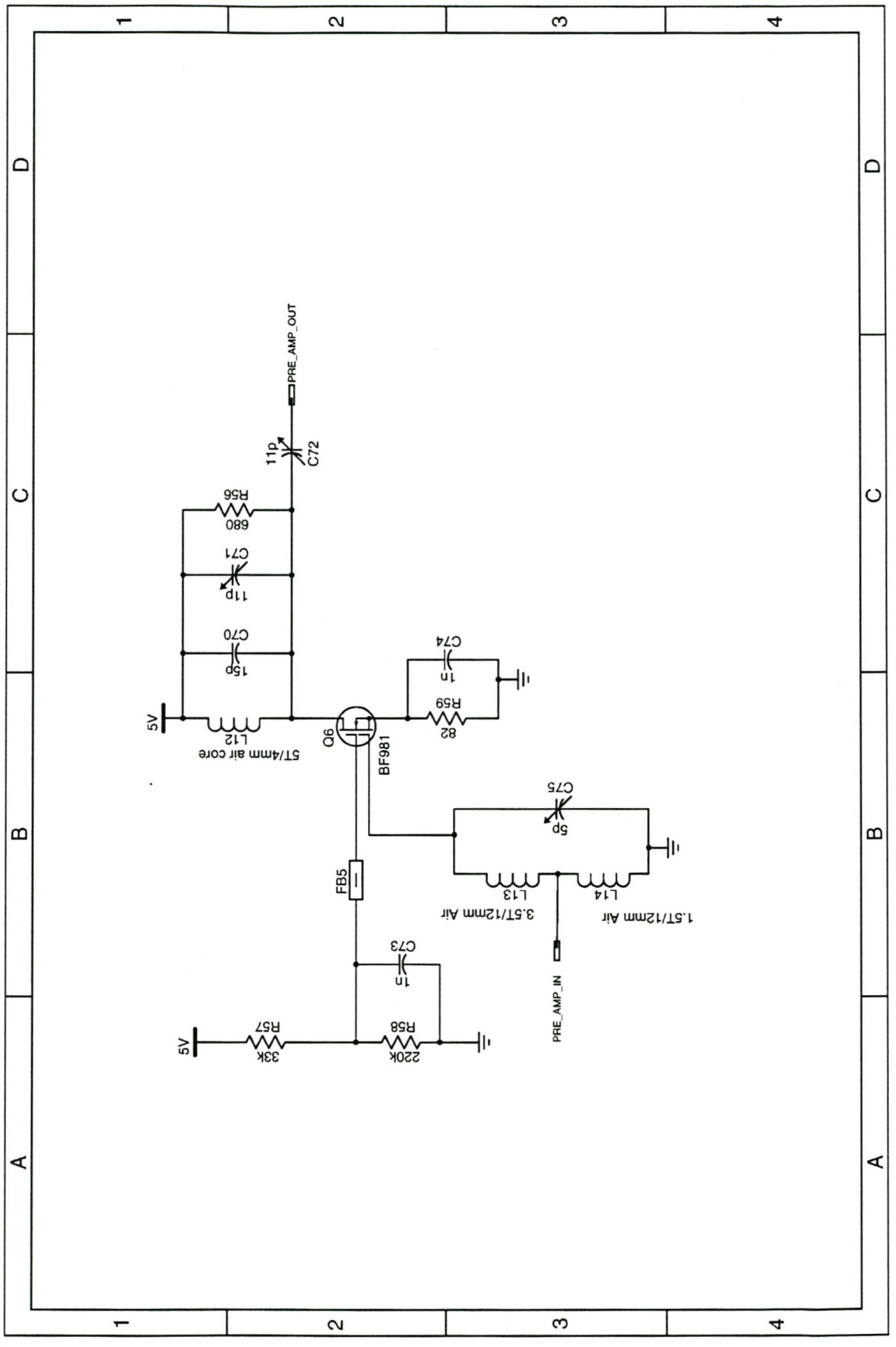

Figure C-6 Receiver -Low Noise Amplifier

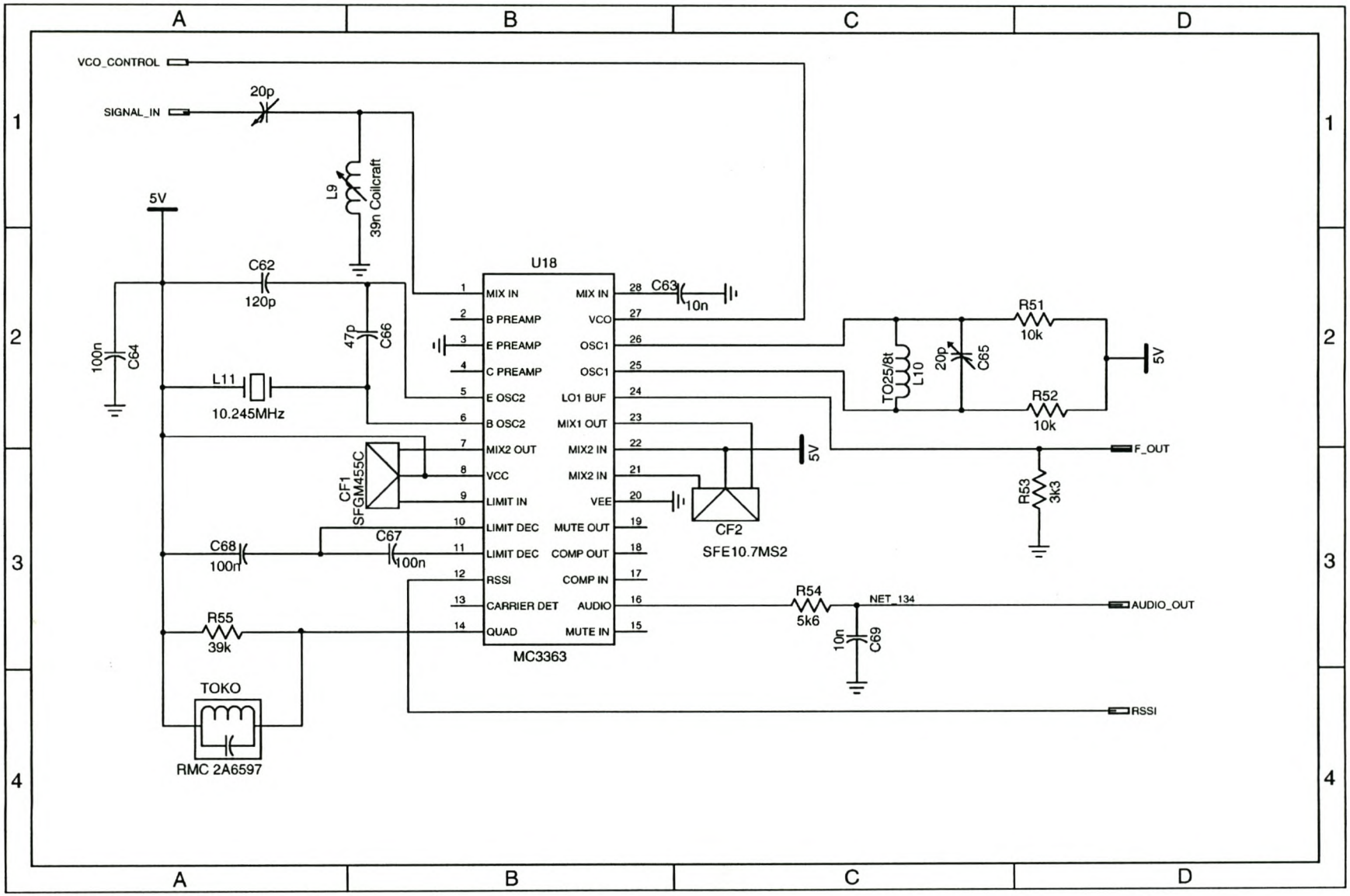

Figure C-7 Receiver - Dual Conversion IC

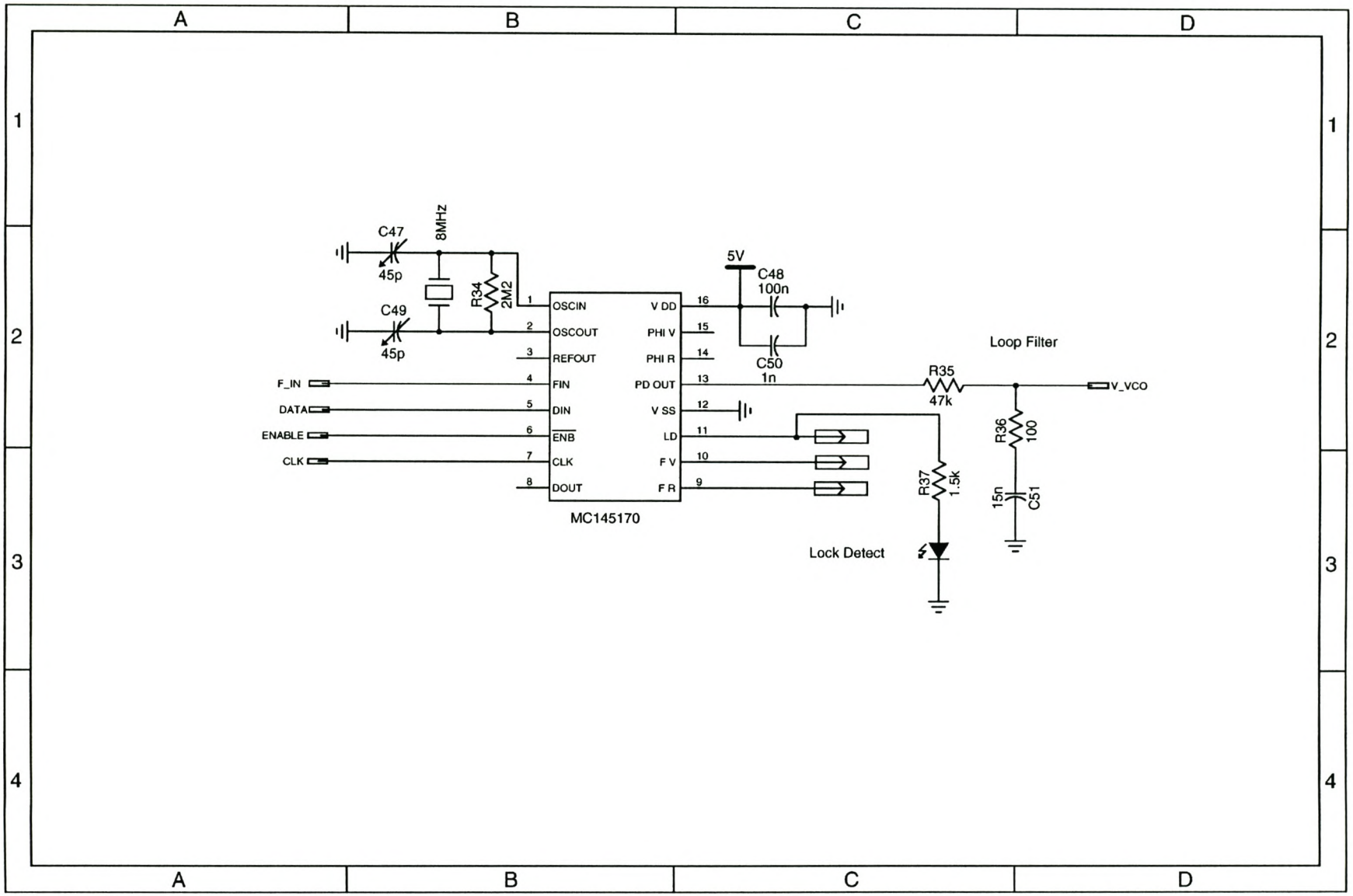

Figure C-8 Receiver - Synthesiser

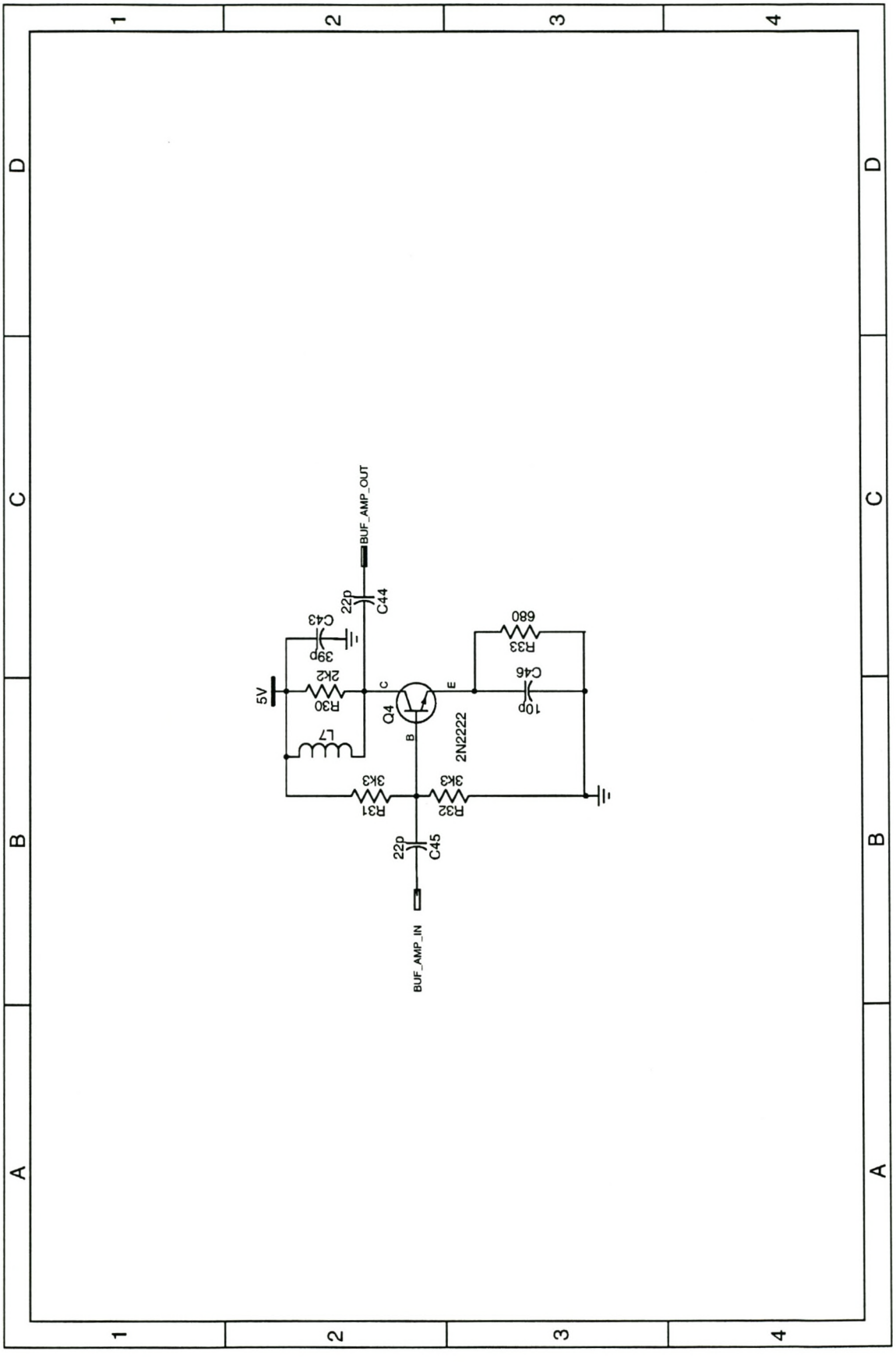

Figure C-9 Receiver - Buffer amplifier

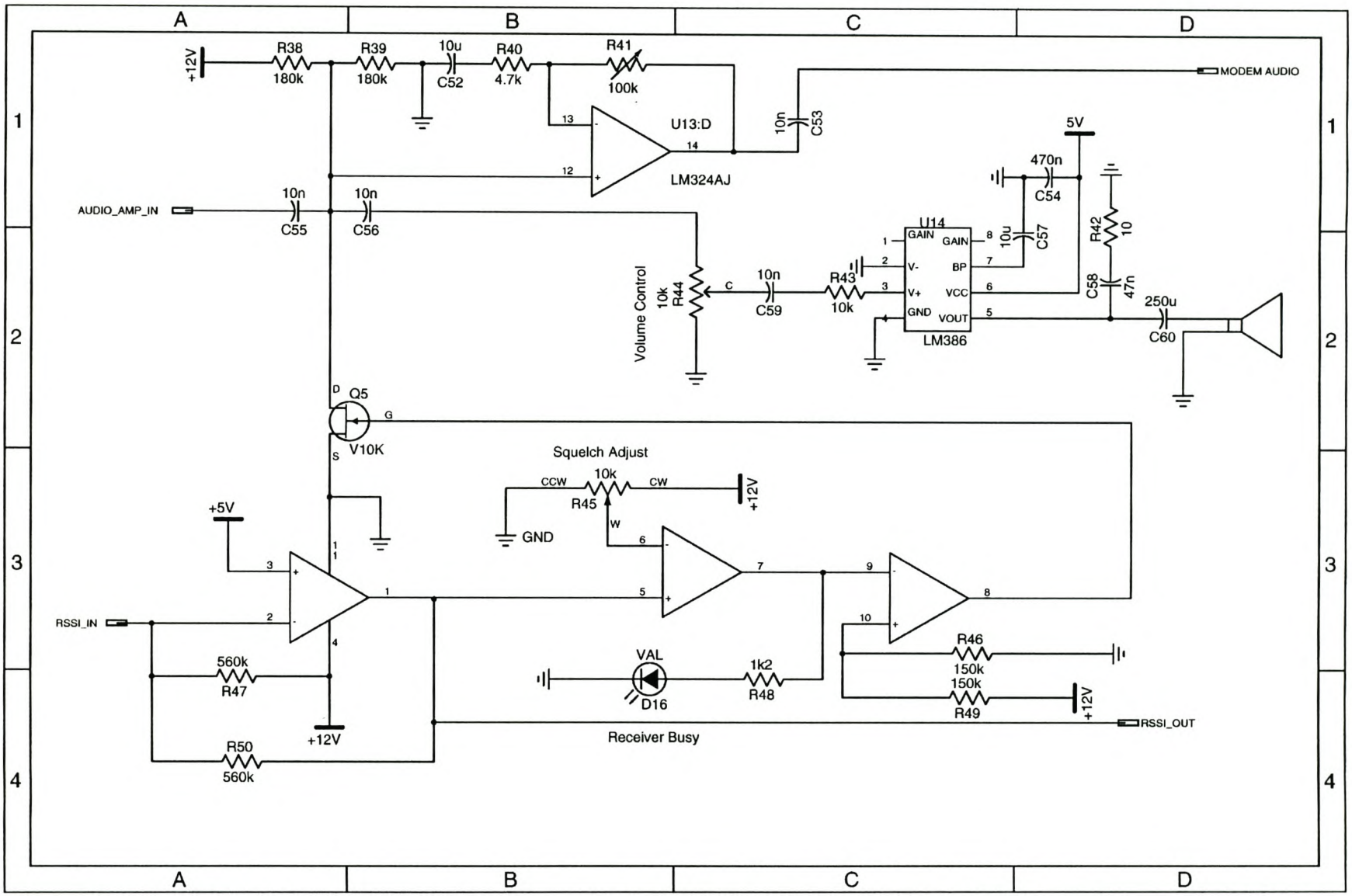

Figure C-10 Receiver - Audio System

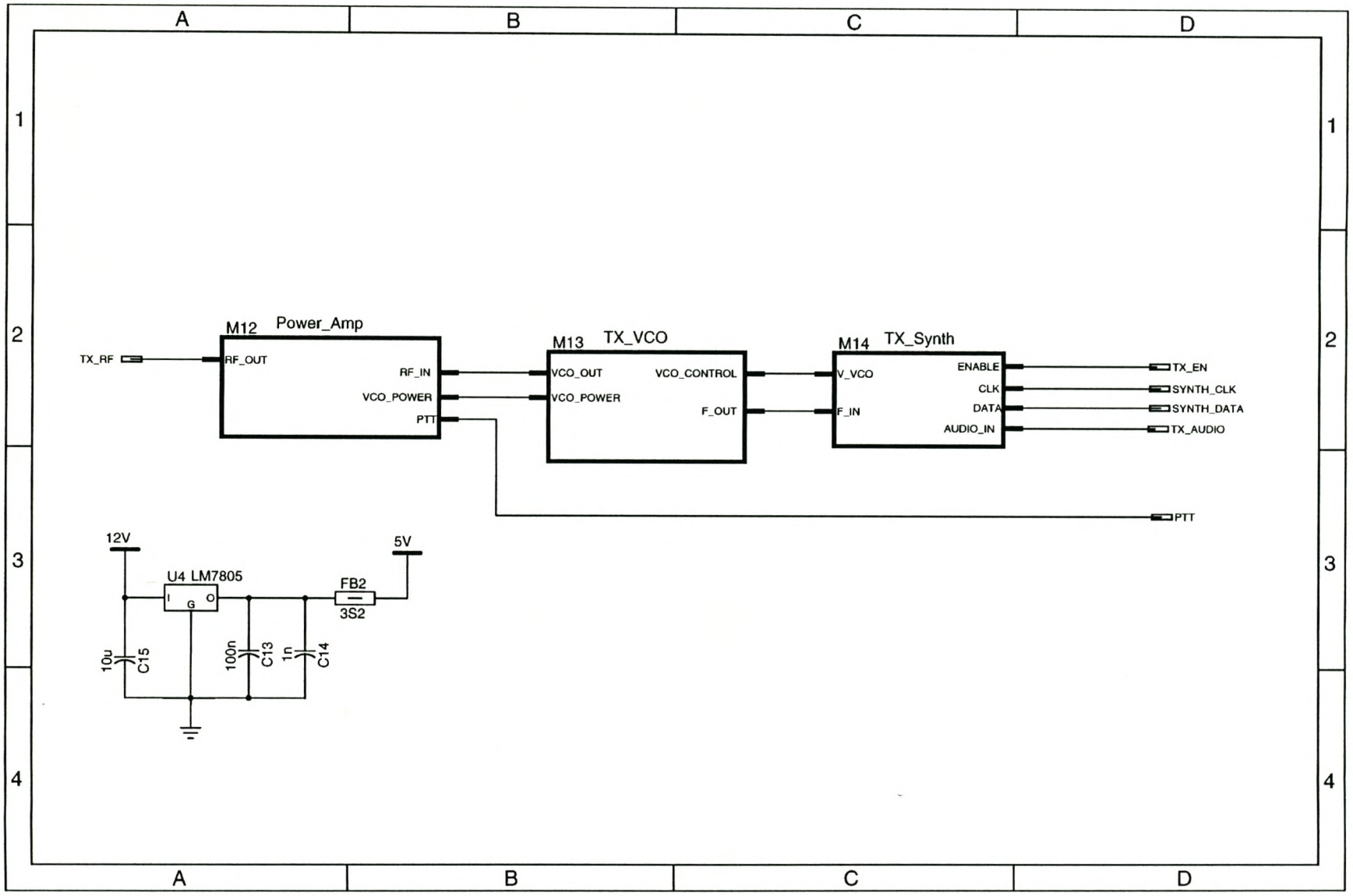

Figure C-11 Transmitter Schematics

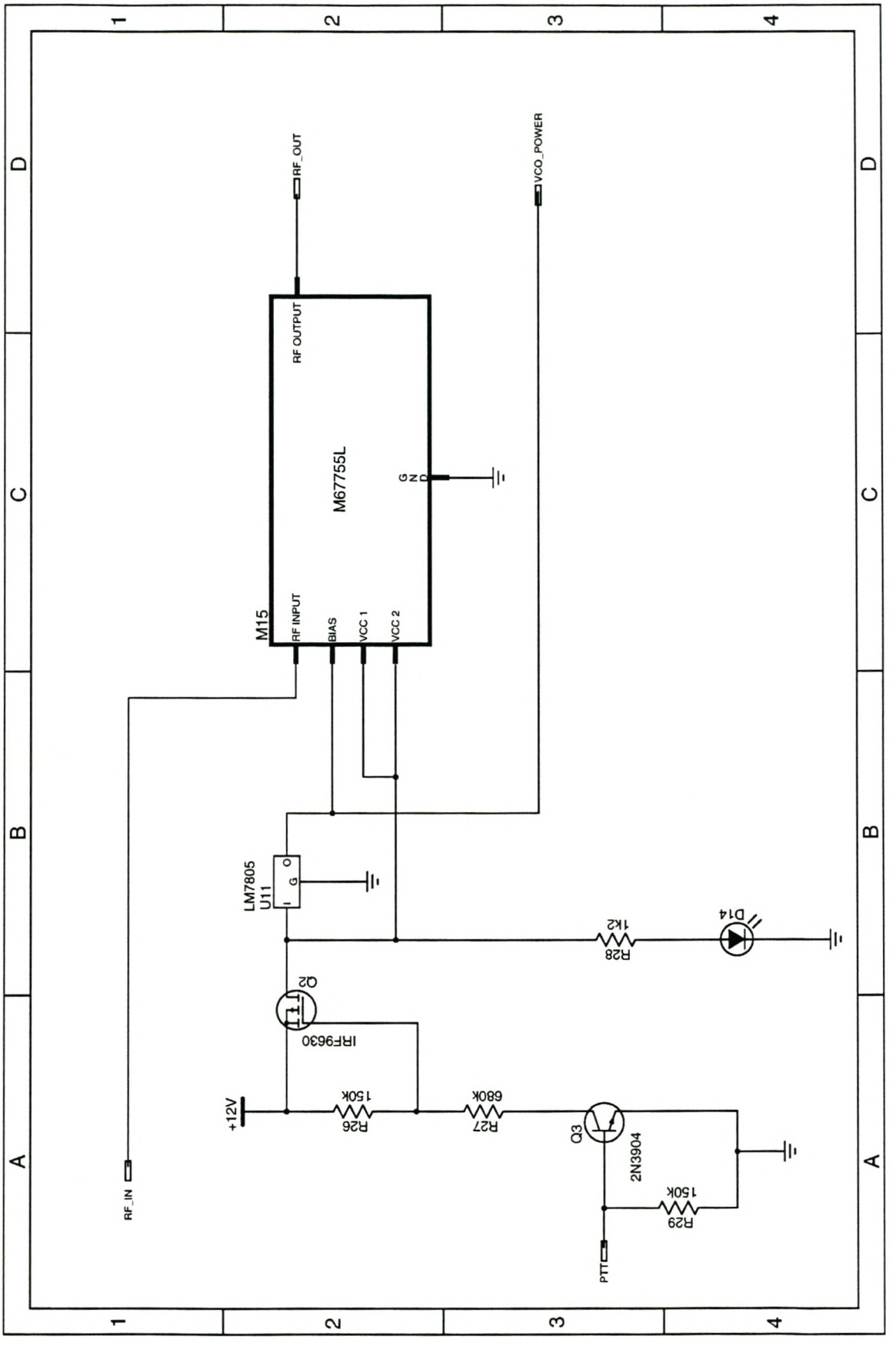

Figure C-12 Transmitter - Power amplifier

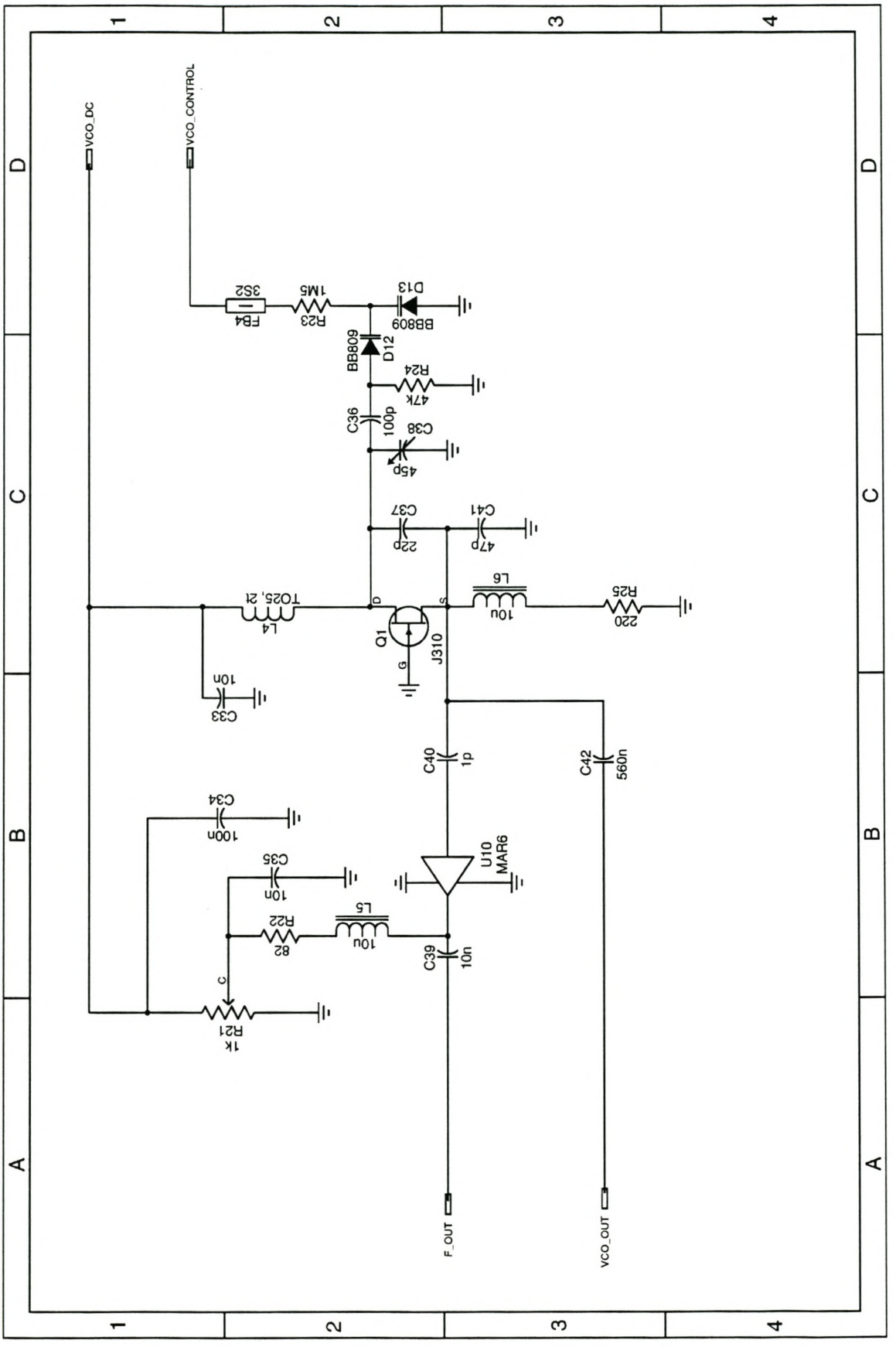

Figure C-13 Transmitter - VCO

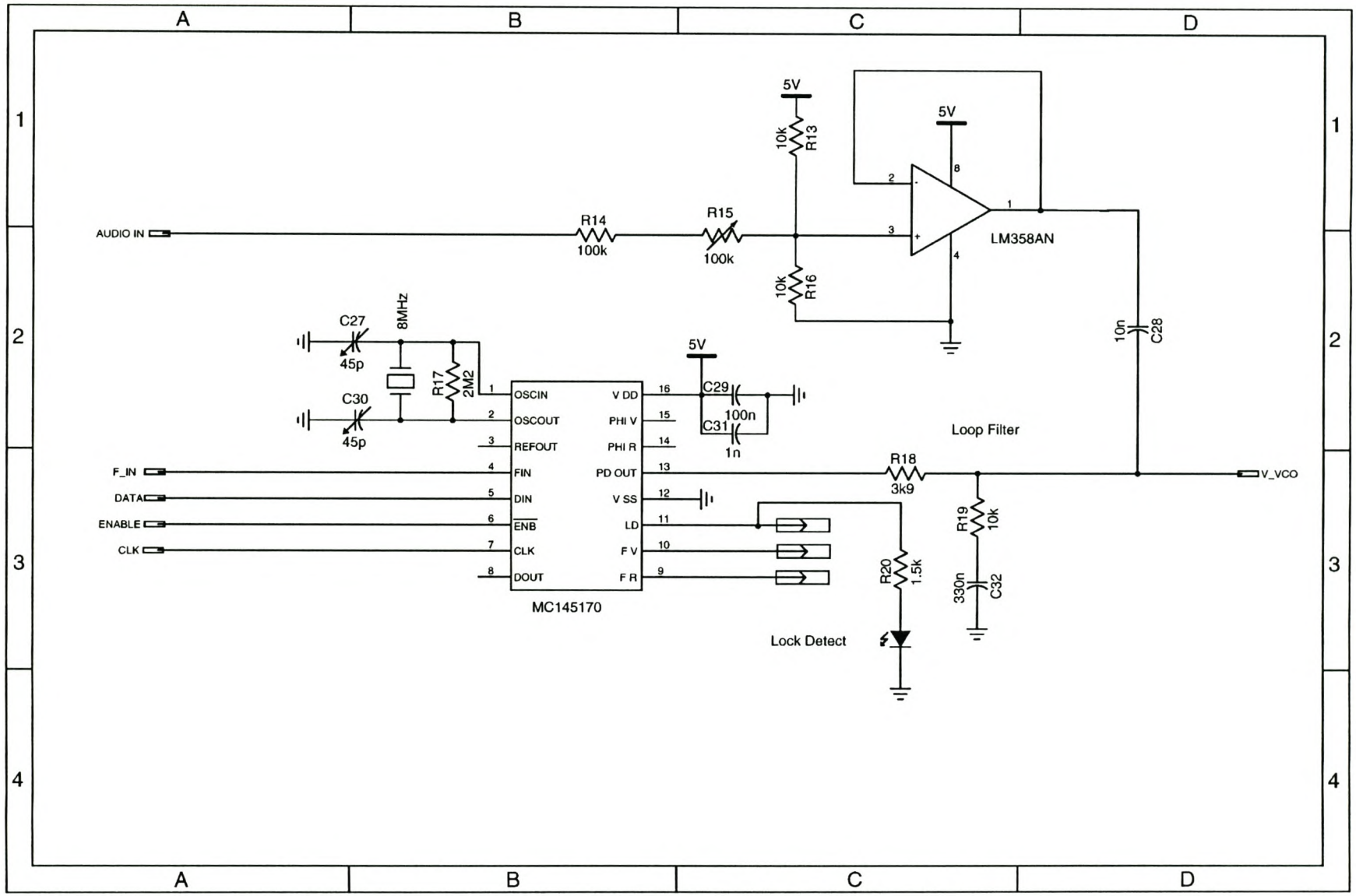

Figure C-14 Transmitter - Synthesiser

Appendix D - List of files on accompanying disk

D.1. Link Budget Files (*See Appendix A*)

Filename	Description
Lbudget.m	Computes the total link budget for the link between the field station and the ***SUNSAT*** microsatellite
P_loss.m	Computes the influence of all the relevant physical phenomena on the link budget
Antgain.m	Includes the influence of the transmitting and receiving antennas on the link budget.

D.2. Synthesiser design files (*See Appendix B*)

Similar files were developed to simulate and design three types of loop filter. In the following table, *n* will be used to distinguish between the files for the following filters:

0 - No loop Filter
1 - Passive loop filter with single pole
2 - Passive loop filter with single pole and zero
3 - Active loop filter with single pole and zero

Filename	Description
Simun.m	Simulates the synthesiser loop for a specified set of parameters
Simuswn.m	Switchyard function for simun.m - Allows the user to see the effect of changing component values on the loop characteristics. Provides GUI buttons.
Plotan.m	Plots the filter bode diagram, open loop bode diagram, closed loop bode diagram, root locus and step response on consecutive screens.
Plotbn.m	Plots the filter bode diagram, open loop bode diagram, closed loop bode diagram, root locus and step response on the same screen.
Hulpn.m	Design tool that plots normalised step responses for different damping ratios to help the designer choose correct loop characteristics
Rn.m	Computes resistor values given loop parameters

D.3. Synthesiser control files

Filename	Description
Athoof_2.asm	Atmel 89c2051 assembly code listing for the synthesiser controller.
Rhoof2.pas	Turbo Pascal code for controlling the receiver and transmitter synthesisers from a personal computer.
Rhoof2.exe	Pascal code in Executable format

D.4. TPK Application

Filename	Description
Tb1.bat	Batch file for setting up the TPK software to function with the field station modem connected to serial port1 of the computer.
Tb2.bat	Batch file for setting up the TPK software to function with the field station modem connected to serial port2 of the computer.
Tpk.exe	Terminal program for using the field station for AX25 data communication
Tfpcx.exe	Software driver for implementing AX.25 protocol on computer
Tncded.exe	Software driver for implementing TNC commands on computer